Effect of drivetrain set up on acceleration, torque, shifting and track times

2021

Supervisor: Mark Lay and Racheal Tighe

Nicholas Piebenga

1285517

Abstract

Every year SAE International organise an international competition to design and race a formula style race car called Formula SAE. The last time WESMO sent a car to competition was in 2018 and the 2018 car had gearing that was very short geared. This resulted in the driver having to constantly change gears, due to the final drive gear ratio being too high. The objective of this thesis was to research into potential way to increase the performance of the future WESMO cars through research into how to the effects of tuning the drivetrain along with potential areas for redesign with the gaol of producing a car that can complete the acceleration event in less than 3.8 seconds. Where practical the majority of the drivetrain components will be retained from the 2018 design,.

Through a combination of optimising the drivetrain gear ratio, researching into new tyres as well as incorporating more carbon into the drivetrain design the proposed car could potentially meet that goal. The incorporation of carbon driveshafts as well as carbon rim shell both increases the efficiency of the torque transfer across the drivetrain as well as reduces the overall weight of the drivetrain. Optimising the gear ratio results in a reduced tendency to wheelspin and minimal shifting required during the acceleration run, while still maintaining high torque at the wheels. Future WESMO teams should also design the car around incorporating 7.5inch wheels, since changing from 6-inch to 7.5-inch wide tyres gives a noticeable increase in traction. The two best options for changing the tyres depend on the situation of future WEMO teams. Changing to 16-inch wheels will give better torque transfer to the wheels and reduces the Unsprung weight of the car but will require extensive redesign of the suspension on the car due to the different outer diameter of the tyre. Changing to the 18x7.5-inch tyres will increase the traction of the car, but also slightly increase the weight, however does not require as extensive of a redesign.

.

Acknowledgements

Firstly, I would like to acknowledge my academic supervisors Mark lay and Rachael Tighe, for their continual guidance throughout this research project and especially during the writing of the report where they would always have the time to advise me as well as answer any questions I had.
Secondly, I would like to acknowledge Scott Harvey for always making the time to drive the car during testing as well as providing accurate setup/testing feedback during each test.
I would also like to acknowledge Jonathan van Harselaar and Larissa Kopf for always being available to ask for technical advice as well as helping out with the maintenance required after each track testing session.

To Sebastian Ashburn for teaching me the basics of Yaw Moment Diagrams and letting me add to his suspension YMD MATLAB code to calculate the YMD for the whole car.

To my family for their continual support during this research project and also helping me by p[roof reading my report to see if I missed any mistakes.

Table of Contents

List of Figures:

List of Tables:

Nomenclature

a	Acceleration	m/s^2
CoG	Centre of Gravity	m
F	Force	kg
Lt	Load transfer	kg
h	CoG in z direction (height)	m
μ	Tyre friction coefficient	
N	Number of teeth on a gear	
GR	Gear ratio	
η	Efficiency	
P	Power	kW
T	Torque	NM
n	Angular velocity	Revolutions per minute (RPM)
ω	Angular velocity	Rad/s
m	Mass	kg
L	Length	m
r	Radius	m
tw	Track width	m
d	Distance	m
Diff%	Differential locking percentage	

Subscripts

X	longitudinal
Y	lateral
Z	vertical
R	rear
F	front
d	dynamic
1	input
2	output
T	traction
i	inside
o	outside
e	effective

1. Introduction

Every year SAE International organise an international design competition to design and race a formula style race car. The competition had over 600 universities compete in 2018 at 10 different competition locations. The car must be designed and built by students at the university and all cars competing must meet the design rules.

At the competition, the car will be judged in both dynamic and static events. The dynamic part consists of 4 events: skid-pad, acceleration, autocross and endurance. There are also 3 static events which are the Presentation, the Engineering design and the Cost analysis. The scoring criteria is outlined in the FSAE rules each year (Figure 1).

Static Events:		
	Presentation	75
	Engineering Design	150
	Cost Analysis	100
Dynamic Events		
	Acceleration	100
	Skid-Pad	75
	Autocross	125
	Efficiency	100
	Endurance	275
Total Points		1,000

Figure 1: Scoring criteria from the 2020 FSAE rulebook

The University of Waikato participates in the Australasian competition, which is held in Australasia competition held in Australia at Winton Motor Raceway (Figure 2).

Figure 2: Winton Motor Raceway

The dynamic events are based on the performance of the car while racing. The acceleration event measures the cars straight line acceleration from a stop. The autocross event measures the cars overall performance on a timed lap of the course. The endurance testing evaluates a formula student cars performance over multiple laps usually 9 -12 laps per driver (18-24 total) depending on the length of the track. The endurance event evaluates the cars overall speed as well as the reliability of the car. To do well overall in the dynamic event the WESMO (Waikato Engineering Student Motorsport Organization) car will have to be well designed with constant referral to previous research as well as thorough research into the tuning of the car once the car is complete. Having a well-designed drivetrain will result in a fast-accelerating car, which is also efficient and will also work in well with the various other aspects of the car, especially suspension. Having these characteristics is vital to the car doing well in the dynamic events.

The static events involve the car being judged based on how well the car was designed, whether good engineering practices were used during the design and manufacturing process, as well as how innovative the design is. The team members are also tested in their knowledge of the engineering principles that were used in the design process of the car. The members are also assessed on the reasoning behind any design choices and an in-depth budget analysis of the design and manufacturing process is also required.

1.1.1. WESMO:

The University of Waikato's Formula SAE team is called WESMO and each year WESMO design, build and race a car in the formula student race series (Figure 3). WESMO enters the internal combustion section of the competition. The last WESMO team to manufacture a car and compete in the competition was the 2018 WESMO team. The 2018 team ended up getting 12th in the Australasian completion which placed WESMO 112th in the world.
It was established that the 2018 cars drivetrain was geared too low. Drivers were required to shift gears too often during the dynamic evets. This frequent gear shifting had a negative effect on the performance of the car, especially in the acceleration event where the car has to accelerate hard from a standing start. If the gearing on the WESMO car can be improved the car could be expected to perform better and place higher in formula student race series.

Figure 3: W-FS-17 testing

1.1.2. Automotive drivetrains

Most modern vehicles use an internal combustion engine to produce the power required to propel the vehicle forward. In a modern internal combustion engine, the kinetic energy needed to move the car comes from combusting hydrocarbons. This works by combusting the fuel in a sealed cylinder and having the expanding pressure exert force on a piston which will be forced away from the explosion in an effort to try decrease the pressure created from the explosion. This piston is then connected to a crankshaft which turns the linear kinetic energy of the moving piston into rotational kinetic energy. This process has a limited range in which it produces power efficiently as the motor can only produce energy while the piston is being forced out. If the rotational speed of the engine is too low limited power is produced due to the increased periods between fuel combustion, but if the rotational speed gets too high, the engine will fail due to the increased stresses exerted in the various parts of the engine. This small optimum range is the reason why all internal combustion engines use multi-gear transmissions so that the torque and rotational speed from the engine can be manipulated to ensure that the engine works efficiently over a vast range of speeds. After the torque from the engine has been compounded via a gear box, the torque then gets transmitted either via a chain and sprockets, or by a driveshaft to the differential.

If the torque is transmitted via a driveshaft to the differential, the differential then has another gear reduction, while also allowing the left and right wheels to turn independently while turning a corner. If the torque is transmitted via a chain the reduction happens during the transmission and the differential just allows each wheel to be able to turn independently while cornering. The torque from the differential is then transferred down each half shaft to the wheels where that torque is then turned back to a linear force.

The car that WESMO is presently using for testing as well as using as the base for future design is the W-FS-18 car. This car uses a KTM Duke 690R motorbike engine along with a Drexler formula student 2010 limited slip differential and Hoosier formula student 18x6-10 R25B Tyres. The 690R engine has an internal 6 speed sequential gear box with a hydraulic clutch. The Drexler formula student 2010 limited slip differential is a 1.5-Way limited slip differential (LSD) meaning that the accelerating and decelerating ramp angles are different. There are 3 ramp angle options to allow tuning of the differential for different applications. The 3 different settings in terms of the ramp angles are, 40º/50º, 45º/60º, 30º/45º with the first smaller ramp angle being the acceleration ramp angle and the second larger angle being the deceleration ramp angle.
If a drivetrain is well designed and optimised for the car it will result in a fast accelerating and efficient car that will be easy to drive and have the potential to do well in the formula student dynamic events .

1.1.3. Problem statement:

In 2017 and 2018, the last two years which WESMO went to competition, the WESMO car has had problems with the selected gear ratio of the drivetrain. This problem usually occurs due to the gear ratio being selected without thorough research and the limited previous research that has been done on optimising the gear ratio has purely been on trying to optimise the gear ratio for maximum longitudinal acceleration. Little to no research has been put into the effect the gear ratio will have on the car during cornering. This was very apparent with the 2018 car as all the drivers complained that the gearing was too short (gears to tightly spaced) and that the drivers were having to change gears too often.
Acceleration has previously been the primary focus as it has the greatest potential for performance increase, as well as being quick and easy enough to produce the required justification needed for the formula student competition. The literature review completed for this project found that there are many different aspects, not just acceleration to consider when selecting a final drive gear ratio. The aim of the current project is to optimise the final drive gear ratio so that the car accelerates as fast as possible while also having the gear ratio and differential setting optimised for the autocross/endurance track.

In previous years there has also been no research into how the ramp angle of the differential effects the handling and performance of the car and the selection process was usually to just use the same settings as the previous year’s WESMO team. The 2018 car had the differential ramp angle on the shallowest ramp angle setting, this means that the differential was running

with high locking percentages. The high locking percentages was one of the likely contributing factors as the why the 2018 car had difficulty making the minimum radius corner of 4.5m and was prone to understeer on low-speed corners.

This research will be carried out by using Excel and MATLAB for theoretical modelling, and Solidworks for the design modelling as well as doing testing on the W-FS-18 car. Both the theoretical and experimental data will be compared to ensure both sets of data are valid.

1.1.4. Objectives:

The main objective of this thesis is to research into potential modifications that could be applied to the new WESMO cars to enable the car to win future acceleration events. To win the acceleration event in 2019 (the last competition before the Covid19 Pandemic) the WESMO car would have had to complete the 75m standing start sprint in under 3.8 seconds. The most recent WESMO formula student car (W-FS-18) completed the acceleration run in 4.3 seconds.
To achieve this objective a formula student car has to optimise power production, design the car to maintain traction, as well as having efficient torque transfer from the engine to the wheels.

The second objective of this thesis is to look into the effects the drivetrain design and tuning have on the cornering performance of the car in the autocross event. This will primarily look into matching the gear ratio of the drivetrain to the layout of the autocross track as well as assessing the impact of changing the differential settings on the handling characteristics of a formula student race car.

A further objective is to determine if selecting new tyre dimensions could increase the performance of the car during the acceleration run as well as estimating the longitudinal performance of the 16in Hoosier tyres.

The final objective is to research into how reducing the weight of the drivetrain could benefit the overall performance of future WESMO cars and research into potential ways of achieving this weight reduction.

1.1.5. Thesis Structure

Chapter one introduces the research topics along with the purpose of the research and the potential outcome and relevancy of the results are also briefly introduced.

Chapter two introduces all the basic principles and general knowledge required to be able to understand the rest of the report. Relevant literature will be used to aid in the development and justifications of the process and approaches used. From this it also introduces some of the underpinning equations that were used in the theoretical calculations in chapter four.

The general methodology of the track testing including further review of any previous relevant research done around the specific car being used for the testing is covered in Chapter three.

Theoretical and track based experimental results are presented in chapter four. A comparison between the two results is completed to demonstrate acceptable agreement between the two.

Conclusions which are drawn from key results are presented in Chapter five. Interdependences between different results are highlighted and a proposal of how these results could be used by future WESMO teams to improve the design and performance of their car is presented.

2. Literature review

2.1. Gear ratios:

The three useful outputs of an engine are torque, rotational speed and power. “Torque, is typically not constant throughout a transmission system. Remember that power equals the product of torque and speed” (Budynas & Nisbett, 2005) (Equation (2.1).

Having the rotational speed drop across a drivetrain can be beneficial, this reduction of rotational speed will result in the torque increasing by the same factor that the rotational speed decreased by. “With a constant power, a gear ratio to decrease the angular velocity will simultaneously increase torque.” (Budynas & Nisbett, 2005)

This drop in speed is measured by the ratio of the speed at the input compared to the output and is given the term “gear ratio” (Equation (2.2)(2.1). A transmission with adjustable gear ratios is needed with an internal combustion engine, due to internal combustion engines having varied power and torque depending on the RPM of the engine. As internal combustion engines do not produce much torque, or power at low RPM, operating an engine in this range will not provide high torque or power and so will not greatly accelerate the car. To remedy this and operate at a more optimum RPM a large gear ratio can be used to compound the torque from the engine, resulting in a large longitudinal thrust provided at the wheels.

$$P_{out} = T_1 * \omega_1 * \eta \tag{2.1}$$

$$Gr = \frac{T_{in}}{T_{out}} = \frac{N_{in}}{N_{out}} \tag{2.2}$$

2.1.1. Final drive:

The final drive ratio is the ratio of the engine output rotational speed (post transmission) to the wheels rotational speed. The selection of the final drive gear ratio will change depending on the application of the drivetrain. In the case of the formula student competition where acceleration is key, the final drive ratios are usually picked for high torque rather than a high top-speed. The final drive ratio also depends largely on whether a car is power limited, or traction limited in acceleration.

There are multiple ways to implement this final drive gear ratio change. The design depends on the application of the car. The final drive is usually the easiest way to change the gear ratios- this is especially the case when designing a car with a motorbike engine as is proposed with the WESMO project.

Chain final drive:

Chain and sprocket design are commonly used as the final drive on motorbikes. Chain final drives have a sprocket with a specific number of teeth on the engine output shaft and a sprocket with a specific number of teeth on the axle (the axle sprocket always has considerably more teeth than the engine sprocket). The final drive ratio is the number of teeth on the axle sprocket divided by the number of teeth on the engine sprocket.
The chain needs to be lubricated occasionally to avoid the resulting decrease in efficiency that comes from an unlubricated chain.
As it is almost certain the WESMO car will use a motorbike engine for the powertrain along with a limited slip differential, this is the more viable of the two final drive designs.

Shaft and differential final drive:

Almost all modern cars use a driveshaft and differential to transport the torque to the axle. The torque transported down the driveshaft is usually low and the driveshaft spins at high RPM. The differential is where the final drive gear ratio increase occurs. This is done to reduce the stress on the driveshaft. The differential in this design usually has a gear ratio of anywhere from 2-4. As the engine used is going to be a motorbike engine this drivetrain/ final drive design is not practical for use in the WESMO car.

2.1.2. Tall versus short gear ratios:

The terms commonly given to drivetrains that do not have optimised gear ratios to suit the application or the car are called “tall” for transmissions with gear ratios too low, and “short” for transmissions with gear ratios too high. Having a tall gear box will result in less acceleration but a greater top speed due to the ratio of the input gear to the output gear being lower meaning that the torque is not increased or compounded much. This also means that the output rotational speed is not decreased which is why the top speed is higher.
A short gear ratio means the transmission will accelerate fast due to the torque from the engine being increased or compounded greatly. The rotational speed of the output will decrease greatly, as a consequence the car will have a low top speed. This quick acceleration and low top speed will mean that the driver will have to change gears often. If a car is power limited the gear ratio selected will often be on the low, or shorter side whereas with a traction limited car the gear selection will tend to the slightly longer, or tall side.

2.2. Transmissions:

2.2.1. General overview on transmissions:

Internal combustion reciprocating engines create power via torque and angular speed. This power gets transferred to the wheels through a gearbox which can adjust the gear ratio of the drivetrain to either under or overdrive depending on the torque requirements as well as the speed of the vehicle. (Heilsler, 2002)

Car transmissions are vital to the overall function of a car as they allow an internal combustion engine to accelerate from low to high speeds while almost constantly enabling the engine to be around its optimum power range. The idea behind a transmission is that in each gear the torque provided will vary depending on the RPM of the engine (Figure 4), the torque tends to increase with the RPM but as the engine nears its maximum RPM the gear ratio needs to change to allow higher rotational output speed, to enable the car to continue acceleration. This increase in rotational speed will decrease the torque at the wheels.

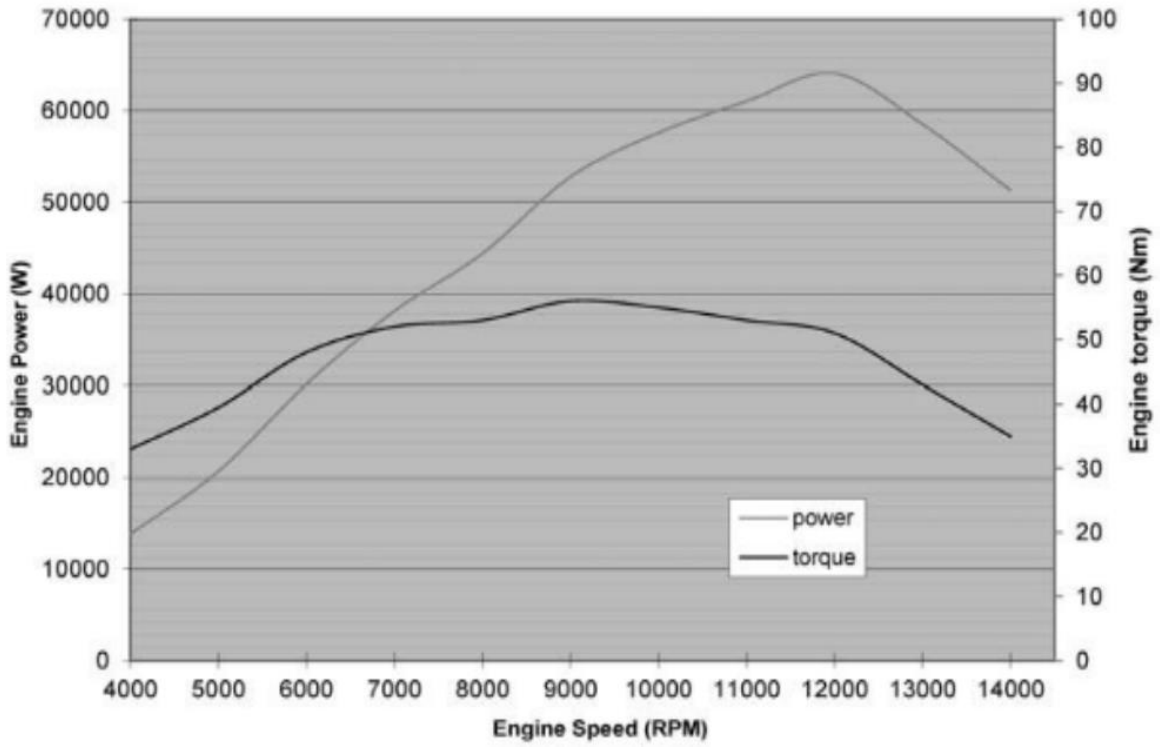

Figure 4: Typical power and torque curve – 600cc restricted motorcycle engine (Seward, 2014)

There are many different styles of transmission used depending on the application of the transmission. The most used transmission in modern cars is an automatic planetary gearbox, but these are not well suited in the motorsport environment as they have a relatively slow shift time, a low efficiency at around 86% and high rotational inertia. In premier motorsport

such as formula one, world rally championship or the various touring car championships either a sequential or a dual clutch transmission are used due to their fast shifting times, whereas a manual transmission is usually used in lower budget race series like the 24 hours of lemons endurance race, or formula ford. In the transmission of an internal combustion engine, the gear ratios in a transmission have a larger gear ratio when in the lowest gears, with first being the largest. The gear ratios gradually decrease with each higher gear until the transmission reaches the top gear, which has the smallest gear ratio of all the gears.
Though all the different transmissions go about changing gears differently, they all follow the same 5 fundamental steps (Figure 5). The different transmission types are explained below.

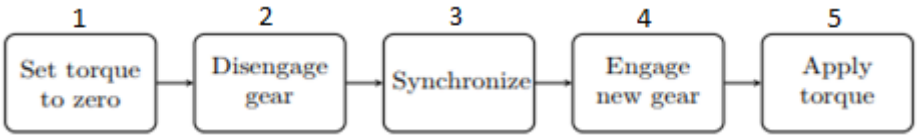

Figure 5: The 5 steps of a transmission shift sequence (Bergman & Byrhult, 2009)

2.2.2. Manual transmission:

A synchromesh manual transmission is the simplest type of transmission, it relies on the driver instead of automation, to engage the clutch and shift the gear lever to the selected gear. Synchromesh manual transmissions consist of two shafts with multiple pairs of interlocked gears of which one is locked to a shaft and the other is freely spinning. To stop the torque from being transmitted through the gear box, the driver then applies the clutch lever/pedal which causes the clutch to disengage, resulting in no torque from the engine reaching the gear box (refer to step 1 Figure 5), once the clutch is fully applied the driver moves the gear lever from the current gear into neutral disengaging the old gear (step 2 Figure 5). The driver then selects a new gear, and the corresponding previously freely spinning gear has a synchroniser pushed up against it gradually locking it to the second shaft (step 3 Figure 5). Once the synchronisation is complete the new gear is engaged (step 4 Figure 5). The clutch can now be slowly released to gradually allow torque through the engine again (step 5 Figure 5) completing the gear change. Manual transmissions are the cheapest and one of the lightest designs of gearbox as they do not need any complicated computers or systems to automatically change gears. They also have the advantage of allowing the driver to skip over gears when changing, which in normal life can be useful but is not very useful in motorsport. The shifting time of a manual car is very dependent on the skill of the driver, with an average shift time of between 0.5 to 1 second (500 – 1000ms) to change gears. A highly skilled driver

could potentially get lower than this but not by much, so manual transmission are inherently slow when compared to other types of transmissions. Due to their design, manual transmissions typically have an efficiency of around 97%.

2.2.3. Sequential manual transmissions:

Sequential gearboxes or variants of, are the main type of transmission used in race cars and motorbikes. Sequential gearboxes are ideal for these applications as they have quick shifting times, are lightweight and often only require the clutch to be used in first gear. Sequential gears can only move up or down one gear at a time and use a dog clutch to lock the gear to the shaft. A dog clutch is made up of two pairs of teeth one on the gear (Figure 6) and the other on the shaft. When the gear is not selected those two teeth are not in contact so can rotate freely. When a gear is engaged those two teeth get pushed together and catch on each other. When sequential gearboxes shift gear, the gear change is quick, with some taking roughly 100ms to change. The shifting of a sequential gearbox is very sudden and creates greater jerk (m/s^3) than most other types of transmission. This is why sequential gearboxes are only used in motorsport applications. As all WESMO cars in the near future will have the KTM Duke 690R engine which has a sequential gearbox and hydraulically activated clutch already built into the engine, a sequential gear box is the type of transmission that will be used.

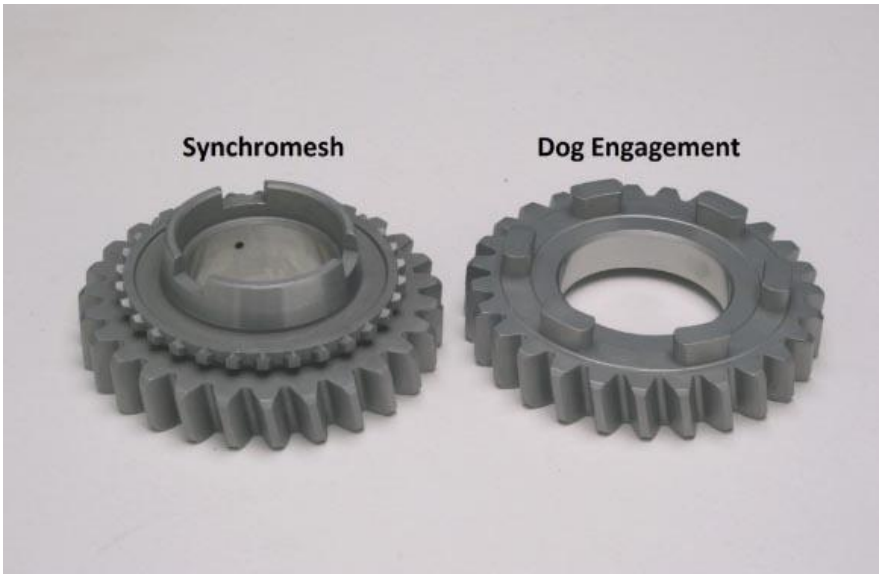

Figure 6: Synchromesh vs dog gear engagement

2.2.4. Dual clutch transmission (DCT):

The dual clutch transmission (DCT) works much like a manual transmission, except that the clutch engagement is automated. DCT transmissions have two different sized clutches usually in a concentric arrangement; the smaller clutch is used for odd gears and the larger one for even gears. DCT's can effectively change gears without interrupting the torque supply to the wheels; the odd gear is supplying the torque to the wheels while the even gears synchronise and engage and vice versa. When the gear needs to be changed, the gear box simultaneously engages one clutch while the other disengages. This results in a smoother gear change than other types of transmissions. DCT's change gears very quickly, an example is the Mercedes Benz SLS AMG's dual clutch gearbox where gear changes can be as quick as 100ms. Although DCT's can change gears fast, they are often considerably heavier and bulkier than other transmission types, limiting their usefulness in FSAE as weight and compactness are vital attributes.

2.2.5. Continually various transmission (CVT):

Continually varying transmission (CVT's) are very different from other mechanical types of gear boxes in that they do not have a fixed number of gears. CVT's work by having a fixed input rotational speed and constantly changing the output rotational speed. This is done by having a V-shaped belt and conical pulleys that can have their width varied on demand. When the pulleys are very wide, the belt is pulled radially inwards and when the pulleys width are thin, the pulleys get forced radially outwards. The gear ratio is changed by changing the effective radius of the pulleys on the input and output shafts. If the belt is forced inwards on the input shaft and outwards on the output shaft, the resulting gear ratio will be high and as the pulleys gradually switch in terms of effective radius (Figure 7), the gear ratio will gradually decrease. CVT's are not generally used in motorsport as they do not work well with high torque inputs and they are generally much less efficient than other designs of transmission, with the efficiency being approximately 88%.

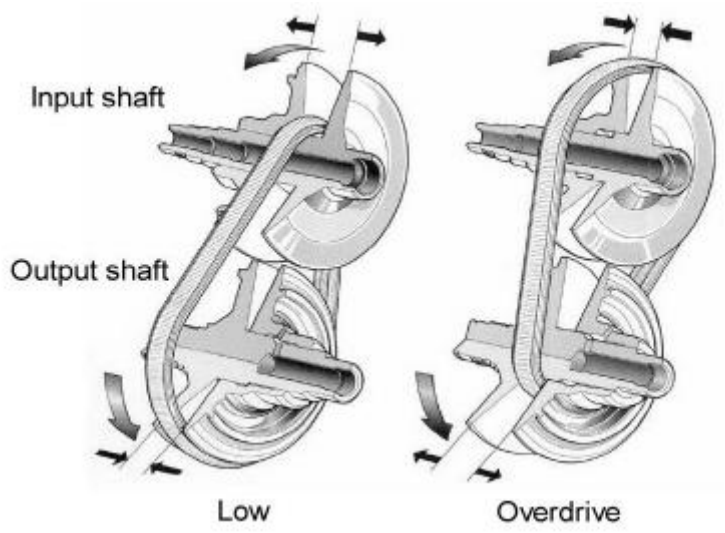

Figure 7: Continually various transmission diagram (Lechner & Naunheimer, 1999)

2.3. Traction:

The overall traction of the wheels is dependent on the tyres, the downforce and the suspension setup. Each of these variables can be manipulated so that the car has maximum traction forces, resulting in the car being fast at competition as well as being a predictable and easy car to drive.

2.3.1. Tyres:

Contact patch basics

When loaded a tyre will deflect vertically which results in the portion of the tyre that is in contact with the road matching the contour of the road as opposed to the round shape when unloaded. This flat region of the tyre which is in contact with the road is the contact patch. Since there is a vertical deflection the radius of the tyre at the contact patch will be smaller than the radius of the wheel. This new radius is called the effective radius of the tyre
Since the loading on each tyre is constantly changing due to the load transfer that constantly occurs during racing the instantaneous contact patch and effective radius is constantly changing as it depends on the downforce applied to each tyre.

The area of the contact patch has quite a large effect on the overall grip of the tyre, according to James Balkwill “Imagine the contact patch as a matrix of discrete elements. A wider tyre reduces the contact pressure at each element for a given vehicle weight which increases the coefficient of friction. With this, each element of the tyre is able to generate a slightly lower force, but this balance is outweighed by the presence of a larger number of elements (contact

area). The effect is a net increase in tyre grip. This also explains why motorsport often uses the largest tyres possible in the search for performance.” (Balkwill, 2018)

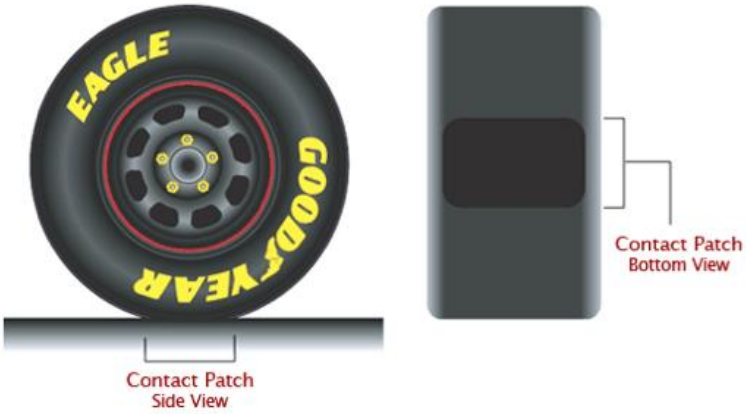

Figure 8: Visual representation of a tyres contact patch (TIRES-EASY, 2012)

In terms of the coefficient of friction (CoF), usually the only factors that affect the friction force are the friction coefficient of the interaction between the two materials as well as the normal force. Though this is always true in linear materials i.e., metals ceramics, this is only true in low stress cases in non-linear materials. As tyres are manufactured from rubber which is a non-linear material when the rubber of the contact patch rubber is exposed to the stresses generated while racing the properties change. If the downforce and traction force on the tyre are kept constant the stress of the rubber at the contact patch is inversely proportional to the contact patch area (Figure 8, Equation(2.3)**Error! Reference source not found.**.

$$\sigma = \frac{F}{A} \tag{2.3}$$

Traction force generation

There are two stress mechanisms that create the traction of a tyre. The first mechanism is adhesion which is where the rubber of the tyre forms intermolecular (Van der Waals) bonds with the road surface. These bonds will hold the rubber to the road surface resulting in traction when a torque is applied to the wheel. When the torque applied to the wheel becomes too high those intermolecular bonds start breaking and the rubber at the contact patch starts deforming (Figure 9**Error! Reference source not found.**).

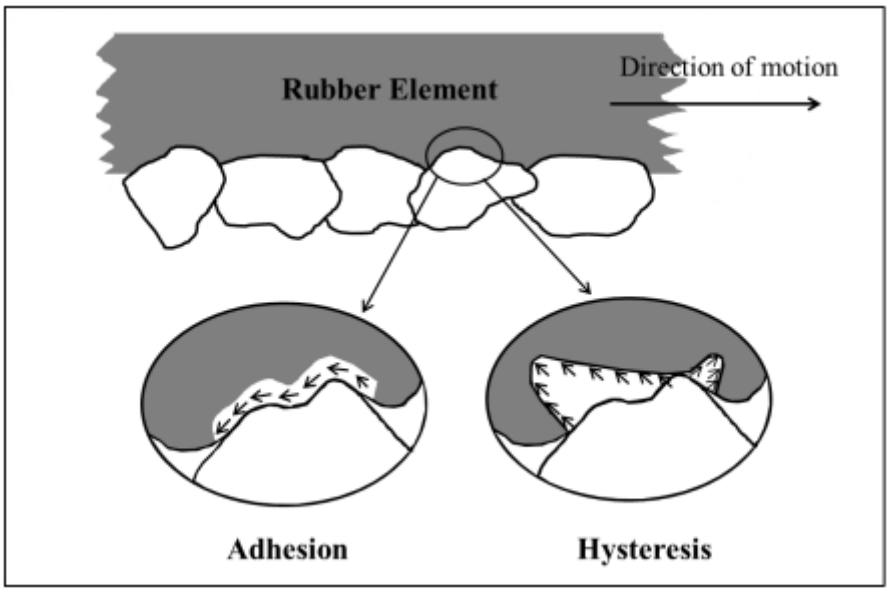

Figure 9: Adhesion vs "hysteresis" of a tyre (Flintsch, McGhee, EIzeppi, & Najafi, 2012)

When adhesion breaks down and the rubber separates from the road, this is technically not hysteresis and has been mislabelled in Figure 9, as the hysteretic property of rubber is most relevant to the force generated from indentation rather than adhesion.

Hysteresis is a property of non-linear materials. Hysteresis is when during the loading of a material, the displacement and strain of that material will be different when being loaded vs when compared with being unloaded (Figure 10). When adhesion breaks down it is not called hysteresis even though hysteresis will still occur due to the effective unloading of the adhesion force.

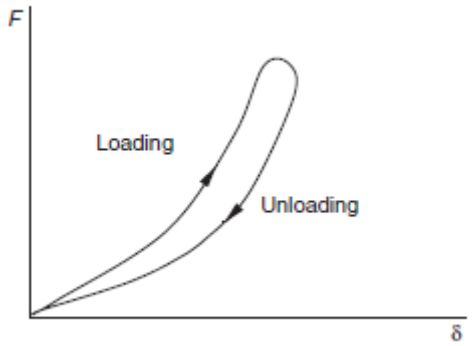

Figure 10: Hysteresis in polymers (Blundell & Harty, 2004)

The second phenomena is Indentation which is sometimes also referred to as hysteresis due to the force being generated by the rubber at the contact patch undergoing hysteresis.

Indentation is where the rubber deforms to match the shape of the road, however due to the

non-linear properties of rubber it does not immediately return and will have different displacements for loading and unloading. This phenomenon is called hysteresis and causes a reaction force which resists slippage and generates traction (Figure 11).

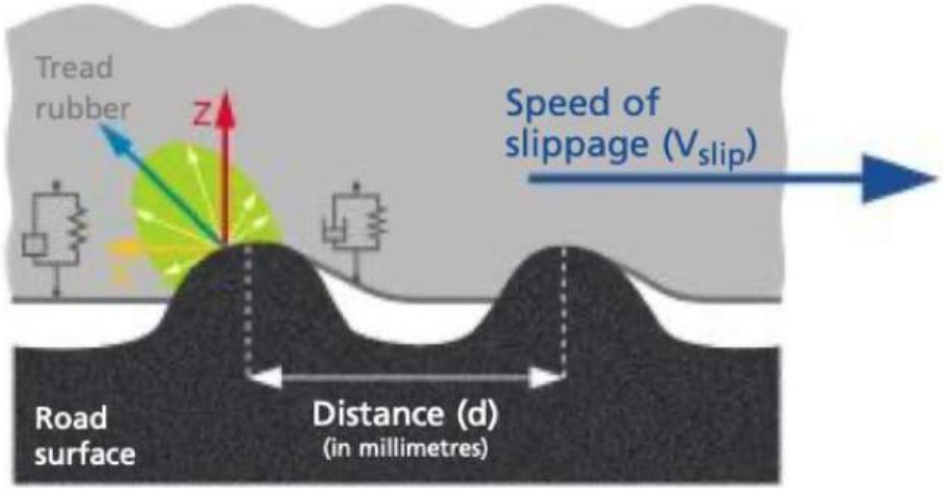

Figure 11: Tyre indentation traction generation (Société de Technologie Michelin, 2001)

How the contact patch effects tyre properties

The area of the contact patch of a tyre mainly depends on two variables, the first is the tyre construction and the second is inflation pressure. The reason the construction of the tyre has a large effect on the area of the contact patch is due to changing factors such as the sidewall size, sidewall thickness and the tread thickness which will affect the overall spring rate (stiffness) of the tyre. Having a larger stiffness results in less tyre deflection under loading and thus affects the rate at which the contact patch changes under load

Tyre inflation pressure also has an effect on the spring rate of the tyre, but under normal operating pressure ranges it has less effect than the tyre construction. In terms of formula student tyres, the internal pressure will always be optimised for the tyre, initially based on tyre data and later verified with testing. Most of the change in overall traction due to changing pressures comes from the altering of the contact patch shape and pressure distribution rather than the change in spring rates. Having the tyre pressure to low will result in a concave contact patch profile. This is due to the inflation pressure being to low so that the force the centre of the tyre is less than the force at the outside edges of the contact patch results in a less pressure on the centre of the contact patch. Having the pressure to high will result in a convex contact patch profile due to the internal pressure forcing the centre of the

tyre outwards resulting in more pressure on the centre of the contact patch, and less pressure on the outside edges of the contact patch (Figure 12).

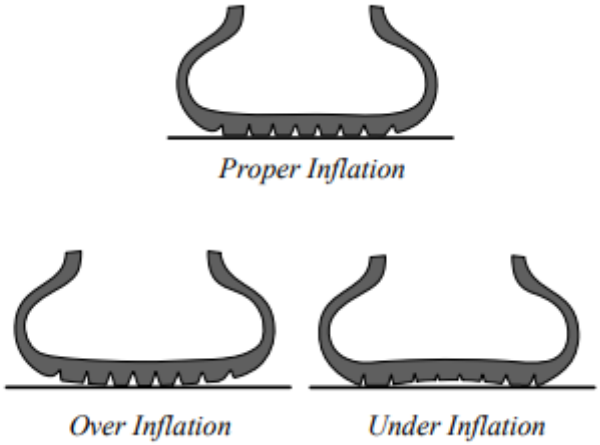

Figure 12: How tyre inflation effects the contact patch (Jazar, 2008)

The pressure distribution of the contact patch also effects the thermal properties of the tyre. Having a slightly overinflated tyre creates more heat in the tyre when compared to an underinflated tyre. This happens as when the tyre is overinflated the centre of the tyre bows out, meaning heat gets applied to the centre of the tyre and disperses outwards across the contact patch. With underinflated tyres the outside edges of the contact patch produce heat and thus some of that heat gets dispersed to the sidewall of the tyre rather than the contact patch. This is the other main consideration when selecting tyre pressures as the overall coefficient of friction of a tyre is very dependent on temperature (Figure 13).

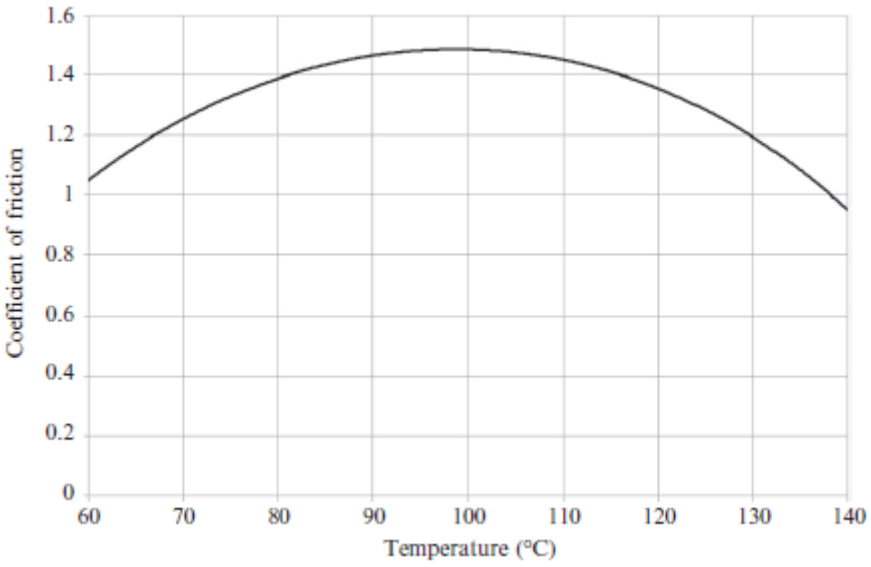

Figure 13: Tyre traction coefficient vs temperature (Balkwill, 2018)

The tyre pressure has a large effect on the overall properties of as tyre. Having the tyres correctly inflated is vital to ensure optimum performance of the tyre.

Longitudinal considerations

A tyre needs to have a portion of the contact patch undergoing slip to be able to produce longitudinal traction forces. This happens because the tyre deforms under longitudinal load or thrust provided by the tyre. This deformation only happens on the contact patch area of the tyre as the tyre is sticking to the road. The remainder of the tyre which is not in contact with the road does not deform. In the area in between the deformed contact patch and the rest of the tyre, the tyre will slip and gradually return to the original position/shape.
When a moment is applied to the tyre, the tyre deforms causing a slanted alignment as opposed to the undeflected radial alignment (Figure 14). This radial defection results in the tyre having slip ratio. According to James Balkwill "The slip ratio involves the ratio of forward velocity to the velocity of a point on the surface of the tyre at the effective rolling radius." (Balkwill, 2018)

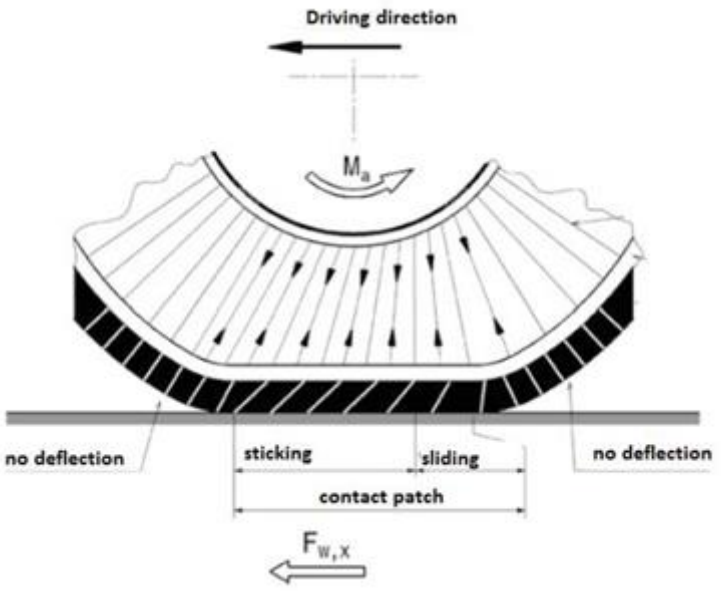

Figure 14: Tyre deformation under acceleration

For example, at a slip ratio of 0.05, the wheel is moving at 1.05 times the speed of the vehicle. The slip ratio is always positive under acceleration, negative under braking, and zero when the tyre is free rolling. As the slip ratio or slippage rate continues to increase, the slip ratio will eventually reach a point where the peak traction force is generated and after this

point the traction decreases sharply, this happens as the tyre is transferring from a static coefficient of friction to a dynamic or kinetic coefficient of friction (Figure 15).

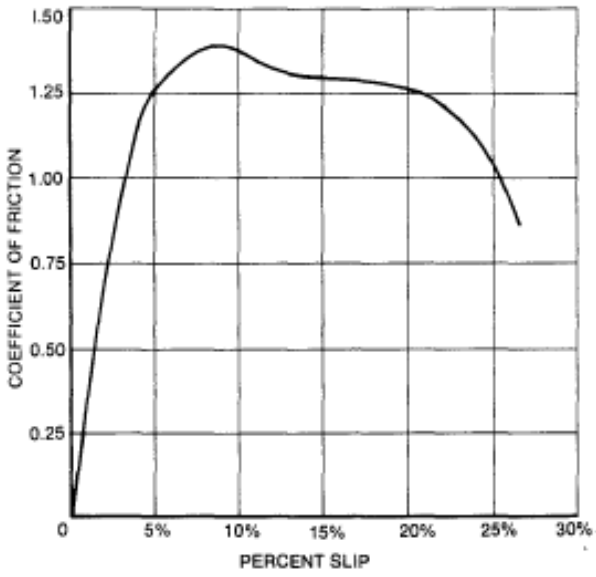

Figure 15: Tyre coefficient of friction vs percent slip (Smith, 1978)

Lateral considerations

Much like for longitudinal traction for a tyre to produce lateral load the tyre needs to undergo slip in the form of a slip angle. A slip angle is a difference in angle (in degrees) between the direction of travel of the tyre and the direction the tyre is pointing (Figure 16). The slip angle is often measured in the form of cornering stiffness which is the lateral force generated per degree of slip. Racing tyres typically have a high cornering stiffness value because they are constructed out of a soft rubber compound.

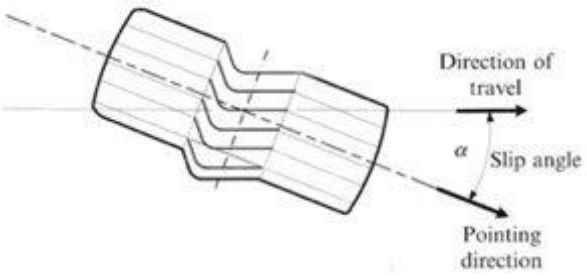

Figure 16: Slip angle of a tyre (Balkwill, 2018)

The slip angle is much like a slip ratio where, as the slip angle increases so does the lateral force but at a certain slip angle the lateral force will start to decrease. The section of the slip vs lateral force graph where the slip angle is greater than the optimum angle is called the

frictional zone due to the coefficient of friction transitioning from static to dynamic (Figure 17).

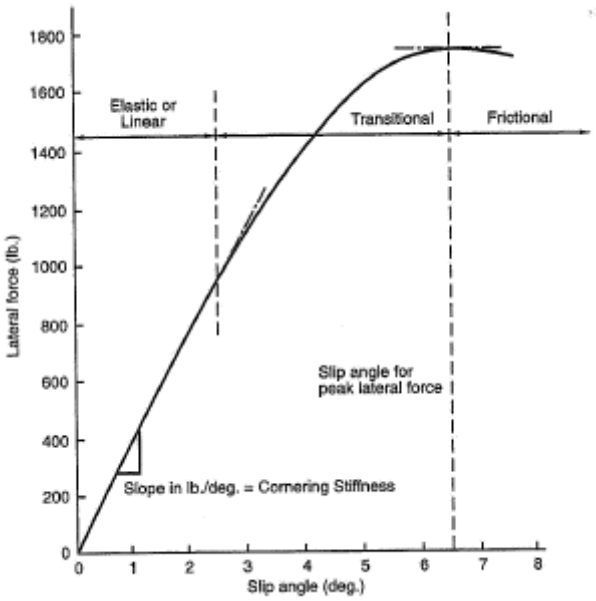

Figure 17: Slip angler vs lateral traction force (Milliken & Milliken, 1995)

Combined traction

A tyres traction can be analysed in terms of either lateral or longitudinal traction, but in most cases while racing there will be a combination of both. When a tyre is exposed to a combined load, increasing the load in one direction causes the available traction in the other direction to decrease. The maximum combined force of a tyre is given by generating a traction circle which shows the maximum combined traction that a tyre can produce.(Figure 18) (Equation (2.4).

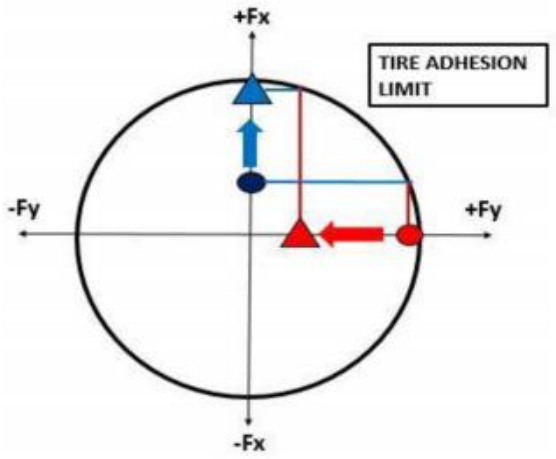

Figure 18: traction circle for a tyre (Kolte, Srinivasan, & Srikrishna, 2016)

$$F_{Tot} = \sqrt{{F_x}^2 + {F_y}^2} \tag{2.4}$$

2.3.2. Tyre testing consortium

The design of modern race cars is very reliant on having accurate and comprehensive data on the performance of the tyres. This data is important as the design of most of the car will be based on the loads which the tyres can withstand and the force which can be produced from the interaction between the tyre and the road, in the form of longitudinal and lateral forces. To determine the forces the tyres can produce the tyre data from the tyre testing consortium is referred to. The tyre testing consortium is a standardised database that has all the data for the most commonly used formula student tyres. The tyre test involves testing each tyre being analysed on a rolling road (Figure 19). Each tyre design is put through three separate tests while on the rolling road. The first two are lateral tests, with the first having constant tyre pressure and having the slip angle varied from +12° to -12°, and the second having constant slip angle, but varying the tyre pressure and camber, or inclination angle Figure 31: Visualisation of camber on a vehicle (Figure 31**Error! Reference source not found.**). The third test is the longitudinal tyre test. The longitudinal test involves accelerating and braking the tyre while on the rolling road. While each of the tests are being conducted the tyre testing machine records everything from the reaction forces in each direction, the pressure inside the tyre, and the temperature of the tyre.

Figure 19: tyre testing machine (Kasprazk & Genz, 2006)

The tyre data is not only used for the design of the car but also the tuning of the car, for example the tyre pressures that are used on race day are based on which pressure gave the optimal performance in the tyre data tests.

The coefficient of friction (traction coefficient) of a tyre is the ratio of how much traction force a tyre can produce per unit of downforce. If a tyre has a traction coefficient of 1.6, this means it can apply 1.6 times more traction force than the downforce applied to it. A tyre will have different traction coefficients for lateral force generation and longitudinal force generation, so each tyre will have both a lateral and longitudinal traction coefficient. Though the coefficient of friction is effectively just a normalized traction force, the traction coefficient is slightly dependent on the downforce and decreases as the downforce on the tyre increases (Figure 20). This means that as the downforce on the tyre increases, the overall traction forces the tyre can provide will increase but the gains in traction diminish as the downforce increases.

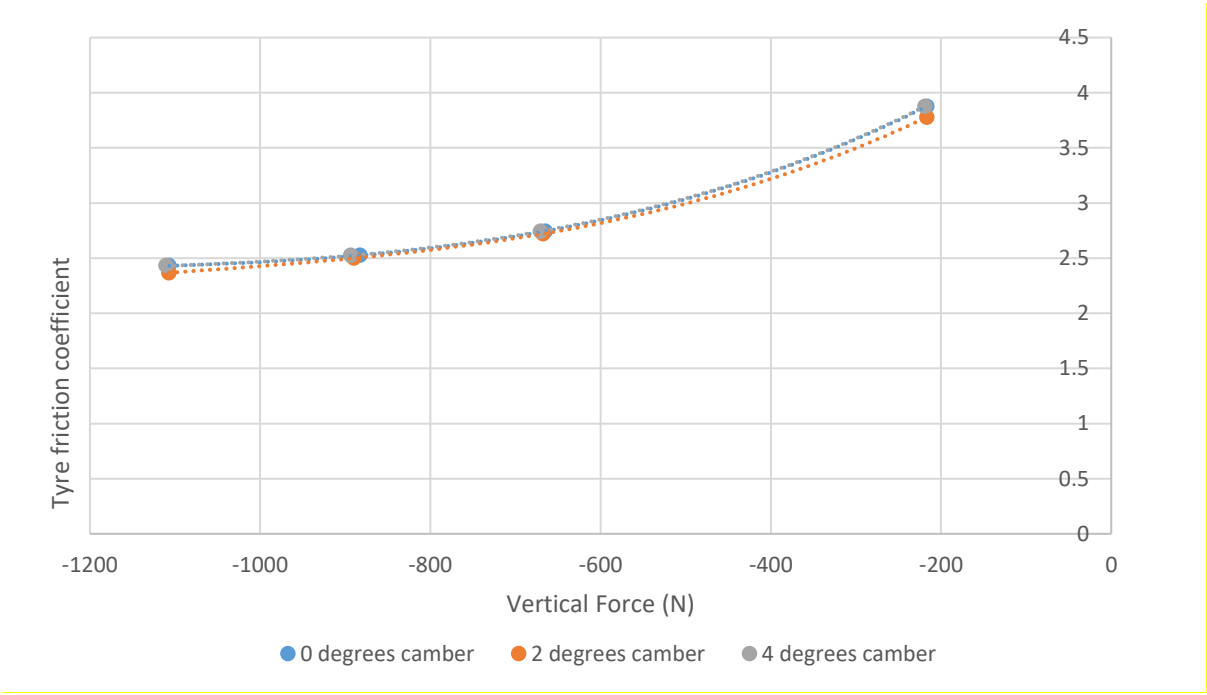

Figure 20: Tyre friction coefficient vs downforce for W-FS-18 tyres

As a tyre has a load applied to it the effective radius of the tyre will decrease due to the deflection of the tyre at the contact patch. The change in the effective rolling radius of the tyre will depend on the design of the tyre.

The two main types of tyre are radial and bias ply. Radial tyres have steel belts that are orientated 90 degrees to the direction of travel while bias ply most commonly have steel and nylon belts that have a 30-45 degree offset from the direction of travel (Figure 21).

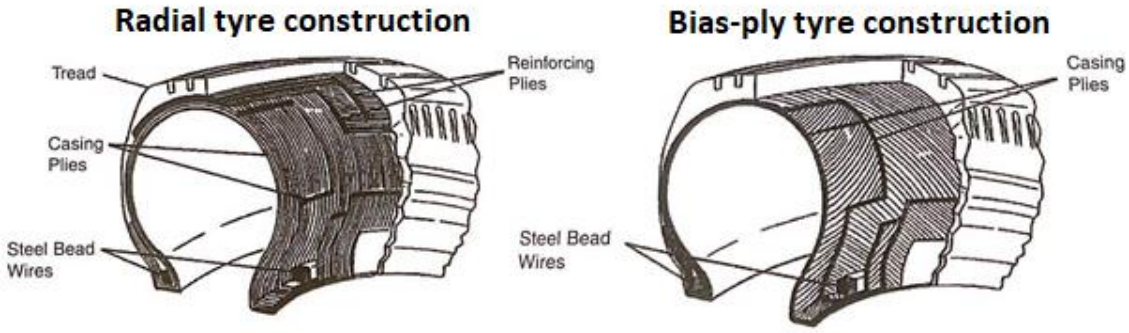

Figure 21: Radial vs bias ply tyre construction (Stone & Ball, 2004)

The effective rolling radius of a radial tyre does not change as much as bias-ply tyres due to how the steel belts react under loads. The deflection of bias ply tyres is large enough that the change in radius will need to be factored in to calculations in this report (2.5) As the Hoosier tyres WESMO currently use as well as the potential tyres that might be used in by future WESMO teams are also bias ply, the effective rolling radius will change with load and will need to be considered.

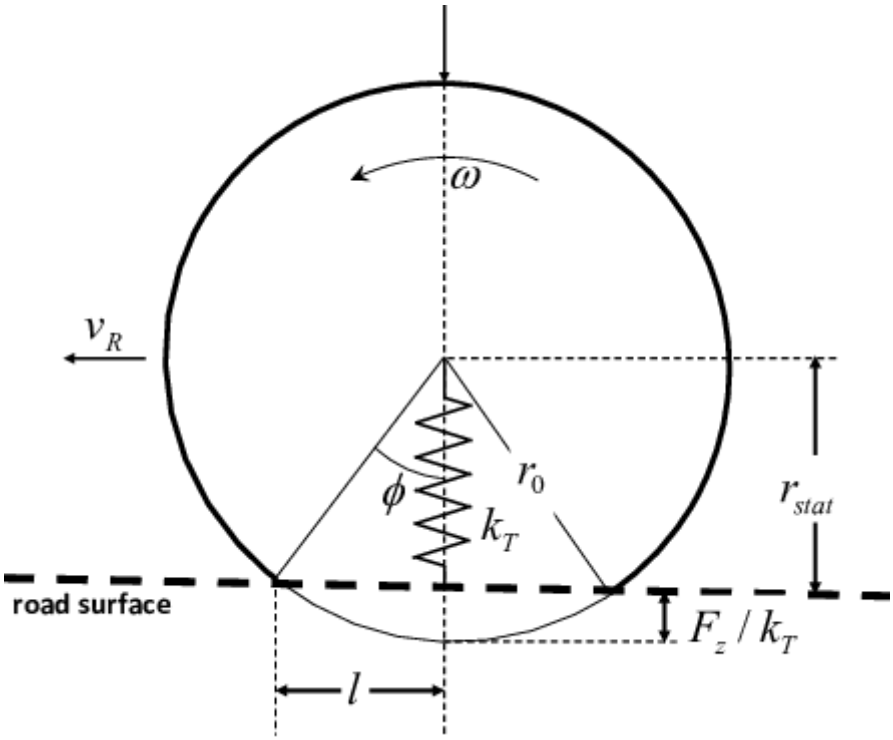

Figure 22: Effective rolling radius (Hoseinnezhad, 2011)

$$F_z = K_t * \Delta r \tag{2.5}$$

2.3.3. Downforce/ load transfer:

The traction of the tyres will change depending on the force applied normal to the support surface. If the tyres have a large amount of downforce applied through them, the traction or grip will increase. This increase is due to the traction of the tyres being proportional to the coefficient of friction between the tyre and the road surface, as well as the normal force applied between the road and the tyre. There are two classifications of downforce, static downforce and dynamic downforce. Static downforce is the weight of the car and driver while the car is stationary (Equation (2.6). In the case of the drivetrain, only the static weight on the rear tyres (R_r) is considered as they are the only ones which have a torque applied to them. The dynamic downforce (R_{ZR}) on the rear wheel's varies depending on the acceleration (a_x**Error! Reference source not found.**) of the car. The downforce due to the weight transferring during acceleration (Lt) increases the traction of the rear wheels while accelerating (Figure 23) (Equation (2.8), Equation (2.9).

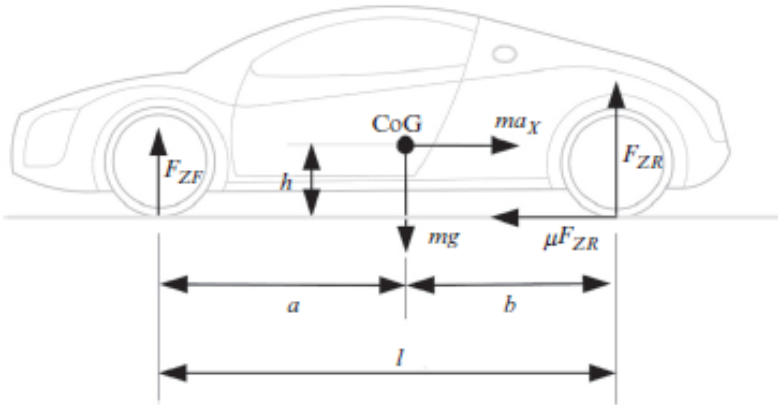

Figure 23: Free body diagram of accelerating race car (Balkwill, 2018)

$$Rr = \frac{m * X_{CoG}}{L} \tag{2.6}$$

$$F = M * a_X \tag{2.7}$$

Once the static downforce is known, the next step is to find the load transfer which will be taken at maximum acceleration (dynamic downforce needs to be calculated iteratively with the initial dynamic downforce being zero). Balkwill uses a and b to denote the distance from the front and rear axle to the COG. For W-FS-18 a and b are equal due to 50/50 weight distribution.

$$\mathrm{Lt} = \frac{\mathrm{M} * a_x * \mathrm{h}}{\mathrm{b}} \tag{2.8}$$

Once both the static and dynamic downforces are known, they can be added together to find the total downforce under acceleration.

$$R_r + Lt = Fzr \tag{2.9}$$

2.4. Differential:

Differentials are used in almost every modern car for both driving on the road or racing on the track. Differentials allow the left and right tyres/axles to spin at different speeds while the car is turning.

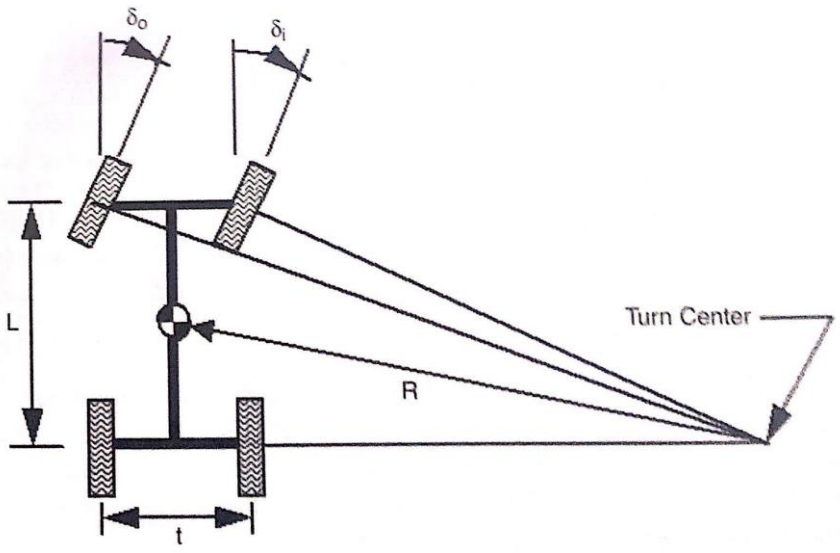

Figure 24: A vehicle in a low-speed turn (Stone & Ball, 2004)

"As the vehicle in Figure 24 negotiates the turn, the two rear (driven) wheels proscribe arcs of different radii. Thus, the outer wheel would tend to rotate more times than the inner wheel. If the vehicle has a solid drive axle, this would result in a twisting of the axle, a phenomenon known as "wind up." The solution is to allow each wheel to turn independently, each at its own speed. This is accomplished with a differential" (Stone & Ball, 2004).
There are multiple different types/designs of differentials used to combat this problem, with the most common design being an open differential as it is cheap and works well in everyday applications.

2.4.1. Types of differentials

Open differential:

The most common differential in an automobile is an open differential. An open differential uses an array of gears and pinions which split the power left and right wheels evenly while still allowing slippage between the left and right drive shafts (Figure 25). Open differentials have the advantage of being cheap and easy to maintain. The main drawback of open differentials is that when one of the wheels lose traction, all the torque through the differential takes the path of least resistance, which is to the wheel with no traction. Sending the power to the wheel with less traction means that the overall longitudinal force is the traction force of just the slipping wheel, which is much lower than if the wheel had full traction. For this reason, open differentials are rarely used in a racing application except for a racing series where open differentials are mandatory. Since the formula student racing series does not have mandatory use of an open differential, it is unlikely that the selected differential will be an open differential.

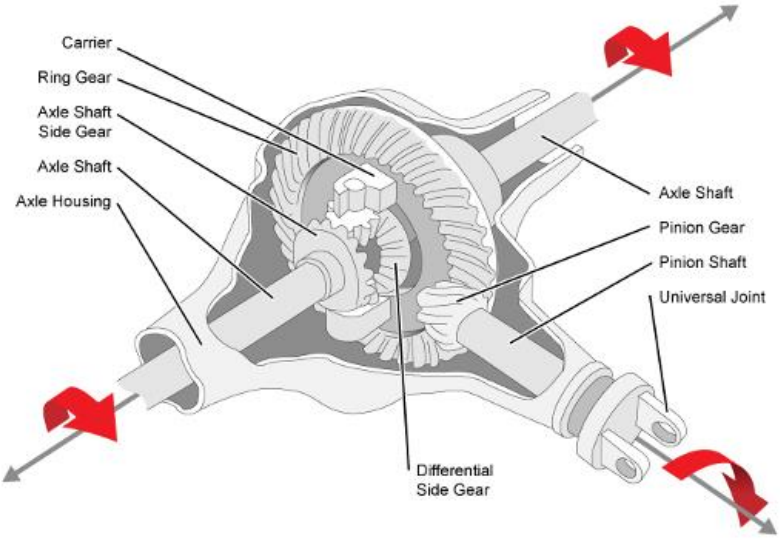

Figure 25: Open differential

Limited slip differential

A limited slip differential works by still having an array of gears, but the gears are set up differently from an open differential, and are used in union with clutch plates and springs (Figure 26). With a limited slip differential, the torque from the motor is only transmitted to each of the drive shafts when that driveshaft provides resistance to the supplied torque. This means that when one of the wheels loses traction the torque applied to that wheel decreases to

effectively zero until that wheel regains traction. This works by having the tangential force between the driveshaft pinion and cross gears create a force that engages the clutch plates inside the differential to grip and transmit all the torque through the driveshaft to the wheel with traction. Once a wheel slips, the torque transmitted to that side drops dramatically, causing the tangential forces of the pinion to drop which causes the clutch plates to separate and slip until the traction is regained. This results in the torque being supplied only to wheels with traction on the road. One of the downsides in terms of performance is that having a limited slip differential does somewhat decrease the predictability of the handling of the car due to the altering of the wheel the torque is delivered to. This sudden change in torque delivery/vectoring slightly upsets the dynamics and thus stability of the car, this influences the handling of the car. This is the type of differential that has been used by previous years WESMO teams.

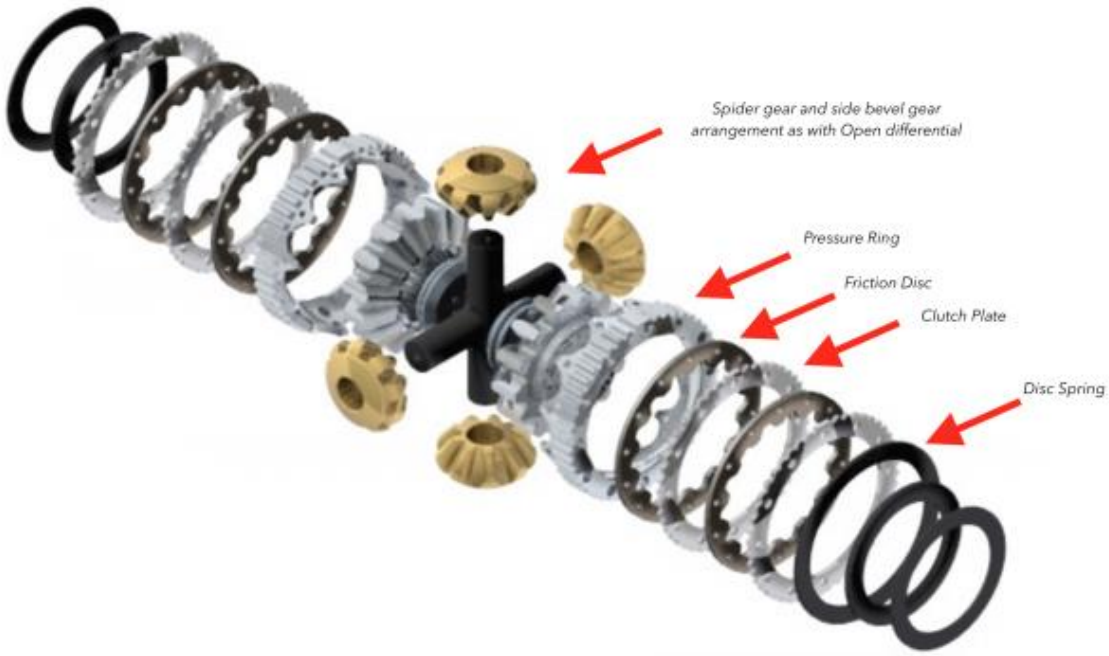

Figure 26: Exploded view of Drexler 2010 FSAE Limited Slip Differential

(Image courtesy of Drexler)

2.4.2. Locked differential/ spool

A locked differential has both rear wheels locked together, most commonly by using bolting both sides together with a spool (Figure 27). This aids longitudinal traction and thus acceleration, due to the power going to both wheels equally. With a locked rear axle, turning

corners will be difficult and the car will understeer badly. This can be solved by reducing spring rates and increasing rear sway bar stiffness. These suspension changes will cause the rear inside wheel to lift, eliminating the understeering problem but this will reduce the traction at the rear of the car because there is only one tyre providing lateral force. This design is still reasonably common in FSAE cars as it is cheap and easy to implement, however the loss of lateral traction means it is not the best option in the FSAE application, where cornering is vital to the performance of the car.

Figure 27: Spool differential (Taylor, 2010)

2.4.3. Differential ramp angle

In a Limited slip differential (LSD), the force with which the clutch plates are clamped together can be changed by adjusting the ramp angle. “Ramp angles determine how much pressure is applied to the clutch plate to increasingly bind the wheels. The torque is transferred from the chain and sprocket to the differential housing. As the housing accelerates relative to the spider axle, the spider axle is wedged in between the ramps of the pressure

rings; forcing them outwards." (Figure 28)

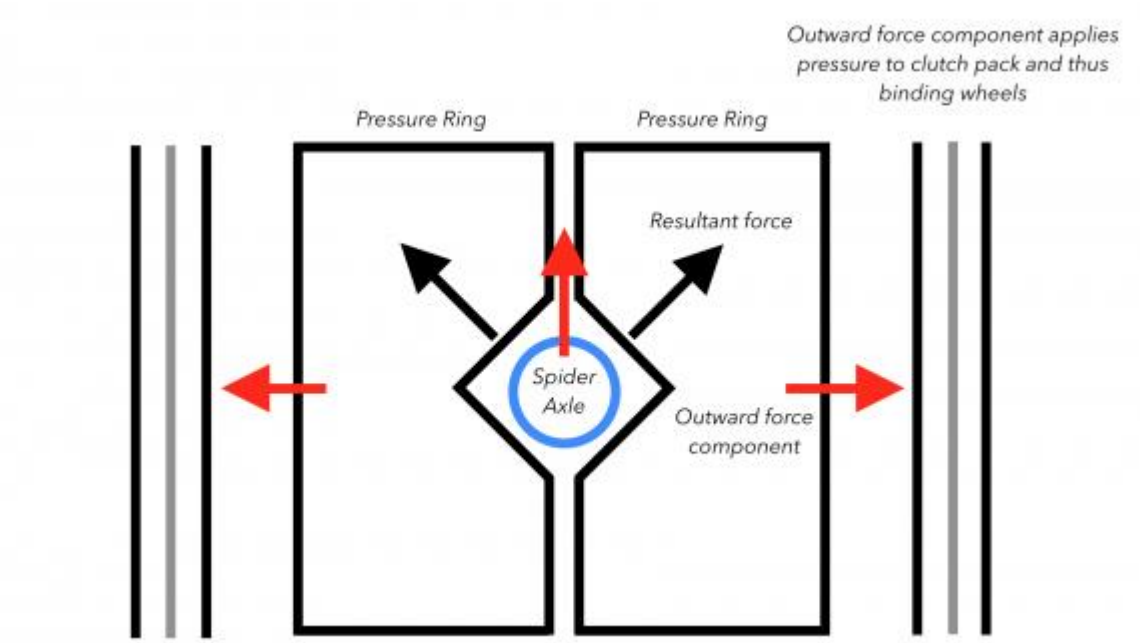

Figure 28: Force diagram of an LSD

The limited slip differential that will be reused in the 2020 car is the Drexler 2010 Formula Student LSD. This LSD is a 1.5-way LSD meaning that the acceleration ramp angle is different from the deceleration ramp angle. The Drexler FS LSD has 3 different options for the ramp angles, these are 40º/50º, 45º/60º and 30º/45º (Figure 29). In the case of the Drexler 2010 differential the accelerating ramp angle is always smaller than the decelerating angle meaning it has a higher locking percentage.

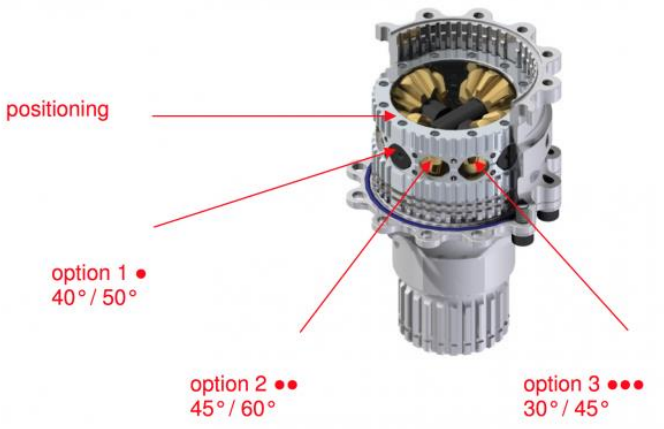

Figure 29: Ramp angles on Drexler Formula Student LSD (Image courtesy of Drexler)

The ramp angles can then be used to find the locking percentage using a ramp angle vs locking percentage plot (Figure 30).

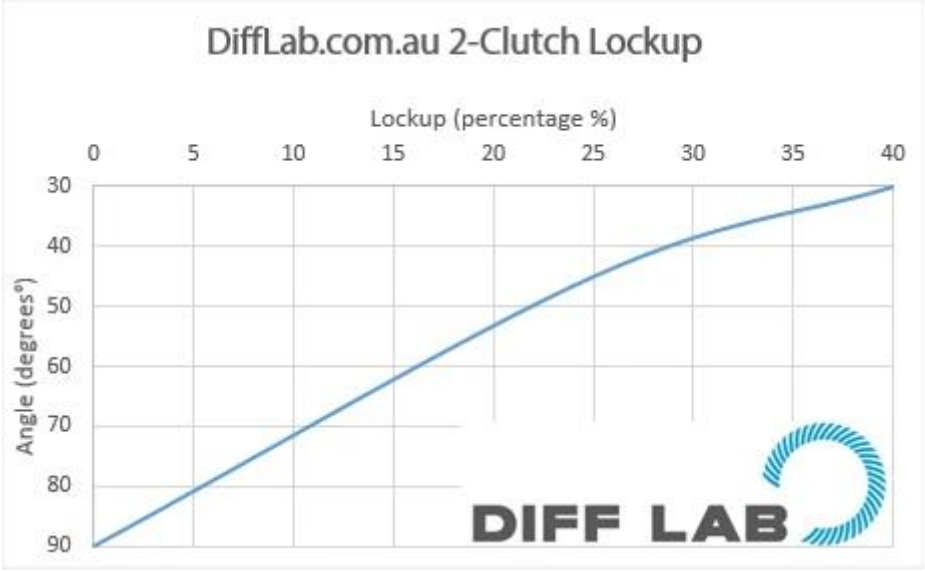

Figure 30: Differential locking percentage vs ramp angle for dual clutch LSD (Image courtesy of Diff Lab)

Longitudinal considerations

The ramp angle on the differential will affect the longitudinal grip as the car will have the most grip when both wheels have equal power being supplied to them. With a limited slip differential this occurs when the ramp angle is smaller as more tangential force is being applied outward on the clutch plates. Having a smaller ramp angle and thus greater locking percentage will result in greater resistance to unequal wheels speeds. This means that if one-wheel spins faster than the other, the differential will try to equalise the difference in wheel speeds proportional to the differential locking percentage. In vehicles that are traction limited during acceleration and cars that are unstable under braking, operating with a higher locking percentage is beneficial as both rear wheels will tend to spin together meaning greater traction while accelerating as well as more stability under braking.

Lateral consideration

Changing the ramp angle on the differential will have quite a large a large effect on the handling of the car as having a differential with high locking percentage will affect the overall yaw rate of a car during turning. This happens because when the differential has a high locking percentage the negative slip ratio of the outside wheel causes a resistive yaw moment, resulting in a decrease in the cars ability to take sharp corners. This is why the ramp

angle of the differential is mainly determined by lateral considerations, because although it has a minor effect on the longitudinal performance of the car, it has a much larger effect on the handling, lateral grip and overall drivability of the car. For rear-wheel-drive cars that tend to understeer using a lower locking percentage is beneficial as decreasing the locking percentage will reduce a cars tendency to understeer as well as helping the car with the initial turn in during a corner but depending on the handling characteristics of the car, this could also induce snap oversteer. Snap oversteer is when the car suddenly losses rear wheel lateral grip when decelerating or coasting due to the load transfer moving forward decreasing the lateral grip of the rear wheels causing the car to oversteer.

2.4.4. Frictional losses:

There will be various losses across the drivetrain due to friction. Some of the areas where losses will occur will be, in the chain drive system, the bearings which allow the limited slip differential to spin freely, and there will also be windage losses due to air resistance on the various parts of the drivetrain as well as fluid drag of lubricants etc.

The frictional loss from the various bearings used in the drivetrain will be minimised by using bearings that have low friction seals. The low friction seals on bearings carry an increased cost but as the limited slip differential is constantly spinning; these low friction seals will increase in efficiency of the drivetrain.

To minimise the losses due to the chain, the chain selected was an O-ring style instead of the more common bushing type of chain. The O-ring style chain has a higher relative cost compared to a bushing type of chain but has a higher efficiency, typically 99% efficient if the chain is properly lubricated at the time of use. Compare this to a bushing type of chain which typically has an efficiency around 95% when properly lubricated. O ring style chains usually have a higher resistance to wear then a bushing type of chain due to minimal metal on metal contact.

There is little that can be done about the various windage losses but in comparison to other frictional losses, windage losses are relatively small.

2.5. Inertia of drivetrain components:

2.5.1. Linear inertia

Linear inertia is equal to the mass of the components. This is the total mass of the components. The linear inertia is only used for calculating linear acceleration and in this calculation is treated the same as a non-rotating part. To decrease the linear inertia of the

drivetrain, the overall mass needs to be reduced. Decreasing the linear inertia by reducing the total mass of the race car will not change the efficiency of the drivetrain but will increase the overall efficiency of the car as the car will need less force/torque to accelerate it at the same rate.

2.5.2. Rotational inertia

Rotational inertia is proportional to the mass of a spinning object and the effective radius at which that mass is rotating about. When calculating the rotational inertia, the effective radius is squared, this means that a small decrease in the radius will result in a large decrease in the rotational inertia of that part. To reduce the rotational inertia of the drivetrain there are two things that could be done, firstly reduce the mass of rotating parts, secondly to decrease the effective radius of the rotating part (Equation (2.10) (Aleksander, 2010). The best way to decrease rotational inertia is to both decrease the mass and the effective radius but this is not always possible. Most of the parts of the drivetrain can be assumed to be a cylinder to find the inertia values (Equation (2.11).

$$r = \sqrt{\frac{I_Z}{m}} \tag{2.10}$$

$$I_{cyl} = \frac{1}{3}MR^2 \tag{2.11}$$

$$T = \alpha * I \tag{2.12}$$

2.5.3. How inertia effects the performance of the car

Inertia is an object's resistance to a change in velocity, whether that be linear or rotational velocity. As a formula student car is a complex system that has both rotational and linear inertias, both must be taken into consideration. The linear acceleration of the car is proportional to the mass (linear inertia) and the force. If the mass of the car were to decrease, it would result in the car's acceleration increasing. Just like the linear acceleration is proportional to the linear inertia, the same goes for rotational acceleration and rotational inertia. If the rotational inertia were reduced, for the same torque, the angular acceleration of the drivetrain would be larger.

Reducing the weight of drivetrain components will reduce both the rotational and linear inertia, so will increase the performance of the drivetrain and race car. By decreasing the rotational inertia of the various parts of the car, the torque from the engine will be used more efficiently to accelerate the car (Equation (2.11). Decreasing the rotational inertia will also

result in the brakes being more efficient as the decrease in inertia means that for the same braking force the brakes will slow the car down more.

There are multiple ways to reduce the overall rotational inertia of a drivetrain. Reducing the mass of components in the drivetrain decreases its rotational inertia. Decreasing the weight is the easiest (but not the most efficient) way to decrease the rotational inertia, as it only decreases the rotational inertia linearly, while also slightly decreasing the liner inertia. Reducing the drivetrains distribution radius of the mass also decreases the drivetrains rotational inertia. Decreasing the radius is harder to achieve but is a much more effective way to decrease the rotational inertia. This is achieved, by using a stronger and stiffer material that does not require as large of a shaft to provide the same strength. It can also be done by removing excess material- for example, cutting slots out of the sprockets.

2.5.4. Durability

While reducing rotational inertia is important, all the components must be strong enough to handle the stress that will be induced in them during the acceleration of the car. Most of the spinning components are round and the stress of those components is inversely proportional to the radius cubed (Equation(2.13), and Equation(2.14). This means increasing the radius of those parts will decrease the stress in those parts and thus, decrease the likelihood of that part failing. To have a high performance and reliable drivetrain, both the strength and inertia need to be taken into consideration when designing and selecting components in the drivetrain. The radius and number of teeth of the sprockets in the chain drive will be set by the gear ratio so it is the width of the chain/sprockets that determines whether the driveline will be durable enough to transfer the torque from the engine without breaking. If the selected chain is not rated for the torque from the engine, then a thicker more durable chain will need to be selected.

$$\tau = T \cdot r / J \tag{2.13}$$

$$J = \pi r^4 / 2 \tag{2.14}$$

2.6. Lateral considerations

The lateral grip of the car will have a large effect on how fast each corner can be driven, this difference in corner speed will ultimately affect the selection of the gear for each corner. Changing the gear ratio will have no effect on the lateral force the car can produce but will affect the acceleration coming out of the corner and thus can improve the cornering

performance of the car. The setting for the differential will also have an effect on the acceleration of the car coming out of the corner, but since most Formula student cars are power limited not traction limited while accelerating, the effect will not be as large as other motorsport applications. The setting for the differential will also effect the handling characteristics of the car, and in terms of formula student this is the major consideration for the setting for the differential.

2.6.1. Suspension:

The tyre pressure, camber, toe and downforce have a large effect on the overall traction of the tyre. In terms of longitudinal grip, the maximum grip is achieved when the camber is zero or neutral, as the tyre sits flat on the road with roughly symmetrical pressure distribution across the width of the contact patch of the tyre (Figure 14). The camber (Figure 31) and toe (Figure 33) are not selected based on longitudinal traction; they are primarily selected to optimise lateral traction, with longitudinal having a slight (but minimal) influence over this decision.

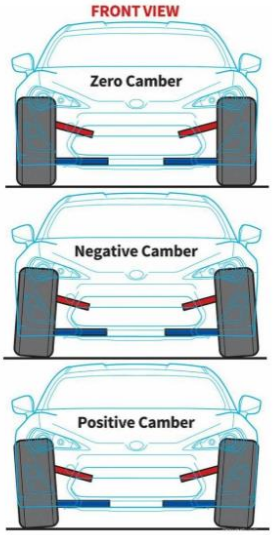

Figure 31: Visualisation of camber on a vehicle (Hunting, 2019)

"The cornering force that a tire can develop is highly dependent on its angle relative to the road surface, and so wheel camber has a major effect on the road holding of a car. A tire develops its maximum lateral force at a small camber angle." (Jazar, 2008). The reason the maximum lateral forces happen at a slightly negative angle is due to the contribution of camber thrust which is an additional lateral force generated by elastic deformation to the tread rubber from the road (Figure 32).

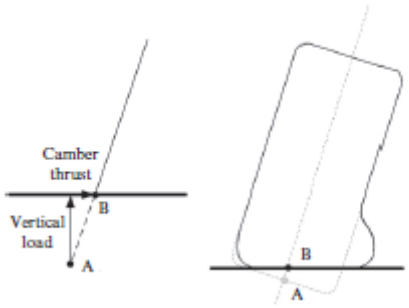

Figure 32: Camber thrust (Balkwill, 2018)

The camber of the tyres will also change due to suspension travel from load transfer, bumps as well as roll due to cornering. This change in camber due to loading is called camber gain and can usually be minimised with a well-designed suspension set-up. Formula student cars usually have around 2 degrees of camber since that gives room in both the positive and negative direction for camber gain.

The toe (Figure 33**Error! Reference source not found.**) of the tyre does not affect the longitudinal traction force but will increase rolling resistance marginally due to the tyres constantly having a slight slip angle thus resulting in a longitudinal resistive force. The toe set up of a vehicle has a large effect on the handling characteristics of a car. The standard convention for toe is to have the rear wheels toe-in. Having toe in at the rear helps reduce oversteer and increases the overall stability of the car, especially at high speed. Having toe out at the front will help reduce a cars tendency to understeer. Toe is adjusted to alter the handling characteristics of the suspension geometry and ultimately should be altered to match the handling characteristics of the car to the driving style of the driver.

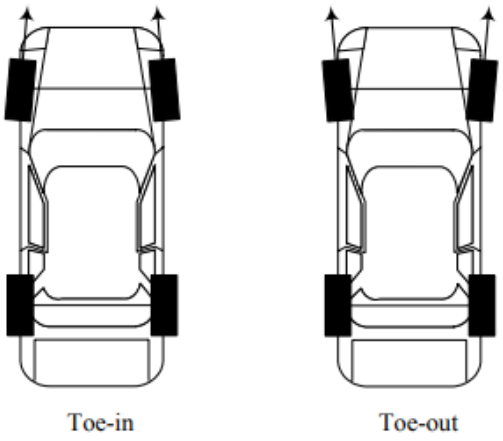

Figure 33: Visualisation of toe on a vehicle (Jazar, 2008)

Anti-squat/ anti-dive

During hard acceleration, a car will often squat due to the load transfer. Squatting is where the rear of the car lowers due to the increased load at the rear, this compression of the rear suspension will cause a change in the camber of the rear wheels. Squatting can be reduced by implementing anti-squat. Anti-squat is where the rear suspension system is designed so that a portion of the load transfer is transferred to the suspension arms instead of the shocks. It works by having the A-arms not parallel, i.e., having one of the A-arms at an angle. Anti-dive works the same way but with the front suspension taking the load transfer loads under braking.

2.6.2. Handling characteristics

Over steer is the condition where the front wheels are still under their traction limit, but the rear wheels are near or over their traction limit (Figure 34a). This happens as the slip angle of the rear wheels is greater than the slip angles of the front wheels. If not corrected via steering in the opposite direction the car will spin out. Understeer is the opposite where the front wheels are close to or over their traction limit, but the rear wheels are not, meaning the front wheels have a higher slip angle then the rear. When a car understeers the front wheels loose traction and the car keeps going straight despite the steering input (Figure 34b).

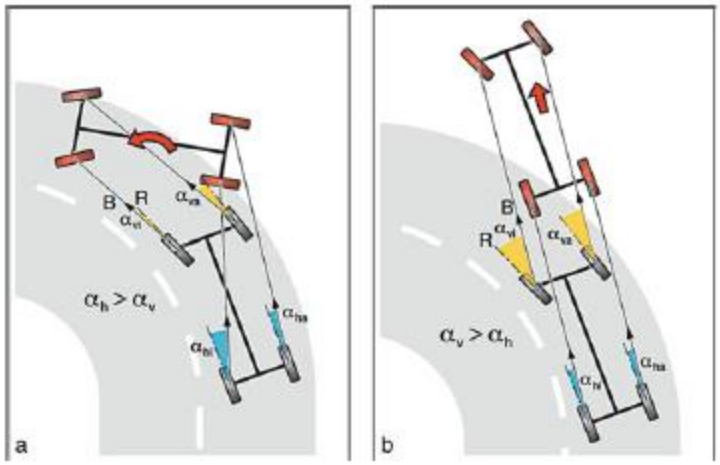

Figure 34: Oversteer (a) and understeer(b) (Pütz & Serné, 2017)

2.6.3. Yawing moment / velocity

"Yawing moment (M_Z) is the component of the moment vector tending to rotate the vehicle about the z-axis, positive clockwise when looking in the positive direction of the z-axis" (Milliken & Milliken, 1995) (Figure 35).

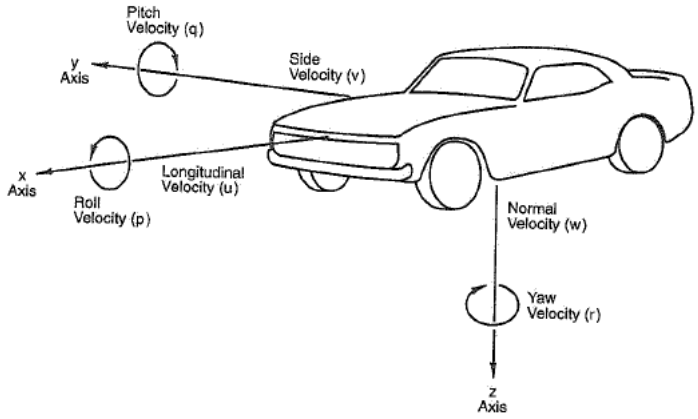

Figure 35: Vehicle axis system (Milliken & Milliken, 1995)

When the yaw moment of a formula student car is calculated, it is usually done using only the suspension and steering data e.g., slip angles, lateral tyre data, Ackerman geometry, and load transfer, but very rarely takes into consideration the effect the differential set up will have on the yaw velocity of the car. The type of differential selected along with how the differential is set up can have a large effect on the yaw velocity of a car. The differential will affect the yaw velocity of a car by either creating an additional yaw moment, which increases yaw velocity, or by creating an opposite yaw moment, that reduces the yaw velocity. With a limited slip differential or live axle, the resulting yaw moment is almost always destructive whereas with an open differential the yaw moment is usually constructive. Cars with a live rear axle often suffer from large amounts of understeer due to this phenomenon. The reason a locked axle increases the understeer tendency of a car is due to the reduced overall yaw velocity of the car which results in a sudden increase in the slip angle at the front wheels. If a car already has high slip angle this further increase in slip angle can result in the tyre transitioning into the frictional zone (Figure 17), thus reducing the lateral force the tyres can produce resulting in the car having understeer.

“Milliken Moment Diagrams (MMDs) are constructed by identifying the lateral acceleration and yaw moment created by a range of vehicle slip and steer angle combinations. The resulting lines of constant vehicle slip, and constant steer are plotted as shown in Figure 36. These diagrams are useful tools for identifying the limits of vehicle performance and understanding many aspects of vehicle behaviour including stability and control.” (Patton, 2013).

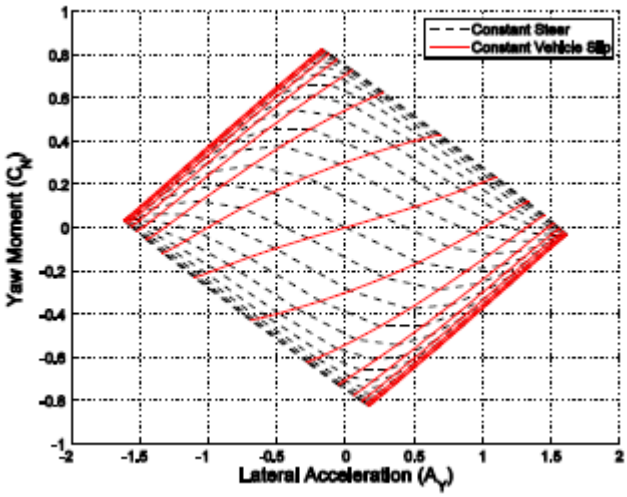

Figure 36:Milliken Moment Diagram –C_N -A_Y – 30 m/s (Patton, 2013)

"The Milliken Moment Method (MMM) is a well-developed approach to deriving a complete description of a vehicle's steady state handling characteristics". The Milliken of yaw moment diagram is one of the easiest ways to predict whether a car will be prone to oversteer or understeer. The ideal handling car is one that has been tuned to be fairly close to neutral, meaning it will have minimal oversteer or understeer tendencies.

The reason that the yaw moment at the maximum lateral acceleration can tell the handling characteristics of the car is because it demonstrates which tyres (front or rear) will break traction first. Assuming the car does not have neutral handling characteristics, the remaining possible traction from either the front or rear will have a potential yaw moment. Whichever wheels do not have a potential yaw moment will break traction first (Figure 37) and thus will determine the handling characteristics of the car.

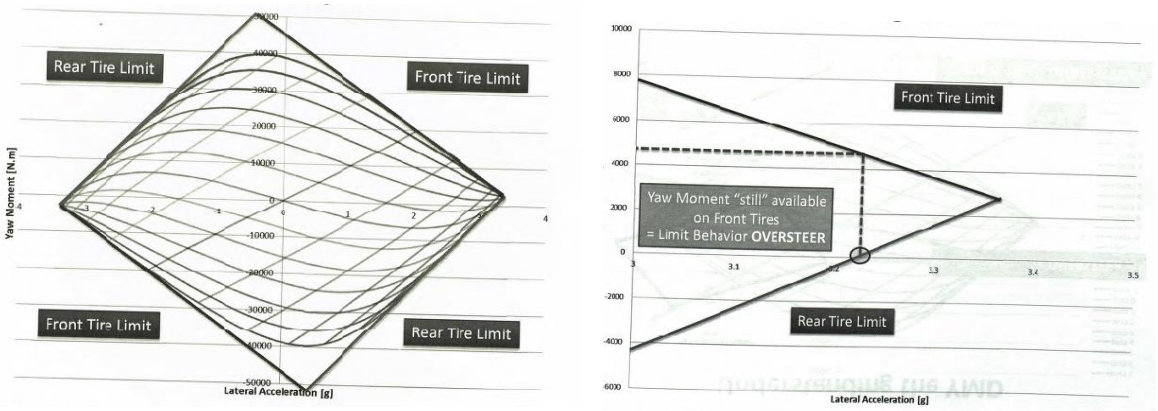

Figure 37: yaw moment diagram handling characteristics (Rouelle, November 2018)

The Milliken Moment Diagram uses a normalised yaw moment C_N otherwise called the yaw moment coefficient. When calculated the yaw moment is often in raw form and will need to be normalised before being plotted on the MMD (Equation (2.15) (Patton, 2013). The conversion from a yaw moment diagram to a Milliken moment diagram is useful for comparing variations of a car but since all comparisons for this research are being made based of the exact same car there is no need to convert the YMD to a MMD.

$$C_N = \frac{M_Z}{mgl} \tag{2.15}$$

2.7. Performance:

2.7.1. Track times/ gear shifting:

The track times of the car will be quickest if the selected gear ratio is optimised to a combination of maximising torque to the wheels to increase outright acceleration and having the rotational output speed large enough so that the driver does not need to constantly change gears because the engine is reaching the RPM limiter too quickly. Having a gear ratio to high not only means the driver must change gears more often but also during the 100 -200ms of time that a gear change takes, the output torque drops to zero momentarily. This temporary stop in torque will mean that during that time the car will not be accelerating. Since W-FS-18 was approximately 200ms off the leader in the acceleration test during the 2018 competition. Having to complete one less gear shift could have been the difference between the third place and first place.

One of the main considerations when selecting a cars gear ratio is to ensure that the car does not fall in an awkward RPM range during inconvenient times. For example, an inconvenient time to change gears is during the initial acceleration period when driving out of a corner, this adds a whole lot of complexity for the driver, as the driver will either need to take one hand off the wheel to pull the gear lever while keeping their racing line or otherwise the driver will need to short shift before coming out of the corner reducing the acceleration of the car right when the maximum acceleration is needed.

2.7.2. 8.2 Fuel efficiency:

The gear ratios selected in the drivetrain have a large effect on fuel efficiency. This is mainly due to the fuel consumption of the internal combustion engine being dependent on how much throttle is being used and the RPM of the engine. As the WESMO car is being used in a racing environment it will most likely be accelerating at close to full throttle. If the driving

conditions were not taken into consideration when the drivetrain was being designed the engine could be regularly operating at high RPM often, which will result in a poor fuel efficiency. Decreasing the inertia of the drivetrain will result in a more efficient transmission of torque and an increase in fuel efficiency.

3. Methodology

The research in this report is split into two sections, the theoretical analysis and the experimental analysis. The experimental analysis involved completing testing on the W-FS-18 formula student car. The testing involved investigating the effect of the gear ratio on acceleration, gear shifting convenience and track times. This testing was carried out at Kartsport Hamilton on two coned testing tracks laid out to effectively test the car in the relevant conditions.

The theoretical analysis involved verifying the results produced in testing through theoretical calculations using a combination of Excel and MATLAB for computational analysis and using Solidworks for any design/geometric analysis.

3.1. Track testing

3.1.1. Testing variables

The W-FS-18 car was used for all testing. This was because it was the most reliable and lightest car built by the WESMO team when compared to previous WESMO cars. All calculations and modelling done for this project were based on the specifications of this car (Table 1). The W-FS-18 has a KTM duke 690R engine which is a single cylinder 690cc motorbike engine that has a 6-speed internal gear box and a manual hydraulic clutch. The car has a wheelbase of 1535mm, and the track width is 1050mm for the rear wheels and 1100mm for the front wheels. The mass of the car that will be used in all calculations is the wet weight. The wet weight of a car assumes the car has a full fuel tank and includes the weights of all the other fluids required for operation of the car.

Table 1: W-FS-18 technical specifications

Specifications	
Wheelbase	1535 mm
Car mass (wet)	191 kg
Driver mass	75kg
Rear weight ratio	50%
Front weight ratio	50%
Height of Centre of Gravity	0.305 m
Track width (F/R)	1100mm/1050mm
Sprung mass	161kg

Unsprung mass	30kg
Peak torque	65N·m
Peak Horsepower	44kw
Camber (all tyres)	-2º
Tyre radius (Diameter/width/Rim size)	18/6.0/10 Inch

Overview of the W-FS-18 drivetrain design

The W-FS-18 drivetrain initially used a final drive ratio of 48:16 or a ratio of three to one with an engine sprocket size of 16-teeth and a drive sprocket of 48-teeth. The torque from the engine was transmitted to the axles through a 520-motorbike chain. The differential used was the Drexler 2010 Formula Student Limited- Slip differential. The LSD was a 1.5 way set up with 3 different options for ramp angles. The three options were 40º/50º,45º/60º,30º/45º with the first smaller ramp angle being the acceleration ramp angle and the second larger angle being the deceleration ramp angle. The differential bearings were SKF 91911-2RS1 on the sprocket side and SKF 61910-2RS1 on the other side of the differential (Figure 38). The drivetrain used hollow unequal length heat treated DIN 1.2767 grade tool steel half shafts along with tripod style CV joints. The hubs and uprights are custom designed and manufactured in house using two SKF 61815- 2RS1 bearings per hub. The gear box that was used is the internal gearbox that comes with the KTM Duke 690R engine.

Figure 38: W-FS-18 Drivetrain components

The total drivetrain components weigh just over 22 kg. The distribution of those weights are shown in Table 2. The majority of the weight from the drivetrain comes from the wheels and

hub assemblies. The hubs and tyre assemblies also have a large effective radius and contribute the most to the overall rotational inertia of the drivetrain.

Table 2: Drivetrain components with masses (grams)

Drivetrain components and mass (grams)	
CV tripod diff (2x)	254
CV tripod upright (2x)	188
CV cup short	560
CV cup long	593
Differential	1430
Half shaft short	856
Half shaft long	904
Bearing 50mm	140
Bearing 55mm	200
Hoosier tyre (2x)	9280
Hub assembly (2x)	4339
Sprocket diff 42 t	390
Sprocket carrier	282
Rim shell inner (2x)	1501
Rim shell outer (2x)	935
Rim centres (2x)	890
Total	**22214**

Engine dynamometer results:

To determine what gear ratio provides optimum performance, the first piece of information required is the torque curve of the engine, as the torque output at the wheels will be greatly affected by the torque being applied to the transmission. The torque curve is found by connecting the engine to a dynamometer and measuring the output torque across the RPM range of the engine (Figure 39, and Figure 40). The power curve is then generated from the torque curve by multiplying the torque in Newton Metres (Nm) at each RPM by the angular frequency of the engine in rad/s (Equation**Error! Reference source not found.Error! Reference source not found.**.

The engine tune that was used in all testing and theoretical calculations was the same tune as in Figure 39**Error! Reference source not found.**. The engine torque and power values used in theoretical calculations were based off the results from that dynamometer test.

$$P_{in} = T_1 * \omega_1 \tag{3.1}$$

The engine was tested on a dynamometer at D-Tech Motorsport in Tauranga. The engine was tested on the dynamometer multiple times with each test using a slightly different tune. The

tune shown in Figure 39 was selected as the best tune as it has a consistent torque output across the entire RPM range of the engine, which results in a smooth power curve that does not taper off too much in high RPM ranges, which is typical of large single cylinder engines.

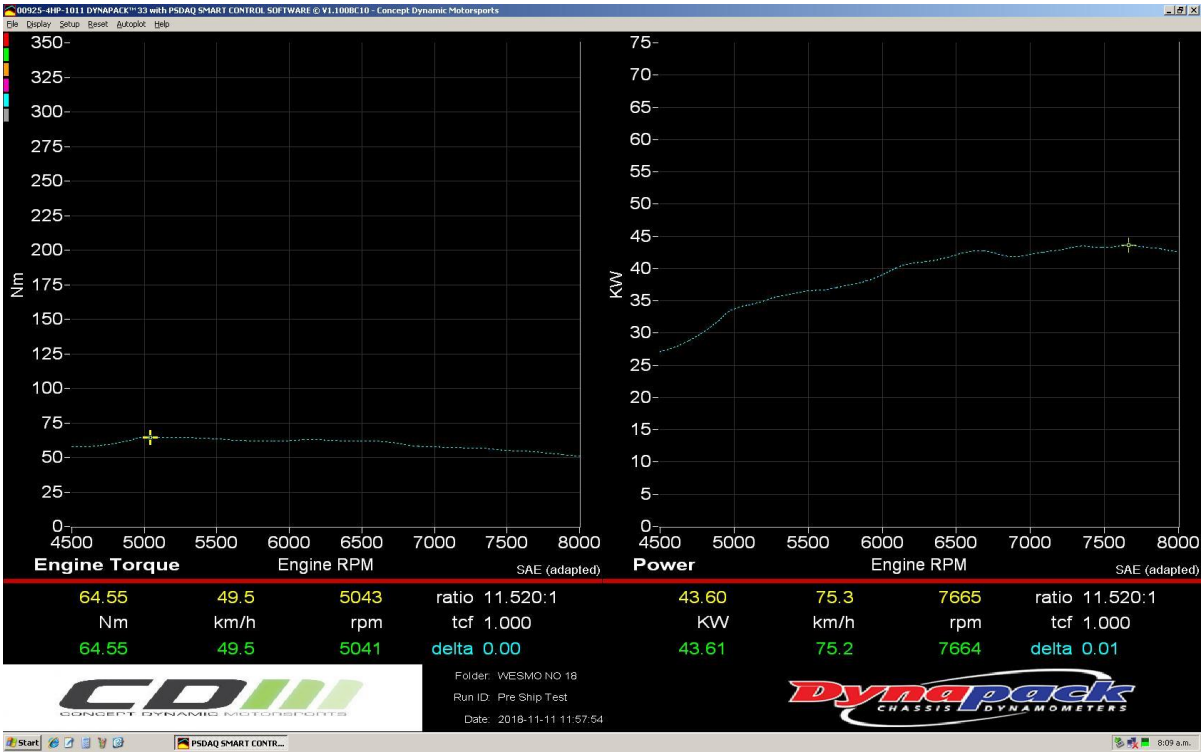

Figure 39: KTM Duke 690R crank dynamometer result graph

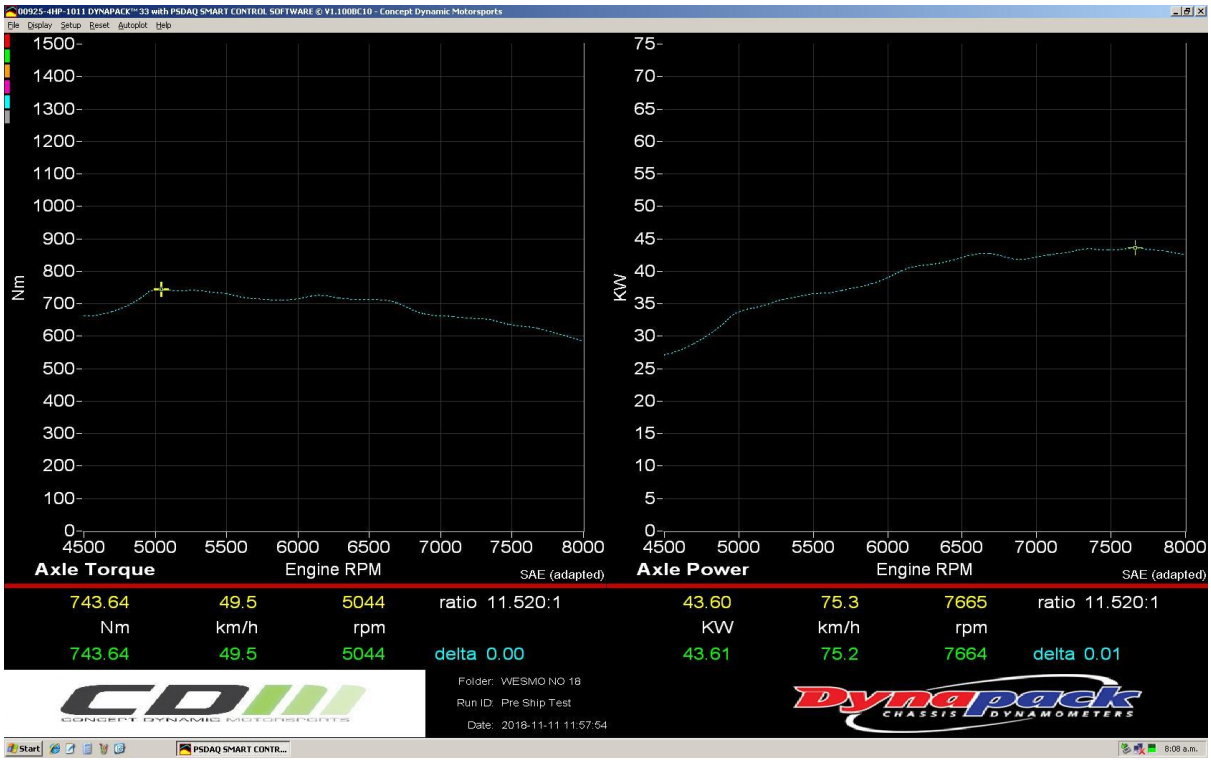

Figure 40:W-FS-18-wheel dynamometer result graph 2nd gear

Track testing

All track testing took place at Hamilton Kartsport. All the straight-line acceleration testing was completed on the start/finish straight where a 75m acceleration course was set up using cones as distance guides. All autocross testing took place on the back section of Kartsport Hamilton (Figure 42**Error! Reference source not found.**). To ensure that all the autocross testing was valid the same track was used for each test. The initial plan was to use the same track set up that was used for suspension research in 2019 (Kopf 2019) but after an initial test the track was found to be too tight (Table 3) (Figure 41) to be able to get any long periods of hard acceleration. The longest straight in the old layout of the track started after exiting a wide slalom and was approximately 25-30m long. In this acceleration zone the W-FS-18 car was accelerating from about 20km/h up to approximately 45-50km/h.

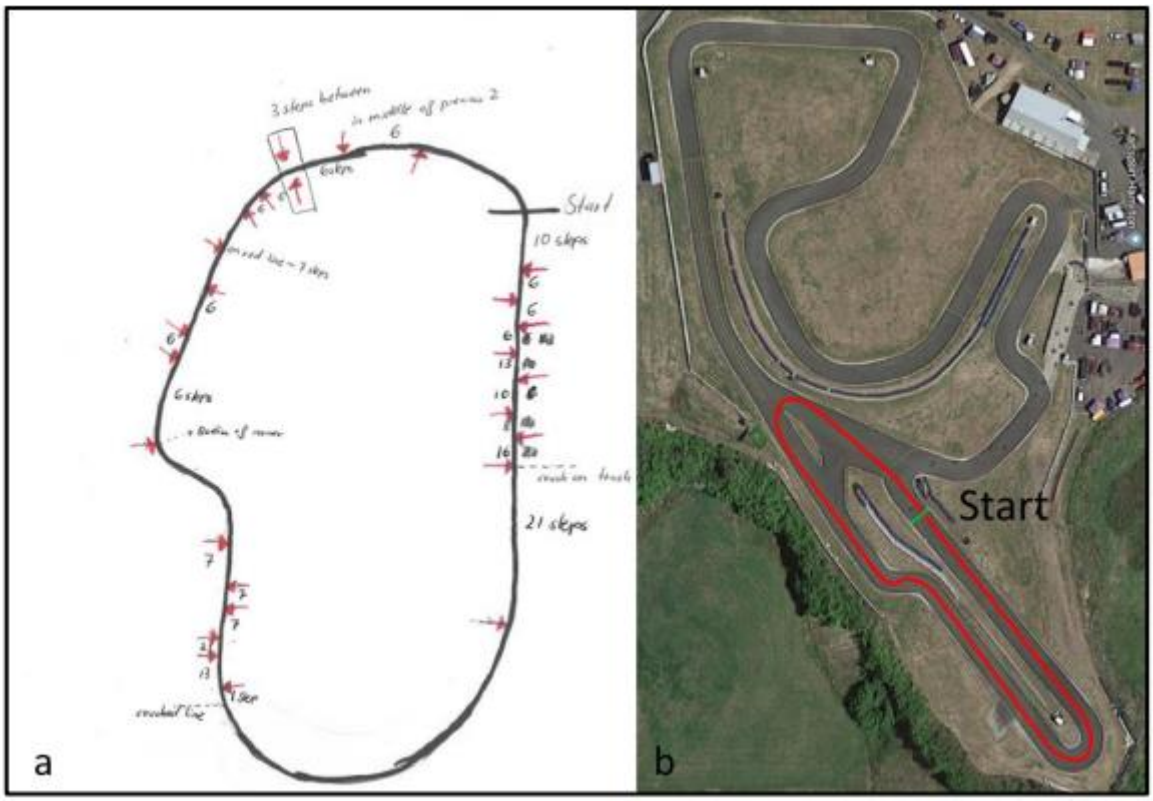

Figure 41: Kartsport suspension testing track and cone layout

The new track design was tailored to facilitate improved testing of the drivetrain. To do this the higher speed slalom on the front half of the track was removed in favour of having a longer open straight. In addition, the radius of the rear slalom corners was increased from 6m to 8m, as well as making the slalom one turn shorter resulting in a new high-speed

acceleration zone. These alterations provided realistic accelerating conditions for analysis of the drivetrain. The main acceleration zone on the new track consists of the car accelerating from approximately 30km/h up to 75-80km/h (Figure 42).

The new track maintains a minimum radius hairpin (4.5m), a low-speed slalom, a highspeed corner as well as a chicane down the back straight (Table 3). The alteration of this course has increased the length of the front straight and has added a high speed straight down the back of the course. This new track layout is a good representation of a FSAE competition autocross/endurance track.

Table 3: Summary of the track features/layout for gear testing vs suspension testing

Gear track	Suspension track
12m long 6m slalom	18m long 6m slalom
46m straight	8-13m variable slalom
Gated wide corner	Gated wide corner
16m long 8m slalom	18m long 6m slalom
4.5m minimum radius corner (135^{o})	4.5m minimum radius hairpin (180^{o})

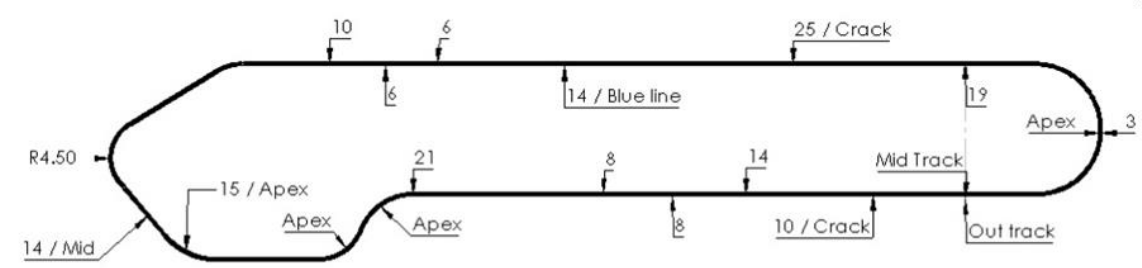

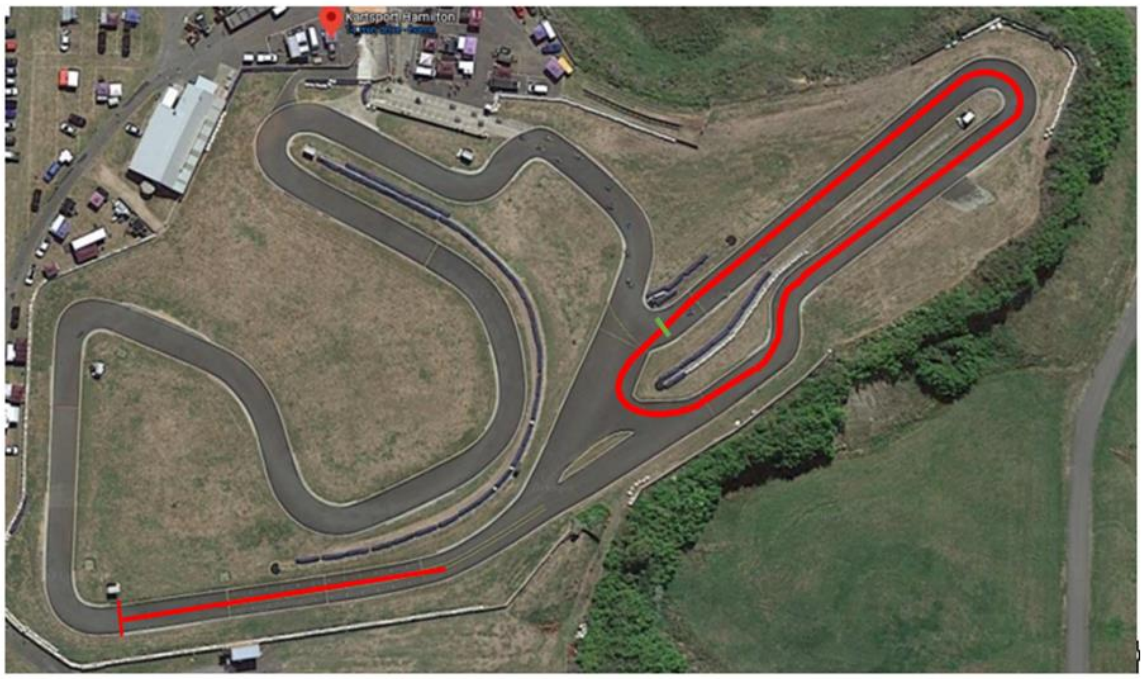

Figure 42: Kartsport drivetrain testing track and cone layout

To ensure the data was collected consistently to minimise variables, all testing was undertaken on a dry track using Hoosier 18.0x6.0-10 R25 formula student tyres at a tyre pressure of 10 psi (cold). Consistency in tyre selection, pressure and track conditions ensure minimal variation of the overall traction of the car. The same driver was used throughout testing to ensure that driver ability is consistent throughout. All the track testing was done in the early afternoon to ensure that the ambient and track temperature are reasonably consistent throughout all the testing. The minor variation in track temperature will have a slight effect on the overall traction but this effect is only a fraction of how the tyre temperature effects the grip. All testing was done after a warmup consisting of approximately 3 laps around the entire go-kart track, both to allow the driver to get accustomed to the track and car set up as well as to warm the tyres up to a consistent operating temperature.

A consistent suspension set up was used for each track day to eliminate any error that could come from inconsistent tuning settings. Since one of the rear anti roll bar (ARB) mounts broke during a previous track testing day, and it was not feasible to replace the ARB mount for this set of testing, all testing was completed without any antiroll bars. Not having the ARB connected had an effect on the drivetrain data in terms of the autocross testing, however the effect was minimal, cornering speed decreased marginally, and there was no effect on longitudinal acceleration. Testing with no ARB did decrease the accuracy of the lateral traction data during testing. This decrease in the handling of the car happened due to the car transitioning from being limited by the traction of the tyres with the ARB installed, to being limited by the roll of the car and the corresponding suspension set up required to operate the car when no ARB was installed. Though having the ARB would be preferable it was just not realistic to install a new rear ARB system in the time available.
The W-FS-18 car has very heavy steering, so any testing must take driver fatigue into consideration. Testing on the car was undertaken ensuring the driver has adequate rest in between each test to ensure that the driver does not suffer from fatigue

Prior to testing, the oil, oil filters and coolant were replaced as well as the differential being rebuilt with new clutch plates and stators to ensure that the car was performing well. The old differential plates also had slightly uneven wear which would have skewed any results gathered during testing. To diagnose the uneven wear on the differential, the two rear tyres were spun in opposite directions. If the differential rotates one way or the other, it means that the wear is uneven, and it will have a negative effect on the handling of the car. After

replacing the clutch plates there was no problem with uneven wear but as a precaution testing the wear of the differential was added to the list of pre track day inspections for all track days.

The autocross testing was split into two halves, the first half consisted of finding the effect the gear ratio has on the performance of the car during the autocross event. This was meant to consist of eight track sessions but due to more setbacks then expected during testing only five of the eight planned testing set ups could be tested. In each session the driver will do as many autocross laps as they can manage around the course at a consistently fast pace. It was initially decided that testing for as many laps as the driver could manage instead of a set number of laps would provide superior results since the timing was going to be used in the analysis of the drivetrain and the logic was, the more laps the greater the accuracy of the timing data. In the end the timing data was not used in the analysis due to the how inaccurate the timing data was when compared to the gearing and traction data.

Before the start of the testing the fuel tank will be completely topped up so that any effects the fuel level will have on performance of the car will be consistent throughout all testing. The whole time during testing the onboard data monitoring MoTeC unit will be recording all the necessary data (Table 5) which will then be processed at a later date. After each track session the car was prepared for the next session ensuring that the driver did not know which set up the W-FS-18 had installed for each track day to eliminate any preconceived bias.
The variables that will be changed during the first part of testing will be the size of the rear sprocket. The rear sprockets that have been selected range in size from 39-tooth to 48-tooth. The front sprocket was chosen to stay the same for simplicity purposes both in terms of the work on the car to change the different testing settings as well as making the analysis easier, while still maintaining a viable range of gear ratios (Table 4). The gear ratio will be analysed both in terms of performance in the acceleration event as well as how well suited the gear ratio is to a typical autocross track layout.
For the rest of the report the change in the overall gear ratio will just be referred to by the rear sprocket size instead of the resulting final drive ratio.

Table 4: Gear ratio testing variations

Front sprocket	Rear Sprocket	Final drive ratio
16	39	2.438
	42	2.625
	44	2.750

	46	2.875
	48	3.000

The second part of the autocross testing will consist of having the optimum rear sprocket installed and changing the differential ramp angle to determine how the ramp angle effects the overall handling of the car. The differential settings will be tested using the optimum gear ratio from the previous testing. Initially the plan was to have a track session with each of the differential settings but due to time constraints only the highest and lowest ramp angle options were tested

3.1.2. Data collection

The MoTeC unit and the Link engine control unit (ECU) were used as data loggers on W-FS-18. These were connected to the sensors listed in Table 5 and recorded data at a frequency of 500Hz.

The main data channels that were used during the analysis of the drivetrain will be the data in the first two columns of Table 5. For analysing the gear ratio, the most important channels were the gear channel which shows the selected gear; the engine RPM which shows the rotational speed of the engine, the throttle position which shows how much the throttle is being applied, the GPS data and the corrected speed which the MoTeC unit calculates based from the wheel speeds.

Table 5: Data recording channels of W-FS-18

GPS, Velocities and Accelerations	Other key information	Engine information	Extra information
GPS Speed	Gear	Engine Temp	Baro Pres
GPS Heading	Engine RPM	Air Temp Inlet	Bat Volts SDL
GPS Time	Throttle Pos	Bat Volts ECU	Lap Gain/Loss Running
GPS Latitude	Wheel Slip (Percent)	Fuel Inj Timing	Lap Gain/Loss Final
GPS Longitude	Susp Pos FL	Ign Advance	Reference Lap Time
Wheel Speed FL	Susp Pos FR	Cam Pos L Inlet	GPS Sats Used
Wheel Speed FR	Susp Pos RL	Cam Pos R Inlet	Light 2
Wheel Speed RL	Susp Pos RR	Lambda 1	SDL Temp Brake
Wheel Speed RR	Odometer	Fuel Pres	Lap Number
Ground Speed	Lap Distance	Eng Oil Pres	Traction Enable Switch
Drive Speed	Lap Time	Fuel Inj Duty	Beacon
G Force Lat*	Brake Pres Rear	Engine Run Time	Trip Distance
G Force Long*	Brake Pres Front	Min Eng Oil Pres	Log Time Remaining
G Force Vert*	Steering Angle	Manifold Pres	Logging Running
GPS Altitude	Running Lap Time	Fuel Actual PW	CPU Usage

GPS Date	Brake Bias Setting	Eng Hours 1	Display Next Line

Having comprehensive and accurate data recording of relevant variables while racing the car is vital to both designing and tuning the car. The data was reviewed after each test to ensure that the car was performing as expected, and the relevant data is used to effectively evaluate the current tuning set up of the car.

Due to space constraints in the cockpit of the W-FS-18 car the 2018 WESMO team decided to mount the MoTeC unit at the back of the car (Figure 43). Since the MoTeC needed to be mounted to a chassis member and the only suitable chassis member was at an angle to the axis of the car the raw MoTeC accelerometer values needed to be corrected.

Figure 43: MoTeC unit mounting location

The actual offset of the MoTeC unit is 61.35º about the x-axis and 14 degrees about the z-axis (Figure 44). To be able to get correct accelerometer data (shown by having a * after the channel name on Table 5) all the accelerations had to be corrected (Figure 44). This was performed inside the MoTeC software using the following equations.

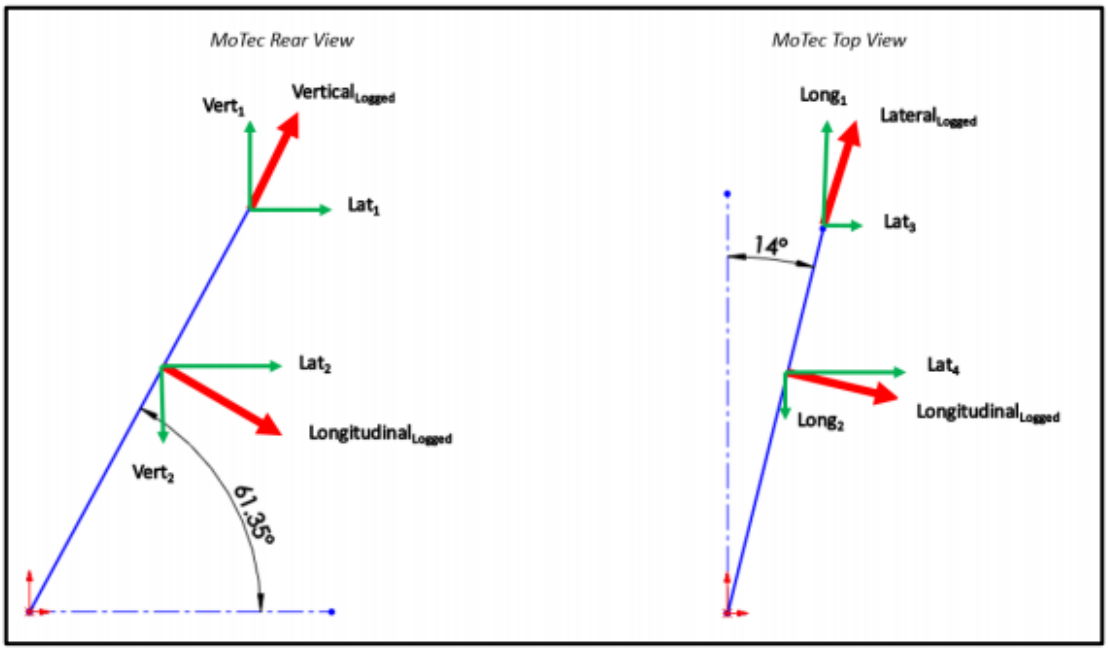

Figure 44:MoTeC unit angular offset (Kopf, 2019)

$$a_{lat,actual} = a_{Lat,1} + a_{Lat,2} + a_{Lat,3} + a_{Lat,4} \tag{3.2}$$

$$a_{Long,actual} = a_{Long,1} - a_{Long,2} \tag{3.3}$$

3.1.3. Modifications to W-FS-18

The chassis of the W-FS-18 car was not designed for easy adjustment to the drivetrain. To adjust the differential all peripheral parts and the engine needed to be removed from the car. Therefore, research was done into whether the rear cross brace that prevents the drivetrain from being removed out the back of the car could be removed from the chassis. The rear cross brace chassis member was initially included in the W-FS-18 chassis design to increase the torsional rigidity of the rear section of the car. Due to the resulting decrease in torsional rigidity the FEA had to be redone to ensure the chassis still meets torsional requirements. With the cross brace, the chassis had a displacement on the bottom corner of 7.493mm (Figure 45). Thought this displacement seems high this is assuming highly improbable loading conditions and this displacement is measured across the length of the chassis. This resulted in the chassis having a factor of safety of 1.16 in terms of torsional rigidity. Without the cross brace the displacement was 7.525mm (Figure 46). This displacement results in a factor of safety of 1.155 in terms of torsional rigidity. The chassis still meets the required stiffness and therefore can have the rear cross brace removed while still meeting specifications (Figure 47).

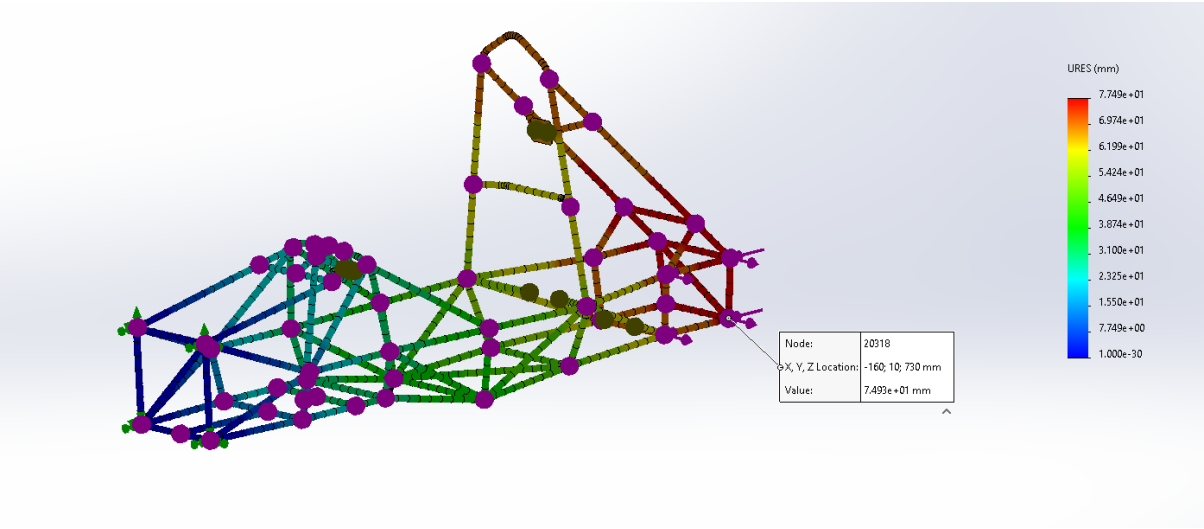

Figure 45: W-FS-18 chassis FEA with rear cross brace

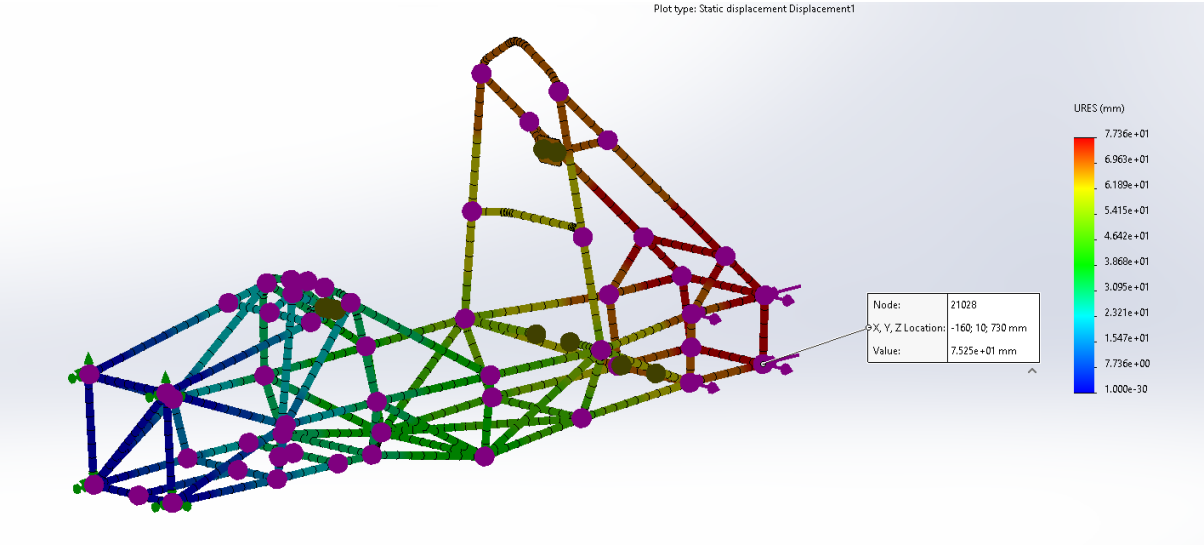

Figure 46: W-FS-18 chassis FEA with rear cross brace removed

Figure 47: W-FS-18 chassis with rear cross brace removed

During testing the GPS sensor stopped working and had to be replaced. The GPS sensor was rated at 5Hz meaning it recorded data every 20ms. At 100km/h this means that the GPS data would be within +/- 6m. It was decided that instead of replacing the GPS sensor with the same sensor, the sensor was upgraded to a sensor which records at 10 Hz ensuring a higher level of accuracy when recording the data, while also being quicker to source, but at a slightly higher cost.

Initially all the gear selection data from MoTeC was generated via calculations based off the engine RPM, the throttle position, and wheel speeds. This has been adequate in all WESMO's previous testing as the gear values had not been used, however upon inspection of the data there appeared to be approximately a 100ms delay from when the gear was actually shifted compared to when the MoTeC registered it as shifting. This delay in registering a gear shift can be seen on the MoTeC data, primarily on the autocross gearing chart with some data points showing the engine RPM has already dropped due to a gear change, but these data points were still registering the car in the previous old gear due to the delay from the calculation process.(Figure 48).

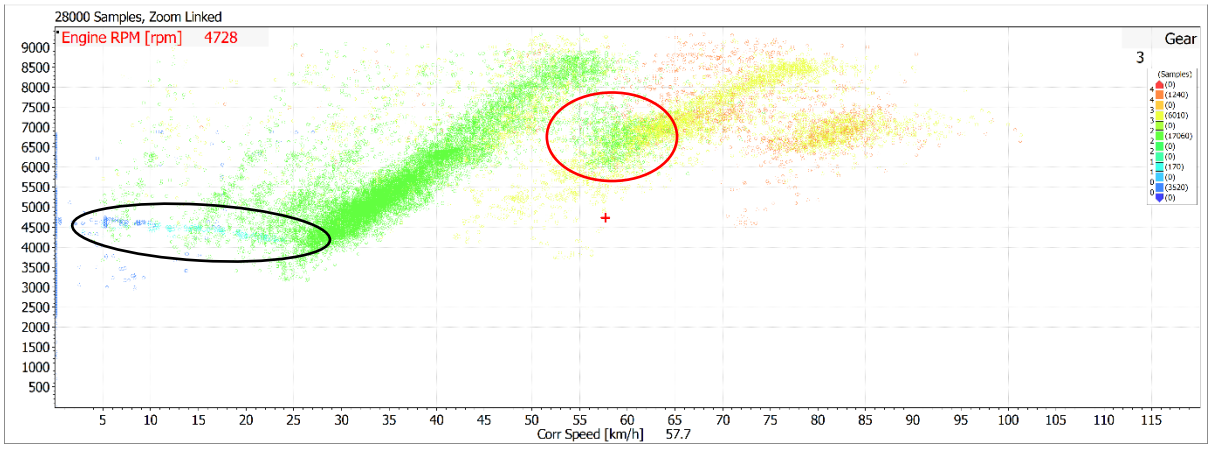

Figure 48: 39 T autocross gearing chart before gear sensor

The engine was supplied with a shifting sensor, but it had been disconnected as all the analogue ports for the Link ECU were being used by sensors that were previously viewed as being more important than the shifting sensor. The solution to this problem was to disconnect the fuel pressure sensor and use its the analogue port in the ECU for the shifting sensor. While fuel pressure is useful for tuning the engine, and determining fuel usage, it was not essential for daily operation of the car.

The lambda sensor (air to fuel ratio) through the MoTeC unit via the Link ECU was used to monitor and control air to fuel ratios. To ensure that the fuel pressure sensor could still be easily reconnected at a later date a male DTM connector port was added to the ECU wire, with a female connector attached to the fuel pressure sensor and gear sensor so the two could be swapped as needed, only, requiring the settings for that port be updated through the Link software.

4. Results

4.1. Theoretical calculations

4.1.1. Calculating maximum traction force:

Before any gear calculations can be undertaken, the overall longitudinal traction, the rear wheels can produce needs to be calculated.

As the traction force of the tyres is proportional to the downforce on the rear wheels, the first step is to calculate the static downforce on each of the rear wheels. When the downforce on each rear tyre is used in the equation for downforce versus the tyre's coefficient of friction from the previous tyre calculations the maximum traction the rear wheel can provide can be calculated (Equation(4.1). The traction force per wheel is then found, with the total rear downforce needing to be halved in order to get the downforce per wheel**Error! Reference source not found.**.

$$F_t = \mu * 0.5 F_r \tag{4.1}$$

The total longitudinal traction force is found by doubling the traction force per wheel. The maximum torque that can be applied to the wheels without loss of traction can now be calculated using the effective rolling radius and the longitudinal traction force (Equation (4.2)**Error! Reference source not found.**.

$$T_t = r_e * F_t \tag{4.2}$$

Finding the actual grip involved iteration of the previous steps as when the car accelerates there was load transfer and so the traction will change depending in the acceleration. Selecting a gear ratio only based on traction is adequate but could result in the driver having to shift the gears too often due to having a short gear ratio. The traction calculations are important, but other mathematical models which take the engine input and driver gear shifting into consideration should be used in unison with these calculations to ensure that final gear ratio gives fast acceleration and that excessive gear changes are not required.

4.1.2. Gear ratio calculations

The KTM Duke 690R engine has an internal transmission with the gear ratios already selected (Table 6**Error! Reference source not found.**). The internal Gear ratio between the crankshaft of the engine and the output sprocket can vary from 5.486 down to 1.908 depending on the gear selected. These gear ratios are essentially set, to be able to alter these a

custom gearbox would need to be designed and manufactured and that would be a very expensive and time-consuming process. To alter the amount of torque at the wheels and the rotational speed in each gear of the transmission the final drive gear ratio will be the gear ratio that will be getting altered in this project.

Table 6: KTM Duke 690R transmission gear ratios

Primary gear ratio	79/36
1st gear (2.5)	35/14
2nd gear (1.75)	16/28
3rd gear (1.33)	21/28
4th gear (1.1)	21/23
5th gear (0.96)	22/23
6th gear (0.87)	20/23

The gear ratio that will be getting optimised will be the final drive ratio. Since the final drive is a chain drive, changing the gear ratio is simple. To change the gear ratio, the number of teeth on either the driving or driven sprocket will be changed. The simplest method of establishing the appropriate gear ratio is to create a table with the rows being the number of teeth for the driven sprocket and the columns being the number of teeth on the driving sprocket (Equation (4.3)**Error! Reference source not found.** (Table 7**Error! Reference source not found.**).

$$N_1 * n_1 = N_2 * n_2 \tag{4.3}$$

Table 7: Final drive ratio of different sprocket combinations

Final drive gear ratios					
Sprocket Teeth	14 T Driving	15 T Driving	16 T Driving	17 T Driving	18 T Driving
36 T	2.571	2.400	2.250	2.118	2.000
38 T	2.714	2.533	2.375	2.235	2.111
40 T	2.857	2.667	2.500	2.353	2.222
42 T	3.000	2.800	2.625	2.471	2.333
44 T	3.143	2.933	2.750	2.588	2.444
46 T	3.286	3.067	2.875	2.706	2.556
48 T	3.429	3.200	3.000	2.824	2.667

Following the creation of Table 7 showing all the final drive gear ratios, a table of the overall gear ratios in each gear was created by multiplying the gear ratio of the selected gear by the primary ratio and the selected final drive ratio. This process needed to be repeated for all of the final drive ratios as well as all of the transmission gear ratios. The results from these calculations were then tabulated for ease of analysis.

Once the overall transmission gear ratios for every possible final drive and transmission selection has been tabulated, the torque at the wheels can be found by multiplying the engine torque, using the torque of the engine found from the torque curve generated on the dynamometer, by the gear ratio of the drivetrain (Table 8**Error! Reference source not found.**).

Table 8: Torque at wheels in first gear with different final drive ratios

Torque at wheels for different gear ratios (N·m)					
1st gear (2.5)	14 T Driving	15 T Driving	16 T Driving	17 T Driving	18 T Driving
36 T Driven	931.0	869.0	814.6	766.7	724.1
38 T Driven	982.7	917.2	859.9	809.3	764.3
40 T Driven	1034.5	965.5	905.2	851.9	804.6
42 T Driven	1086.2	1013.8	950.4	894.5	844.8
44 T Driven	1137.9	1062.1	995.7	937.1	885.0
46 T Driven	1189.7	1110.3	1040.9	979.7	925.3
48 T Driven	1241.4	1158.6	1086.3	1022.3	965.5

The longitudinal force generated at the ground can be found by multiplying the torque applied to the wheels by the radius of the wheels. This calculation will need to be repeated for all the different final drive ratios and transmission gear ratios as when either of those two ratios change the torque at the wheels will also change (Equation (4.4)**Error! Reference source not found.** (Table 9**Error! Reference source not found.**).

$$F = \frac{T}{r} \tag{4.4}$$

Table 9: Output force at wheels for different final drive ratios

Output longitudinal force (N) in first gear					
1st gear (2.5)	14 T Driving	15 T Driving	16 T Driving	17 T Driving	18 T Driving
36 T Driven	4050.43 N	3780.40 N	3544.12 N	3335.64 N	3150.33 N

38 T Driven	4275.45 N	3990.42 N	3741.02 N	3520.96 N	3325.35 N
40 T Driven	4500.47 N	4200.44 N	3937.91 N	3706.27 N	3500.37 N
42 T Driven	4725.50 N	4410.46 N	4134.81 N	3891.59 N	3675.39 N
44 T Driven	4950.52 N	4620.49 N	4331.71 N	4076.90 N	3850.40 N
46 T Driven	5175.54 N	4830.51 N	4528.60 N	4262.21 N	4025.42 N
48 T Driven	5400.57 N	5040.53 N	4725.50 N	4447.53 N	4200.44 N

Once the longitudinal force was calculated the maximum acceleration of the car was found using Equation (4.5 (Table 10)**Error! Reference source not found.Error! Reference source not found.**. The mass of the car for the acceleration was assumed to be 266 kg of which the car is 191kg (wet) and the driver is 75kg. This initial calculation does not account for the torque loss due to rotational inertia.

$$F = M * a \tag{4.5}$$

Table 10: Maximum acceleration of gear ratio

Acceleration from output force (no traction limit) (m/s^2)					
1st gear (2.5)	14 T Driving	15 T Driving	16 T Driving	17 T Driving	18 T Driving
36 T Driven	18.113	16.905	15.849	14.917	14.088
38 T Driven	19.119	17.845	16.729	15.745	14.871
40 T Driven	20.126	18.784	17.610	16.574	15.653
42 T Driven	21.132	19.723	18.490	17.403	16.436
44 T Driven	22.138	20.662	19.371	18.231	17.219
46 T Driven	23.144	21.601	20.251	19.060	18.001
48 T Driven	24.151	22.541	21.132	19.889	18.784

The next step is to calculate the torque lost due to the rotational inertia of the drivetrain using Equation (2.12) (Table 11**Error! Reference source not found.**). The inertia of the drivetrain was found using the Solidworks models of all the parts. As everything in the drivetrain apart from the chain and driving sprocket rotates at the same rotational speed, the rotational acceleration of all the parts in the drivetrain will be the same. The rotational acceleration of the drivetrain was calculated by dividing the linear acceleration by the radius of the tyres (Equation (4.6**Error! Reference source not found.**)

$$\alpha = \frac{a}{r} \tag{4.6}$$

Table 11: Drivetrain assembly inertia values

Inertia of drivetrain components	mass (kg)	inertia (kg/m^2)	maximum torque loss (Nm)	torque loss (%)
Differential assembly	2.616	1.90E-03	0.089	0.43%
Wheel assembly	16.944	0.435	20.434	98.50%
rim assembly	3.325	0.0371	1.739	8.51%
axle assembly	2.108	3.03E-04	0.014	0.07%
Sprocket assembly	0.672	3.85E-03	0.181	0.87%

Once the rotational acceleration of the car is known the torque loss can be calculated by multiplying the overall inertia of the drivetrain and the rotational acceleration of the drivetrain (Equation (2.12) and then tabulated for each of the potential gear ratios (Table 12**Error! Reference source not found.**).

Table 12: Dynamic torque loss due to inertia for

Inertial torque loss (%)			
Gear	48 T	44 T	39 T
1st	34.0%	33.1%	29.7%
2nd	26.5%	25.4%	22.9%
3rd	21.6%	20.8%	18.5%
4th	18.4%	17.8%	15.7%
5th	16.5%	15.9%	14.0%
6th	15.2%	14.7%	12.9%

These results were then used to correct the torque that is provided to the wheels as the previously calculated values did not consider that there will be torque loss in the drivetrain (Table 13). Once the inertial loss is included in the calculations the reduction in acceleration from this will mean that the inertial loss is now incorrect. This calculation will need to be iterated as both the linear and rotational acceleration will decrease when a new higher gear ratio is selected, thus the overall inertial torque loss decreases as well (Table 12). This decrease in inertial torque loss is dependent on final drive ratio, with a higher gear ratio, with quicker acceleration resulting in a greater torque loss then a lower final drive gear ratio

Table 13: Wheel torque with 48 tooth sprocket after inertial

Torque including inertial losses 48-tooth (Nm)	
1st	721.07
2nd	561.37
3rd	456.13
4th	389.47
5th	348.15

6th	321.24

The next step is to calculate the output force including the inertial torque loss with the goal of predicting whether the car with the current gear ratio will have wheelspin. This was done by using conditional formatting on the output force table. To differentiate the outcomes two rules used were to display orange if the output force was greater than the static traction limit of the rear tyres, and red if the output force was greater than the dynamic traction force. The reason Table 14 was formatted this way is that if the cell is red the car will wheelspin at full throttle regardless of whether the clutch is suddenly released or released slowly. For the gear ratios that will not dynamically lose traction, the formatting is a gradient format where the darker the orange the more likely the car is to wheelspin if the clutch is suddenly released and the lighter the shade of orange the quicker the clutch can be released without breaking traction.

Table 14: Output longitudinal force with traction warning

Output longitudinal force (N)					
1st gear (2.5)	14 T Driving	15 T Driving	16 T Driving	17 T Driving	18 T Driving
36 T Driven	3947.20	3684.06	3453.80	3250.64	3070.05
38 T Driven	4166.49	3888.73	3645.68	3431.23	3240.60
40 T Driven	4385.78	4093.39	3837.56	3611.82	3411.16
42 T Driven	4605.07	4298.06	4029.44	3792.41	3581.72
44 T Driven	4824.36	4502.73	4221.31	3973.00	3752.28
46 T Driven	5043.65	4707.40	4413.19	4153.59	3922.84
48 T Driven	5262.94	4912.07	4605.07	4334.18	4093.39

Knowing the peak acceleration that the torque from the motor can produce is important, however this torque may not necessarily all be applied into accelerating the car as for some of these gear ratios the overall traction force that the tyres can produce will be exceeded and the torque will create wheelspin. The maximum traction force that the W-FS-18 cars rear tyres can produce is 4033N which will result in the car having a traction limited maximum acceleration of 15.162m/s^2 (Table 15). Based on the peak longitudinal traction of the rear wheels being 4033N the optimum gear ratio that will not be traction limited in first gear is using at 42-tooth driven sprocket in combination with a 16-tooth driving sprocket. This combination should not be able to lose traction.

Table 15: Maximum acceleration of gear ratio (traction limited)

Acceleration from output force (traction limited) (m/s^s)					
1st gear (2.5)	14 T Driving	15 T Driving	16 T Driving	17 T Driving	18 T Driving
36 T Driven	14.823	13.835	12.971	12.208	11.529

38 T Driven	15.162	14.604	13.691	12.886	12.170
40 T Driven	15.162	15.162	14.412	13.564	12.810
42 T Driven	15.162	15.162	15.132	14.242	13.451
44 T Driven	15.162	15.162	15.162	14.920	14.091
46 T Driven	15.162	15.162	15.162	15.162	14.732
48 T Driven	15.162	15.162	15.162	15.162	15.162

The traction limited table shows that the current gear ratio that is being used in the W-FS-18 car is traction limited in first gear. In terms of the acceleration run this is not ideal as it means that the driver cannot use the full power that the engine can provide until the car is in second gear. The traction limited table does not show the complete picture though as this table is showing the acceleration assuming that there is time for the load transfer to happen which will only happen if the clutch is released slowly, not suddenly.

To accurately evaluate each potential gear ratio the key variables that need to be calculated are the top speed, potential acceleration (Equation (4.9)**Error! Reference source not found.** and also time it takes to accelerate through each gear(Equation(4.8)**Error! Reference source not found.**. Once all these variables have been calculated a theoretical acceleration run for each gear ratio can be generated.

Prior to calculating theoretical acceleration runs a general overview of each gear, for each potential gear ratio was produced, an example of this is Table 16, which shows the data for the 48-tooth gear ratio in first gear . This table has the summary of all the key information needed when calculating a theoretical acceleration run.

$$a = F/M \tag{4.7}$$

$$\Delta T = \Delta V/a \tag{4.8}$$

Table 16: Gear ratio selection table

Engine sprocket number of teeth	16
Differential sprocket number of teeth	48
Gear	1
Gear ratio	16.4
Torque at wheels (exl losses) (Nm)	1086.25
Torque at wheels (inc losses) (Nm)	716.93
Longitudinal output force (exc losses) (N)	4751.75
Longitudinal output force (inc losses) (N)	3136.16
Top speed (Km/h)	48.17
Top speed (m/s)	13.38
Expected acceleration (m/s^2)	11.57

Expected acceleration (g)	1.18
Time in gear (s)	1.16
Max rotational acceleration (rad/s^2)	50.62

4.1.3. Theoretical acceleration run

A theoretical acceleration run of the car is then calculated for each gear ratio using the values in the gear ratio selection table (Table 16). This was created by using the acceleration, top speed and time in each gear to find the distance and velocity of the car at different points during its 75m run (Equation (4.9)**Error! Reference source not found.**. This data was then plotted on an XY plot to enable easy visual analysis of the results (Figure 49). In Figure 49 and Figure 50 each time the driver changes gears, there will be a pair of dots on the graph. These dots denote the time which the car is shifting and thus has no acceleration.

$$D = V_i * T + 0.5 * a * T^2 \quad (4.9)$$

When calculated theoretically, all the gear ratios showed similar results in terms of the time to complete the acceleration run. This does seem counter intuitive as it would seem that the decrease in torque would cause the car to have a slower acceleration. After more analysis it was found that this advantage is cancelled out by the fact that a drivetrain with a lower gear ratio will also spend more time in a lower transmission gear. The difference between the gear ratios of each of the transmission gears, is much larger than the difference between the different final drive ratios. When the car is in a lower gear, even with a lower final drive gear ratio, the car will have more torque than the same car with a higher final drive gear ratio being in a higher gear. This means that while the car with the lower final drive ratio is still in the lower gear it will have greater acceleration then that same car with the higher final drive gear ratio in a higher gear.

The distance plot initially does seem deceiving though, because in first gear from a standing start the faster accelerating gear ratios have a shallower gradient and appear to cover less distance in the same time as the slower accelerating lower gear ratios (Figure 49). In reality this is not the case as the distance covered is not linear, however the theoretical model is plotted using a linear line fit between data points. Using a plot that has a linear line fit also makes it appear that the speed suddenly increases when changing gear but, as there is no acceleration at this point, the gradient of the line during the gear change should be the same as the gradient right before the gear change. Using a linear chart with straight lines does not significantly decrease the accuracy of the chart though as the initial and final points in each gear are still correct and the graph is only used as a visual representation.

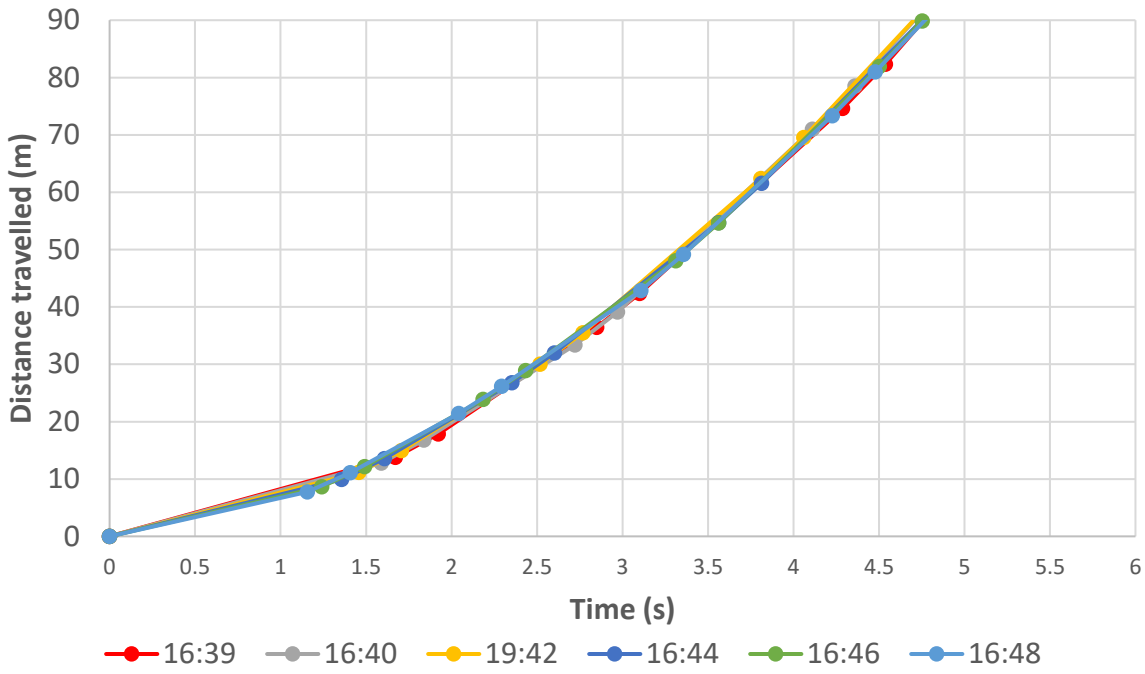

Figure 49: Distance vs time plot of acceleration test with different gear ratios

The velocity plot was mainly used as verification of the distance plot. Since the car will cross the line at around 100km/h, this means that the time to accelerate from 0 to 100 will not be far off the time to complete the 75m acceleration run.
The velocity plot is also the best visual representation of which gear ratio has the greatest acceleration as the steeper the gradient of the line the faster the car is accelerating (Figure 50) as well as being considerably easier to see when the can is shifting gears.

Initially the gear ratio does not seem to have much effect on how quickly the WESMO car can do the acceleration run, in both track testing and theoretical calculations the gear ratio does not seem to have much of an effect.
Under closer scrutiny all the gear ratios from 16:42 – 16:39 only have to change gears 3 times whereas the others have to change gears 4 times. This is an important factor to consider as whenever the driver needs to change gears there is always a chance of the driver making a mistake and losing time. The other major consideration that is ignored on these plots are the likelihood to wheelspin. When accelerating off the start line the higher gear ratios are much more likely to wheelspin, meaning that a higher level of driver skill will be required to consistently launch the car without either spinning the wheels or changing gears at an engine RPM that is below the optimum (short shifting).

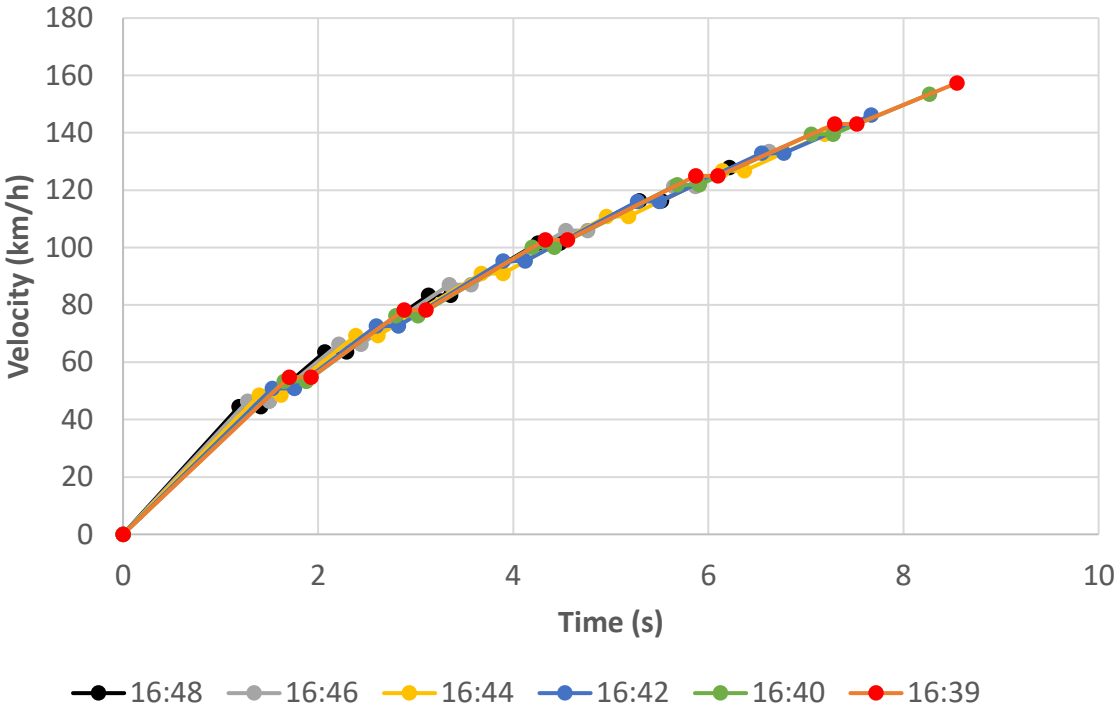

Figure 50: Velocity vs time plot of acceleration test for different gear ratios

4.1.4. Weight reduction effect

According to the theoretical acceleration runs the easiest way to see a large improvement in the acceleration event would be to reduce the overall weight of both the driver and car. Just reducing the weight of the car by 6kg as well as having a driver that weighs 60 kg instead of the usual 75kg saves approximately a tenth of a second in the completion time of the acceleration run. Reducing the car by 6kg would not be too difficult as the car could be tested and raced with minimal fuel. Operating the car without an undertray and having 2 L (1.5kg) of fuel instead of 4 L (3kg) would have already saved 3kg from the total weight of the car.

Reducing the weight increases the acceleration of the car meaning that car reaches higher speeds in the same period of time. In Figure 51 this can be seen from the car reaching the top speed of each of the gears quicker, both in terms of distance as well as time.

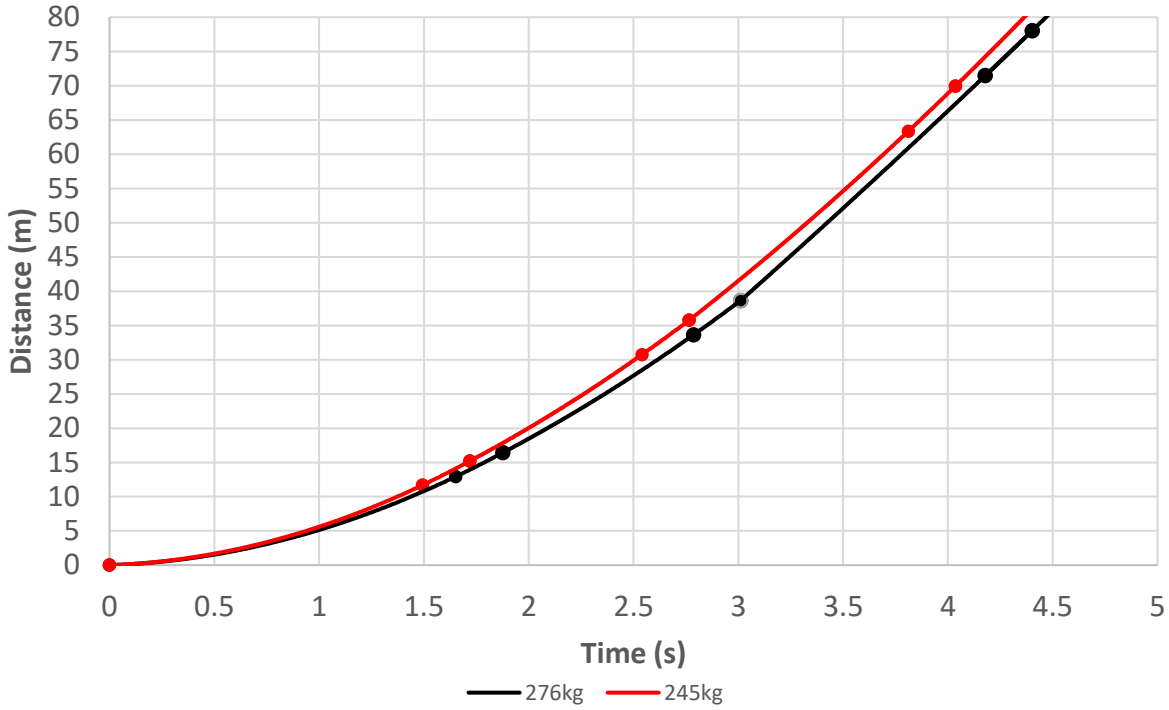

Figure 51: Theoretical acceleration run for 276kg ca r with driver vs 245kg car with driver

4.2. Track testing

One of the plots that is autogenerated by MoTeC is the gearing chart. The gearing chart autogenerated by the MoTeC unit, plots the RPM of the engine against the speed of the vehicle. This plot can also be generated to have different coloured data points depending on which gear the car is in. This gearing chart can be used to find the top speed in each gear as well as how well suited the selected gear ratio is to the track that the car is racing around. This is useful for both analysing the gear ratio for the acceleration event as well as the autocross event.
In the acceleration testing the gearing chart indicates whether the car undergoes wheelspin or not. The gearing chart could also be used to find the ideal RPM to launch the car at which is vital to ensure quick acceleration times.

4.2.1. Autocross testing

The ideal gear ratio for an autocross track will have the data points for the next gear start at approximately the speed where the previous gear was reaching the RPM limit of the engine. The final drive ratio is to low if there appears to be a large amount of data points in lower gears but very little in higher gears. The large amount of data points in lower gears is due to each gear having a much higher top speed and might not be able to get out of first gear on many corners due to tight nature of the testing track. If a final drive ratio is too high the car will require shifting too often and will be much more likely to require shifting at an awkward time. To prevent having to shift at an awkward time the driver will often short shift. Short shifting is easy to see on a gearing chart as there will be a bunch of data point in low RPM ranges. In low RPM ranges the ca r does not produce power very efficiently and the acceleration will suffer.

The 48-tooth rear sprocket gear ratio is clearly too short as can be seen by the amount of data points that fall at low RPM ranges (Figure 52). This means that the gear ratio is very short, and the driver is having to short shift often. This will definitely have a negative impact on the performance of the car as the acceleration coming out of the corner will be drastically lower than if the car was in the optimum gear.

The gearing chart for the 44-tooth char appears to be the best in terms of how well the gears suit the autocross testing track (Figure 53). This can be seen by having the data points gear reasonably well distributed between the different gears as well as almost no data in low RPM ranges. Having little data points in low RPM ranges means that the driver never felt like they

was required to short shift and that they would have enough time in the current gear to finish the corner before needing to change gears. During the 44-tooth autocross test the car was stopped mid test as the car was making a unusual sound. The sound was coming from the chain tensioner which was starting to fail. It was decided to continue the testing as only a few more laps were required to complete the data. The tensioner did not fail but needed to be replaced after the testing session. The stationary data values had to be filtered out and so when it came to processing the data the easiest way to achieve this was by adding a gate to the data to remove any data where there was zero lateral acceleration, this only happens when the car is stationary.

When analysing the 39-tooth gear chart it can be seen that there is an excessive amount of data points in first gear and almost no data points in third gear (Figure 54). This is one of the key signs that the 39-tooth gear ratio is much too low and is not optimised for the autocross track. There are also lines of data points that vary from the normal trend shown by red circles on Figure 54. These data points happen when the car downshifts and the slip ratio of the rear wheels increases due to the additional engine braking force. These alternate lines are not as apparent in the other data sets due to the other gear ratios in the gears being much shorter and thus having a smaller difference in speed between each gear. Having a large difference in speed between each gear means that during a downshift the change in RPM of the engine is much larger.

The 48-tooth and 39-tooth autocross data were collected before the gear shift sensor was connected. The 39-tooth sprocket was meant to be retested with the gear sensor connected but due to time constraints and the multiple breakdowns of the W-FS-18 it was decided that this data is accurate enough to be included in the analysis.

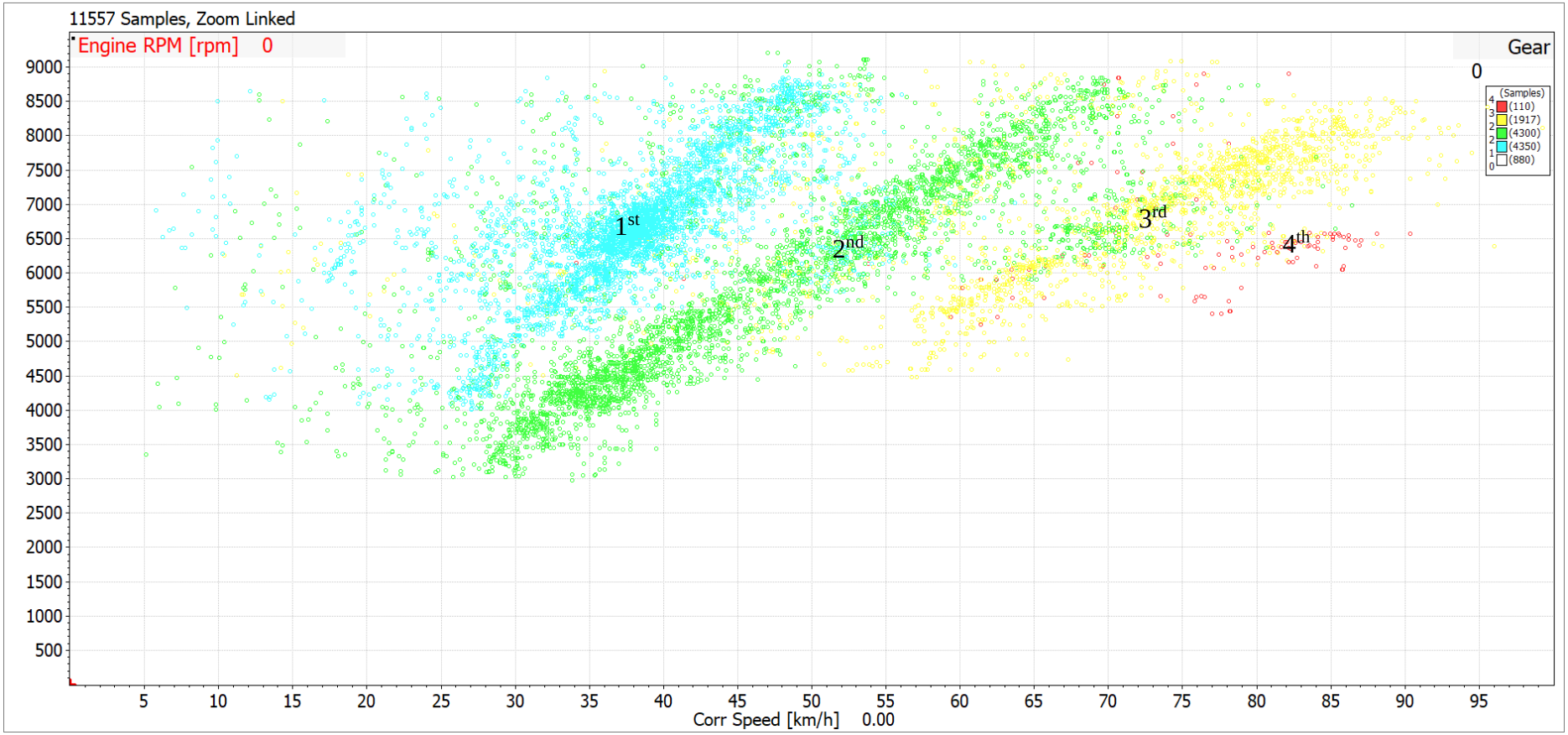

Figure 52:48-tooth rear sprocket MoTeC autocross gearing chart

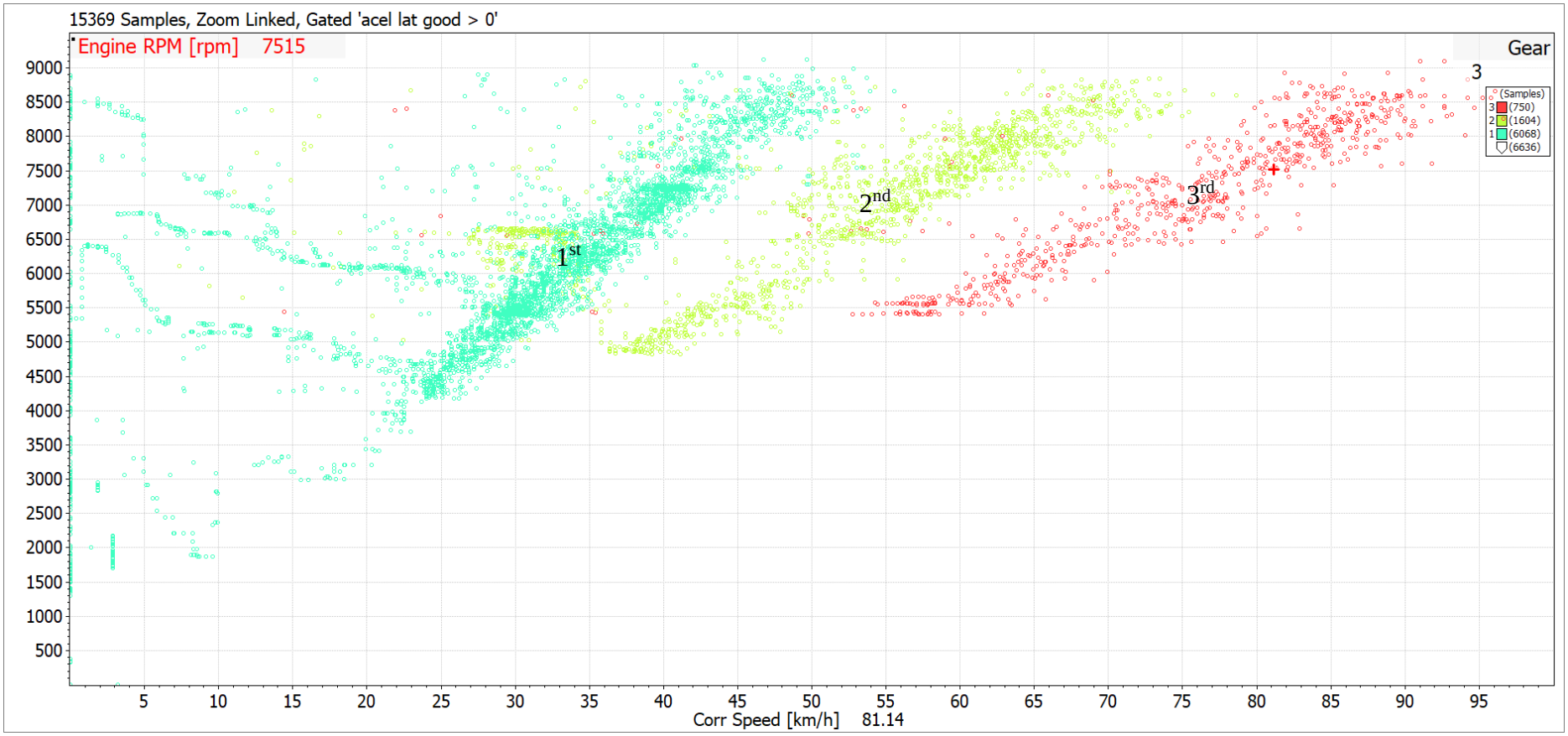

Figure 53: 44T rear sprocket MoTeC autocross gearing chart

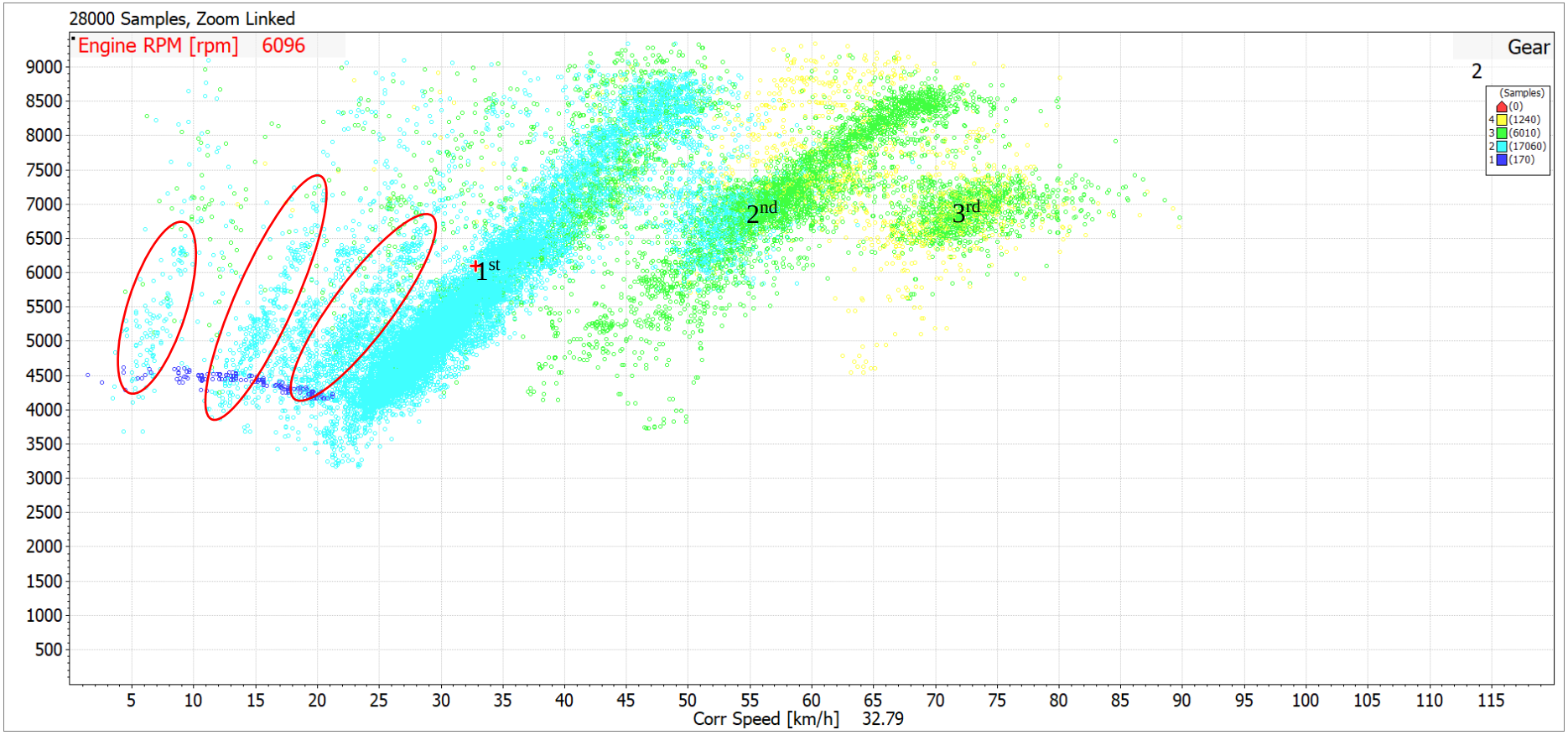

Figure 54: 39-tooth rear sprocket MoTeC autocross gearing chart

4.2.2. Acceleration

During the 75m acceleration testing it is useful to know how fast the car can go in each gear as well as how many gear shifts are required to complete the acceleration run.

Using the gearing chart is a good way to accurately analyse the selected gear ratio, as the top speed of each gear, when the gear shifting occurs, as well as if the car is undergoing wheelspin. For easy analysis, each different gear has different coloured data points and each gear is denoted by a line (Figure 58). The key data that of the acceleration gearing chart is the trend of the data in first gear as well as how many gear shifts were required in the duration of the acceleration test.

The data points for the initial launch of the car in first gear can very accurately tell whether a car had excessive wheelspin or not. Wheelspin results in the car accelerating slower and thus wheelspin decreases the performance of the car in the acceleration event. The ideal acceleration would have minimum wheelspin and would require as few gear shifts as possible. Wheelspin can be seen on the gearing chart by having data points that follow a very steep gradient as the motor RPM rapidly increases but the velocity of the car does not increase much.

In the 48-tooth rear sprocket acceleration run the gear ratio is clearly too short. This can be seen primarily in the data for first gear. The data shows that the car had major wheelspin almost instantly from launch and the driver had to reduce the throttle to regain traction before the car could accelerate again. (Figure 58). Either having excess wheelspin or short shifting have a noticeable negative impact on the overall performance of the car during the acceleration testing. The 6th run was the only one where there was minimal wheelspin and no short shifting which resulted in it being the quickest to complete the 75m. (Figure 55**Error! Reference source not found.**). The first two runs where slightly slower than run 6 as the driver was short shifting and run three through five were much slower due to having excess wheelspin. The large variation in the completion time of the acceleration runs shows that the 48-tooth gear ratio is not ideal for the acceleration event.

	Kartsport Hamilton, 48 T track testing Scott Harvey, W-FS-18 24/02/2021, 4:10:08 PM, 48T accel run							Eclectic
	Lap 1	Lap 2	Lap 3	Lap 4	Lap 5	Lap 6	Lap 7	
Acceleration track	00:04.436	00:04.434	00:04.589	00:04.580	00:04.555	00:04.405		00:04.405
Restart loop (Start)	01:14.421	01:04.388	01:02.612	01:03.393	01:02.742	01:06.627		01:02.612
Restart loop (End)		00:00.963	00:00.078	00:00.859	00:00.828	00:01.063	00:00.408	00:00.078
Restart loop							01:22.634	01:22.634
Totals	01:18.857	01:09.785	**01:07.279**	01:08.831	01:08.125	01:12.095	01:23.042	02:29.730

Figure 55: 48 tooth sprocket acceleration run times

The 44-tooth rear sprocket proved to be easier to launch with less of a tendency to wheelspin then the 48-tooth gear ratio. This can be seen by the increase in consistency when compared to the 48-tooth gear ratio, with every acceleration run apart from one being within 0.1 seconds of each other.

The 44-tooth had the problem that the driver said he was either having to shift a few meters before the finish line or stay in the same gear and lose acceleration for those last meters due to the engine being at its RPM limit. This can be seen by the car finishing the acceleration course at a slightly lower speed then the other acceleration runs. This is a problem and will have had a negative effect on the testing times. If there was more time testing with a 42-tooth sprocket during an acceleration run would have been optimal as it has a little more top speed and would be able to complete it in third gear without hitting the RPM limiter.

	Hams, 04/05/21 track day SH, W-FS-18 4/05/2021, 4:49:51 PM, 44 t acceleration Final							Eclectic
	Lap 1	Lap 2	Lap 3	Lap 4	Lap 5	Lap 6	Lap 7	
Restart loop (End)	00:00.330	00:00.158	00:00.082	00:00.098	00:00.234		00:00.384	00:00.082
Acceleration Run	00:04.373	00:04.444	00:04.345	00:04.404	00:04.365	00:04.345		00:04.345
Restart loop (Start)	00:56.549	00:54.754	01:26.877	00:54.082		00:59.686		00:54.082
Restart loop					00:52.800		01:24.204	00:52.800
Totals	01:01.252	00:59.356	01:31.304	00:58.584	**00:57.399**	01:04.031	01:24.588	01:51.309

Figure 56: 44-tooth acceleration runs

On the acceleration run that was completed before the exhaust snapped the W-FS-18 got very close to a sub four second acceleration time (Figure 57). On the final 39-tooth sprocket testing day, the driver was launching very consistently with every launch apart from the

fastest being within a tenth of a second of each other (**Error! Reference source not found.**). This matches up to what was predicted as the driver could launch at higher RPM and had more time to react before needing to shift out of first.

	Kartsport, 39T track day SH, W-FS-18 27/04/2021, 4:12:32 PM. Final 39T accel						Eclectic
	Lap 1	Lap 2	Lap 3	Lap 4	Lap 5	Lap 6	
Restart loop (End)	00:00.485	00:00.095	00:01.365	00:00.550	00:00.255	00:00.072	00:00.072
Acceleration track	00:04.316	00:04.258	00:04.271	00:04.312	00:04.272	00:04.251	00:04.251
Restart loop (Start)	00:56.803	00:53.540	01:26.515	00:54.155	00:52.823	00:59.327	00:52.823
Totals	01:01.604	00:57.894	01:32.150	00:59.018	**00:57.350**	01:03.650	00:57.146

	Hams, 23/03/21 track day , 23/03/2021, 2:51:15 PM, accel run exhaust
	Lap 1
Restart loop (End)	00:00.040
Acceleration track	00:04.035
Totals	**00:04.075**

Figure 57: 39-tooth sprocket acceleration run times (both sessions)

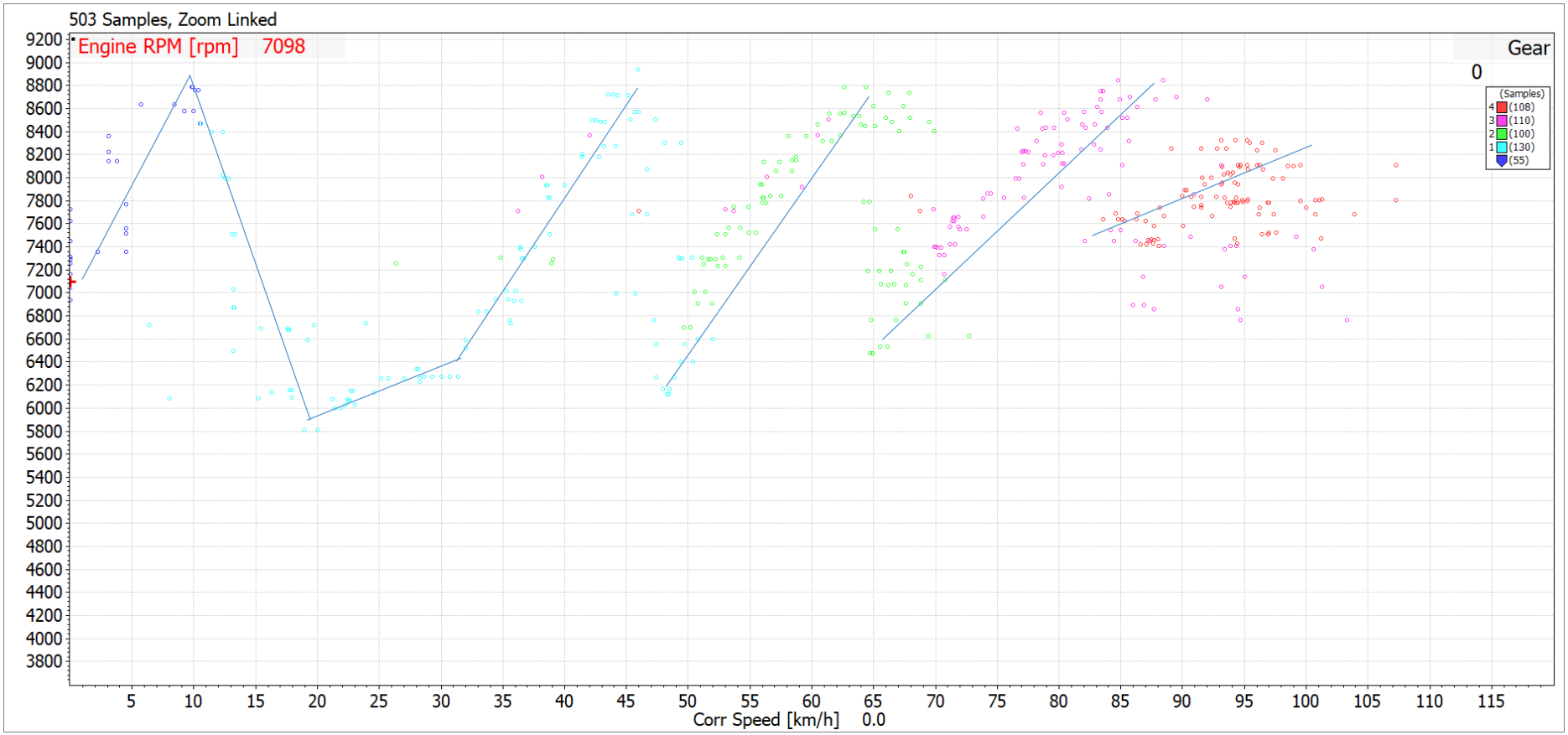

Figure 58: 48-tooth rear sprocket MoTeC acceleration gearing chart of run 3

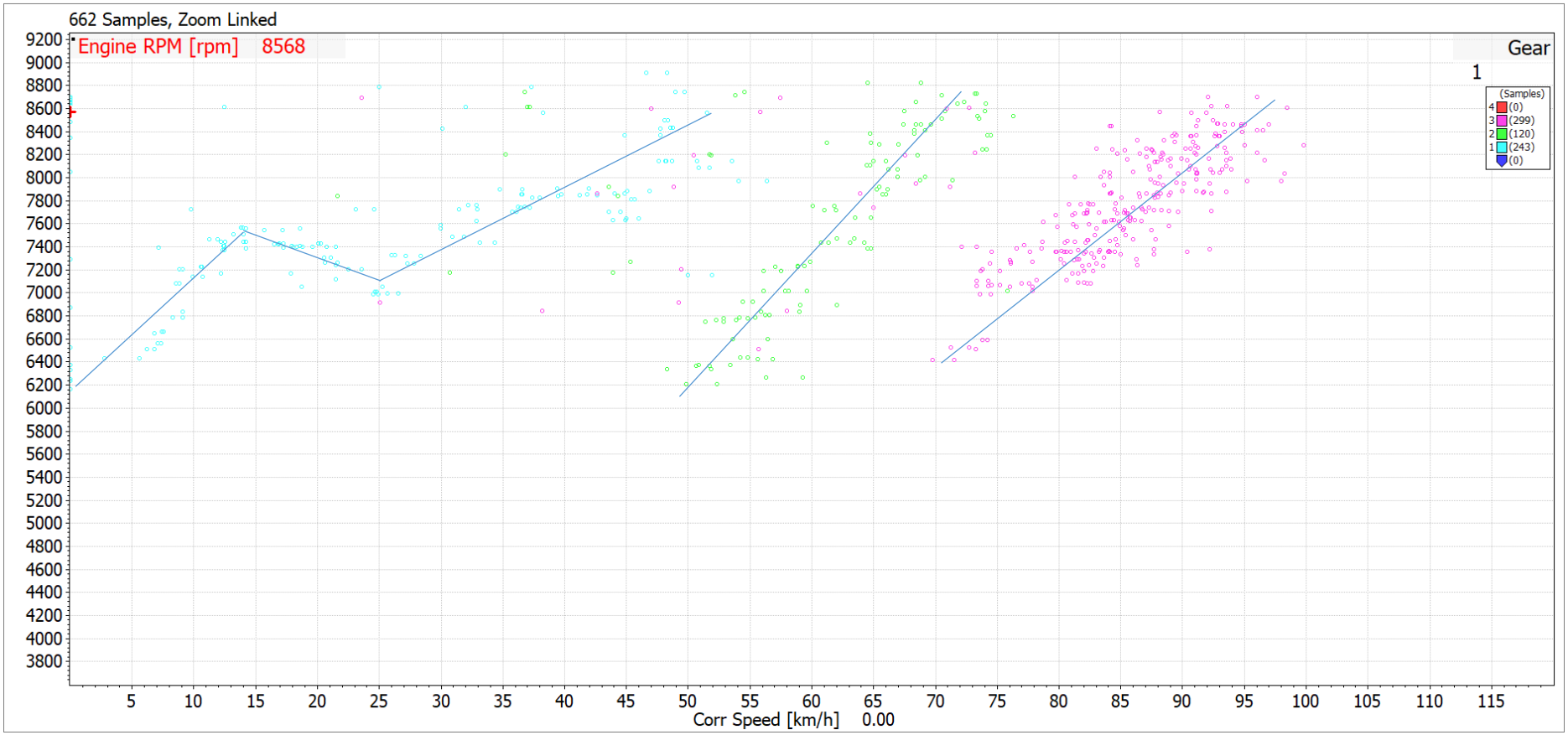

Figure 59: 44T rear sprocket MoTeC acceleration gearing chart of run 4

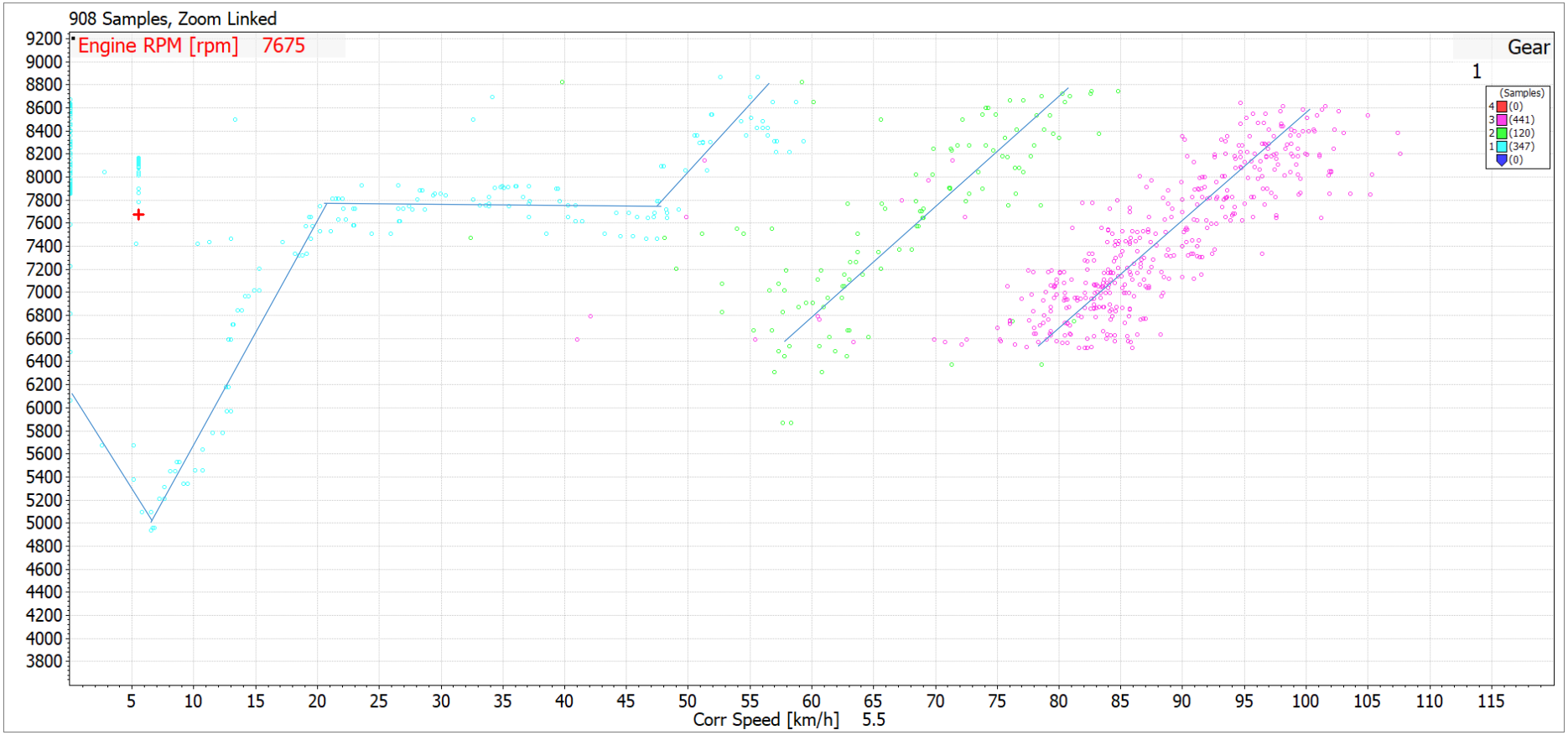

Figure 60: 39-tooth rear sprocket MoTeC acceleration gearing chart of run 4

The theoretical and testing gearing chart for the 48-tooth gear ratio matches up reasonably well, with only a slight variation between the two (Figure 61). The gear shifts in this testing run also match up very well with the theoretical shifting points which were selected as 9000 which is 250 RPM short of the engines RPM limiter.

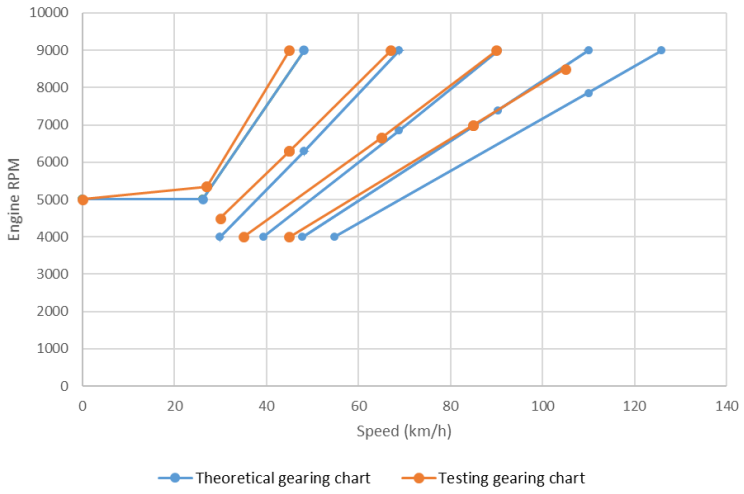

Figure 61: 48-tooth rear sprocket theoretical vs testing gearing chart

The 39 and 44-tooth theoretical gearing charts matched up reasonably well to the experimental gearing chart (Figure 62). However, during both of these runs the driver was shifting slightly earlier then the optimum point to change gears, especially with the 39-tooth gear ratio.

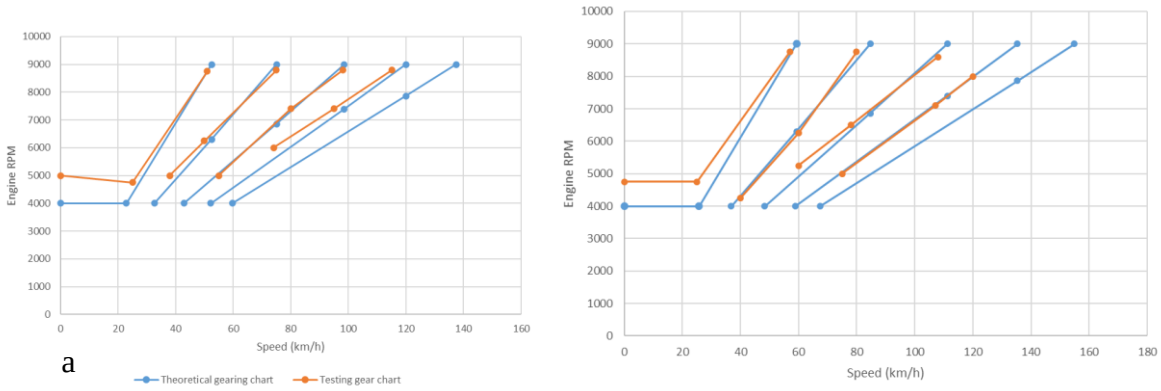

Figure 62: 44-tooth (a) and 39-tooth rear sprocket (b) theoretical vs testing gearing chart

The 39-tooth rear sprocket resulted in almost no wheelspin (**Error! Reference source not found.**), this is shown on the gearing chart with there being no cluster of data that has high RPM while also having low speed. Having no wheelspin means that the contact between the wheels and the road will be in the static coefficient of traction, resulting in a much larger maximum traction force and greater acceleration. During the acceleration run with the 39-

tooth sprocket thew car also had to only change gears twice as the car was just hitting the RPM limiter in third right on the finish line. Having the driver only have to change gears twice instead of three means that the car has at least 0.25 seconds more time with power provided to the wheels, due to having one less period where the torque provided to the wheels is zero. Having two gear shifts instead of three coupled with the reduced wheelspin could be one of the reasons why the acceleration runs were all considerably quicker, with the W-FS-18 car recording its first ever sub 4 second acceleration run.

The acceleration times that the driver putting down for testing were fairly consistent not only between his runs, but the acceleration run times when running the 48-tooth rear sprocket was also consistent with the official times that the W-FS-18 achieved during the 2018 Formula student competition. One thing that was apparent was that the times were very dependent on the start. The runs where there was little or no wheelspin were consistently faster as is to be expected. Having a gear ratio that has slightly less torque supplied to the wheels will hopefully reduce the likelihood of wheelspin and potentially help get consistently faster times.

4.3. Inertia reduction

4.3.1. 16-inch tyre

Changing to smaller 16-inch tyres is one of the ways that the overall inertia of the drivetrain components could be reduced. However, this reduction of inertia will be slightly offset by the fact that all the drivetrain components will have a greater rotational acceleration. The reason the rotational acceleration will increase is because the radius of the tyre has decreased and to accommodate this the gear ratio will have to decrease to offset the smaller radius of the tyre. The smaller gear ratio will decrease the torque but also have less of a decrease in rotational speed.

The 2018 WESMO team decided it was a good idea to change wheels from the 20.5x7 inch wheels that had been used by previous years WESMO teams and replaced with smaller 18x6 inch wheels. This change in wheels resulted in a large decrease in the rotational inertia of the drivetrain and thus would have resulted in a much more efficient transfer of torque from the

engine to the wheels (Figure 63).

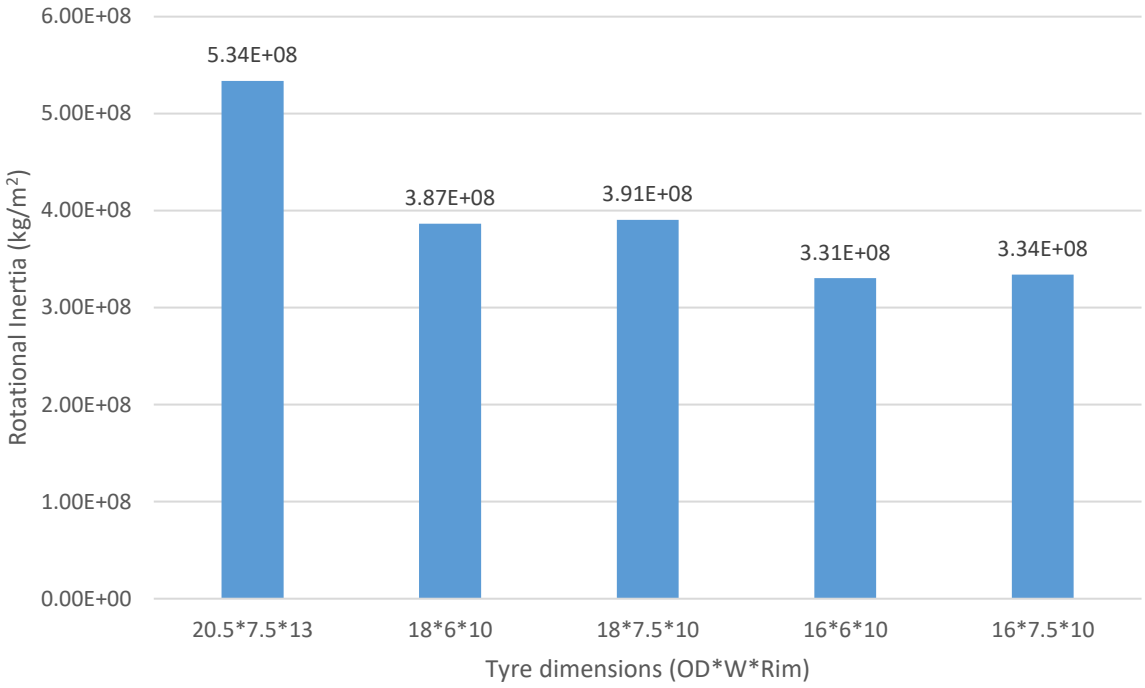

Figure 63: Rotational inertia of different Hoosier formula student tyre dimensions

Since the gear ratio needs to be adjusted depending on the radius of the tyre, in order to generate the torque loss comparison, the gear ratios were adjusted so that with the same torque applied the wheels will all have the same force applied at the contact patch. This also means that the linear velocity of the tyres at the contact patch will be ethe same. From these calculations it can be seen that as the radius of the tyres decrease so does the inertia even though the rotational speed does have to increase to compensate for the decreased radius of the tyres (Figure 64).

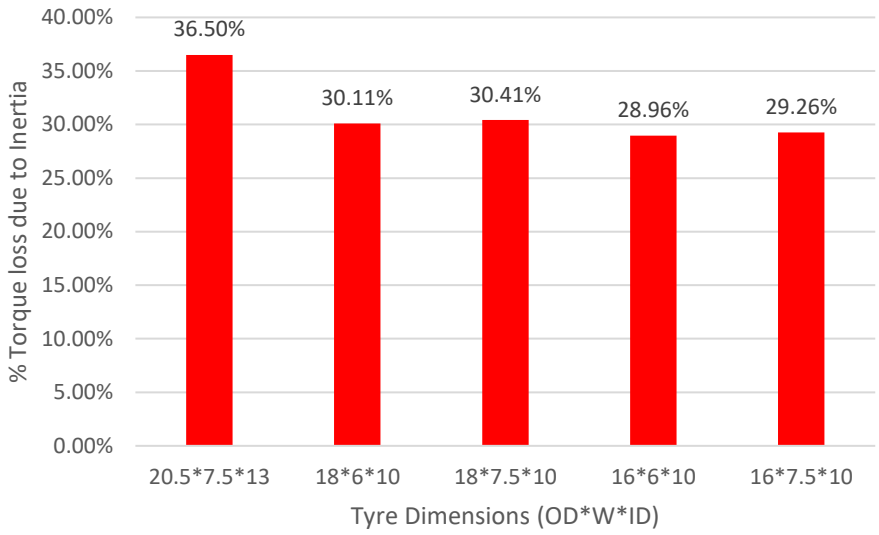

Figure 64: Inertial torque loss of different Hoosier tyre dimensions

The inertial torque loss due to the increase in rotational speed from the 16-inch wheels is smaller than the decrease in inertial losses due to the reduced moment of inertia of the drivetrain with the 16inch wheels. Not only do the 16-inch tyres result in a more efficient drivetrain, but they are also just over 460 grams lighter per wheel meaning that changing the wheels results in a 1.8kg weight reduction.

With the 7.5-inch wide 16inch tyre the overall torque loss will slightly decrease when compared to the current tyres 18x6 inch tyres (Figure 64), however with the increase in width of the 16x7.5 inch tyres the overall traction will also increase.

4.3.2. Alternate materials

Another way the overall inertia of the drivetrain could be reduced would be by reducing its mass via incorporation of alternative materials. One such approach could be through incorporating more carbon fibre into the design. Carbon fibre is increasingly being used in high performance motorsport. For comparison, the specific strength of Carbon Fibre is around 2400kN·m/kg whereas the specific strength of 6000 Series Aluminium alloy is 115kN·m/kg and for Din2.67 tool steel it is around 200kN·M/kg. The reason carbon fibre is only used in high performance applications is due to the increased cost and complexity in manufacturing, due to the parts having to be set in a mould. Carbon fibre also cannot be easily machined after it has been set without causing damage such as delamination.

Carbon fibre half shafts

One part that could be manufactured out of carbon fibre would be the half shafts. Carbon fibre driveshafts are increasingly being used in high-performance cars due to the high stiffness and light weight of the resultant parts.
The current half shafts are made out of DIN2.63 tool steel which has an extremely high strength but is also very heavy. The reason that the driveshaft is made out such a high grade of steel is because the rear drivetrain can have close to 900Nm of torque applied to it on a regular basis. This means that each half shaft has close to 450Nm going through it under normal operating conditions. However previous half shafts that had been designed to take 600Nm have snapped due to extreme loading cases so the half shafts need to be designed to take 800Nm of torque. The reason the shafts are designed to a rating of 800Nm is because the maximum grip of the rear wheels is 4033N and the half shafts were designed to a factor of safety of 1.75. Using the traction limit and the factor of safety, the calculated torque that each of the half shafts are rated to 801.6Nm.

Most of the current ways to manufacture carbon fibre driveshafts is to roll wrap the carbon fibre into a tube with metal insets glued in each end. The insert at each end is required because manufacturing a carbon fibre spline is almost impossible, as the carbon needs to be layered over a mound and set and the shape of a spline is too intricate and complex for this process. A spline also cannot be machined into the carbon fibre after its set either, leaving metal inserts as the optimal method for adding a spline to carbon.

Since the stress that half shafts will be exposed to is torsional stress, the orientation of the carbon layers will have a large effect on the overall strength of the part. The optimum orientation for torsion is 45º so a good starting laying setup would be laying the sheets at ±45º. Some driveshaft manufactures also include layers that are ±30º to decrease the torsional stiffness of the shaft allowing some flex across the driveshaft. This flex of the driveshaft decreases the stress on other parts in the drivetrain but reducing the angular impulse caused by a sudden increase in torque.
Designing a driveshaft out of carbon fibre requires a large amount of research into how to effectively bond the metal inserts to the carbon fibre as this is the most commonly where driveshafts fail. In 2004 it was experimentally proven that the strength of a bond increases linearly as the circumference of the tube increases however the strength increases asymptotically as the length increases. This phenomenon is called Volkersen theory with flat

surfaces but also works with cylinders. Applying this theory, it would be logical to increase the diameter of the half shafts to increase the strength of the adhesive bond, while also considering that increasing the diameter of the half shafts will increase their rotational inertia.

Table 17 shows an example calculation for the minimum radius of the half shafts such that the shear stress in Henkel Loctite® Hysol® EA 9658 Aero Epoxy Adhesive (Equation (4.10), a common carbon-metal adhesive is below the allowable shear stress. This calculation assumes that the adhesive has a thickness of 0.2mm and that the adhesive fails and not the bonding between the adhesive and the material. 0.2mm (0.08 in) was used as research done by MIT into the optimum thickness of adhesive for carbon-metal bonding (Cobi, 2012). Experimental research would have to be done on how to prepare the tool steel prior to applying adhesive to ensure the bond is strong enough.

$$\sigma = \frac{F}{A} \tag{4.10}$$

Table 17: Calculation for Hysol® EA 9658 shear strength

Henkel Loctite® Hysol® EA 934NA Epoxy Adhesive	
Shear strength (psi)	4500
Shear strength (Pa)	31026420
Shear strength (MPa)	31.02642
Factor of safety	1.5
Allowed shear strength (MPa)	20.68428
Torque applied (Nm)	800
radius of insert (mm)	10.5
radius of insert (m)	0.0105
glue thickness (m)	2.03E-04
length of bond (mm)	60
length of bond (m)	0.06
Force (N)	76190.47619
Bonded area (m^2)	0.003958407
Stress (Pa)	19247763.34
Stress (MPa)	19.24776334

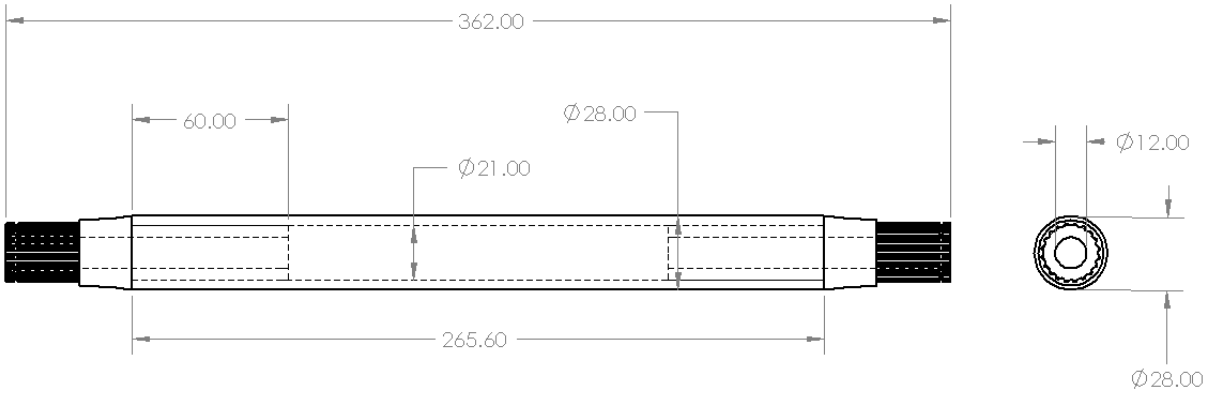

Figure 65: example carbon fibre half shaft design used for inertia comparison

The longer of the tool steel half shafts weighs 903 grams and has a rotational inertia value of $6.85x10^{-5}kg/m^{2.}$ An example of the same shaft made from carbon fibre (Figure 65) weighs 580 grams and has a rotational inertia value of $5.6x10^{-5}kg/m^2$. The insets are made out of the same steel as the current half shafts and the properties of the carbon were based from the material properties of the carbon fibre used by K. Cinar, for his research into designing carbon fibre driveshafts (Figure 66). If the shorter half shaft was also made from carbon fibre it would weigh 524 grams and have a rotational inertia of $4.9x10^{-5}kg/m^2$.

	Resin	HS Carbon fiber (24K)	Adhesive
Viscosity (mPas)	750 ±150		120
Density (g/cm^3)	1.10 ±0.05	1.79	0.97
Tensile strength (Mpa)	75-80	4900	22.6
Elastic modulus (Gpa)	3.2 -3.7	250	1.55

.

Figure 66: Carbon fibre properties used in carbon driveshaft (Cinar, Ersoy, & Unal, 2018)

If carbon fibre half shafts were to be implemented by WESMO, more research would need to be done on the best fibres, weave patterns as well as layer orientation to ensure that the carbon fibre does not fail.

Carbon fibre rims

Another part that could potentially be made out of carbon fibre is the rims. Manufacturing the outer shell of the rims is also not very complex but would be a lot more expensive than half shafts due to needing much more material since the rims have a larger geometry. Making wheel centres out of carbon fibre is a complex and expensive process and is usually only done by those with access to specialised manufacturing facilities. Most of the expense comes

from creating the mould cavities which the carbon fibre will be moulded to. The most common way that formula student team do this is by using a CNC machine to manufacture the mould out of a piece of billet aluminium. Manufacturing the moulds is not that complex as it is based on a CAD file of the part. Using the CAD file of the part, an accurate mould can be created using the cavity/mould tool on Solidworks, ensuring that the parameters of their cavity and the design is able to be easily milled using a CNC mill. The design will also have to have a reasonably simple geometry that is designed to be easy to layup without inclusion of flaws such as voids and wrinkles. If the final part has any voids or wrinkles the part will fail at much lower stresses, then the part was designed to withstand. This occurs as voids create stress concentration while wrinkles result in the fibres being in the wrong orientation which decreases the strength and stiffness and increases the chance of delamination.

With the wheel centres making up only a small percentage of the overall weight of the rim, and considering that their effective radius of mass and rotational inertia is small, and these parts having a high level of complexity in manufacturing, building this part out of carbon fibre would not be recommended as the benefits are not worth the extra cost and complexity of manufacturing.
Making the rims out of carbon fibre is beneficial due to the large rotational inertia caused by the outer rims which have a much larger effective radius then the rest of the drivetrain parts. The large inertia value results in a large torque loss meaning that any reduction in the mass of the rims will have a noticeable reduction of the overall torque loss, meaning a higher torque is provided to drive the wheels.

The loading conditions on rims are constantly varying and will usually have combined loading. Selecting the orientation of the carbon fibre layers often takes a considerable amount of research and background knowledge due to carbon fibre directional properties.
The loading on the rims can have any combination of torsion for longitudinal acceleration, bending due to the downforce applied through the rims as well as compression/tension during lateral loading. With metal rims this variety of loading directions does not matter much as metals have isotropic properties. Carbon fibre is an anisotropic material, which results in exceptional strength in the same plane as the fibres but very little strength and stiffness in any other direction. This is the main reason Formula student teams who design their outer rims out of carbon fibre often have a problem of the tyres debeading due to excessive displacement of the rim bead. This displacement happens due to the nature of the loading of

the rims which can result in the stress being applied perpendicular to the orientation of the fibres, which results in a lower stiffness of the rim than the designed stiffness.

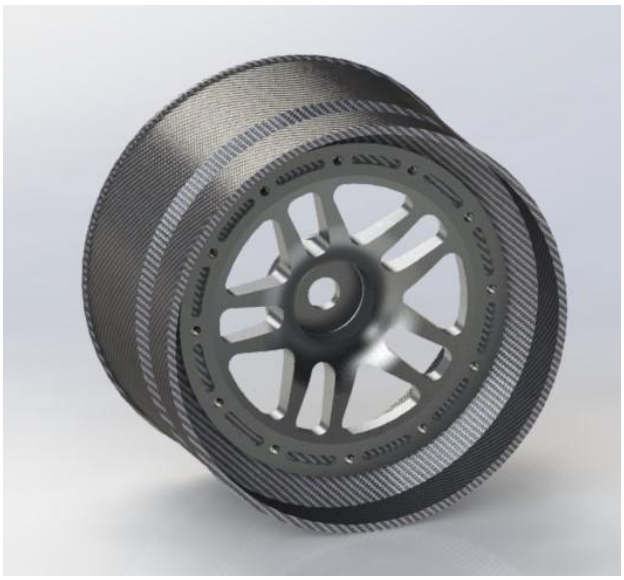

Figure 67: Example Carbon fibre rim For W-FS-18

The mass of the carbon fibre outer rim combined with the aluminium wheel centres (Figure 67) is 1.46 kg per rim with a rotational inertia of $1.26x10^{-2}kg/m^2$. By comparison the mass of the 6061 series aluminium is 1.97 kg per rim and has a rotational inertia of $1.95x10^{-2}kg/m^2$. If carbon rims were used for all four tyres on the car, there would be an approximate weight saving of 2kg and also decrease the torque loss due to inertia by 3%.

Before either of these parts could be designed out of carbon fibre and implemented onto the car, they would need to have comprehensive research completed on their feasibility, including how to manufacture parts out of carbon fibre in such a way that the end product meets the required specifications. Once the knowledge of carbon fibre manufacturing techniques processes is well researched, these parts can be properly designed and manufactured out of carbon fibre, tested and then redesigned iteratively until the design meets specifications. Designing and manufacturing both of these parts out of carbon fibre would be a good research and design project for a future WESMO design team member.

4.4. Traction

The research into improving the drivetrain included research into whether switching the tyre dimensions would be beneficial to the car. Each of the potential tyres will be analysed by finding the overall traction vs slip, both in terms of longitudinal and lateral traction. Since the

Calspan tyre testing machine requires a spacer to be able to test the smaller 16-in tyres, the drive brake test was not possible. In order to be able to compare the 16-inch tyre to the other tyres an estimation of the longitudinal traction was generated.

The tyres that will be evaluated for longitudinal performance are tyre sizes that have either been used on previous or current WESMO cars. Alternate widths were also analysed as they could still potentially be used if a future WESMO team decided the alternate tyre size could benefit the car.

Table 18: Analysed tyre dimensions

Evaluated tyres
18x6 in
20.5x6 in
*16x6 in
18x7.5 in
20.5x7 in
*16x7.5 in

The tyres that were analysed are shown in Table 18. The 16-inch tyres have a * in front of them as these tyres were only able to be analysed in terms of lateral performance and the longitudinal data will be calculated.

The first step when analysing a formula student tyre is to go onto the tyre testing consortium and download the testing data of the tyre that is currently being analysed. The raw data set will have many runs that are not relevant, therefore the data will need to be filtered so that the data only shows the relevant runs. In the case of the WESMO car the inclination/ camber is set to 2 degrees and the tyre pressure is selected at 10 psi. Any data that is at another inclination angle or pressure is filtered out.

4.4.1. Testing traction circle

Due to the short length of the autocross track, there are not many data points on the experimental traction circle. The traction circles that were autogenerated by the MoTeC unit were incorrect due to the offset of the MoTeC unit and the corrected acceleration had to be calculated and plotted on the traction circle.

The peak lateral acceleration during testing was considerably lower than previous values, further proving that not having no ARB installed reduces the maximum lateral acceleration the W-FS-18 can achieve. The lateral acceleration the W-FS-18 car could reach decreased from approximately 1.8g to approximately 1.6g.

The traction circles that were generated during testing are heavily weighted to one side in terms of the lateral acceleration that the car was exposed to. This imbalance of lateral acceleration is caused due to the circular nature of the testing track, which was always tested in a clockwise direction. Having a circular track means that the majority of the corners were right hand corners which will result in a positive lateral acceleration (Figure 68).

For the 48-tooth testing the peak lateral acceleration both for left and right-hand turns appear to be fairly equal in magnitude, this is to be expected as the limiting factor for lateral acceleration will be a combination of both the tyres as well as the suspension setup, due to the lack of ARB. For the longitudinal acceleration however the braking and accelerating peak values are considerably different with the peak acceleration being approximately 0.65g whereas the peak deceleration was approximately 0.9g. this difference in the accelerating vs decelerating is due to the fact that while decelerating the car is traction limited however while accelerating the car is power limited.

The maximum braking capability of the W-FS-18 car is actually much larger than what has been achieved in the 48-and 39-tooth testing. The 44-tooth testing achieved peak braking values that are much closer to the theoretical braking ability of the W-FS-18 car. The main reason for the difference in peak braking between the tests will most likely be due to the driver becoming more comfortable with the car and test track. The testing sessions with which the traction circles for the 44-tooth and 39-tooth autocross testing were generated from were the first two testing sessions. The 44-tooth gear ratio was tested on the autocross track towards the end of the track testing, so the driver had much more experience with the layout of the testing track and had time to optimise his braking points during the many previous laps.

Judging from the peak acceleration values achieved during the 48-tooth autocross testing, the car was in second or third gear for a lot of the acceleration zones on the testing track (Figure 68). This estimation comes from the fact that the bulk of the acceleration values were under 0.8g which is the theoretical peak acceleration in second gear.

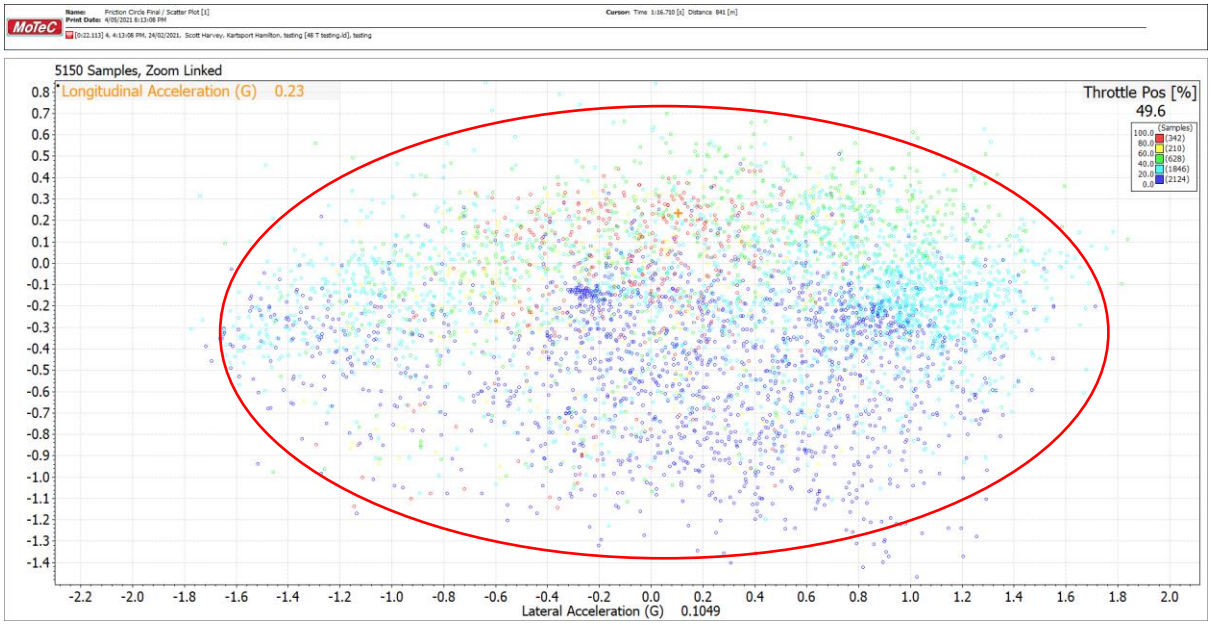

Figure 68: Testing traction circle with 48 tooth sprocket

Both the 44-tooth and the 39-tooth gear ratios achieved their highest longitudinal acceleration while still having some lateral acceleration (Figure 69 and Figure 70). This combination happens while the car is accelerating out of a corner. In the case of the autocross testing these high acceleration values will most likely happen when the car is accelerating out of the rear corner and approaching the 8-metre slalom. The reason this maximum acceleration happens while still having some lateral acceleration is because commonly when accelerating out of a sharp corner the car will be in first gear, thus will have the highest torque provided to the wheels. The longitudinal acceleration at no lateral load was consistently lower than the maximum acceleration that can be achieved in first gear. This happens as by the time the car reaches either of the straights it will be out of first gear and thus the peak acceleration that can be achieved at that point will be peak acceleration in the selected gear which is much lower than the maximum acceleration the car can achieve.

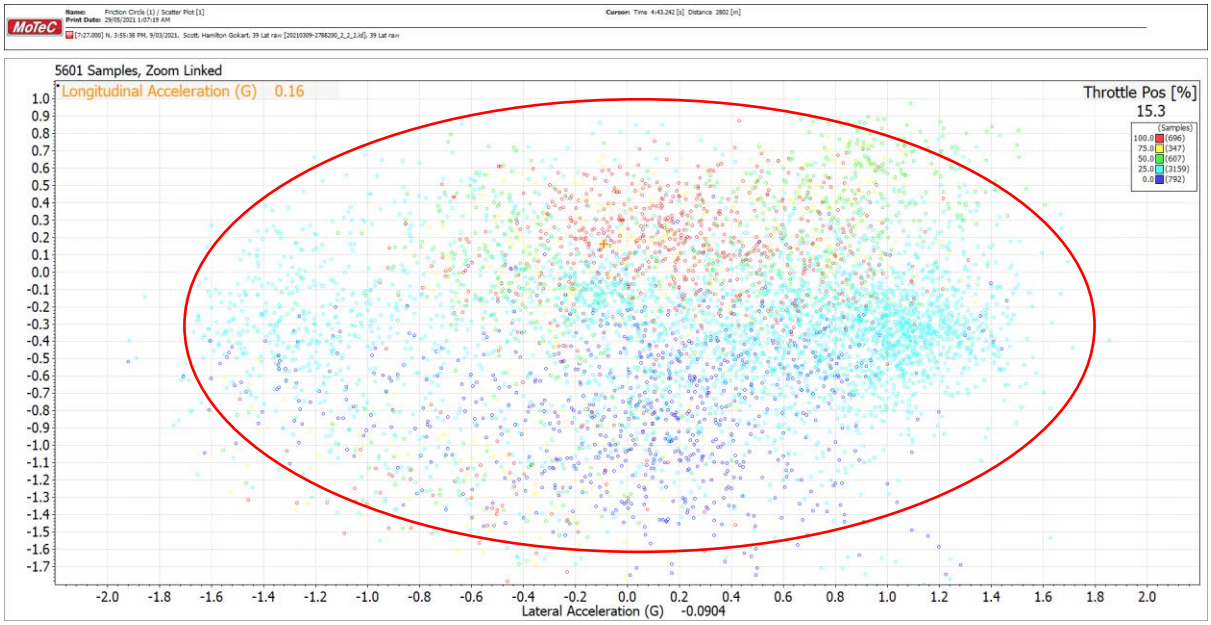

Figure 69: Testing traction circle with 44-tooth rear sprocket

The 48-tooth sprocket achieved the same acceleration results with no lateral acceleration, when compared to the acceleration which included sight lateral acceleration. This will be occurring due to the car coming out of the corner in an already higher gear. Since the car achieved the same acceleration coming out of the corner than it did on the straight, this shows that the car would have been in the same gear in both situations. This is definitive proof that the driver was having to short shift with the 48-tooth gear ratio.

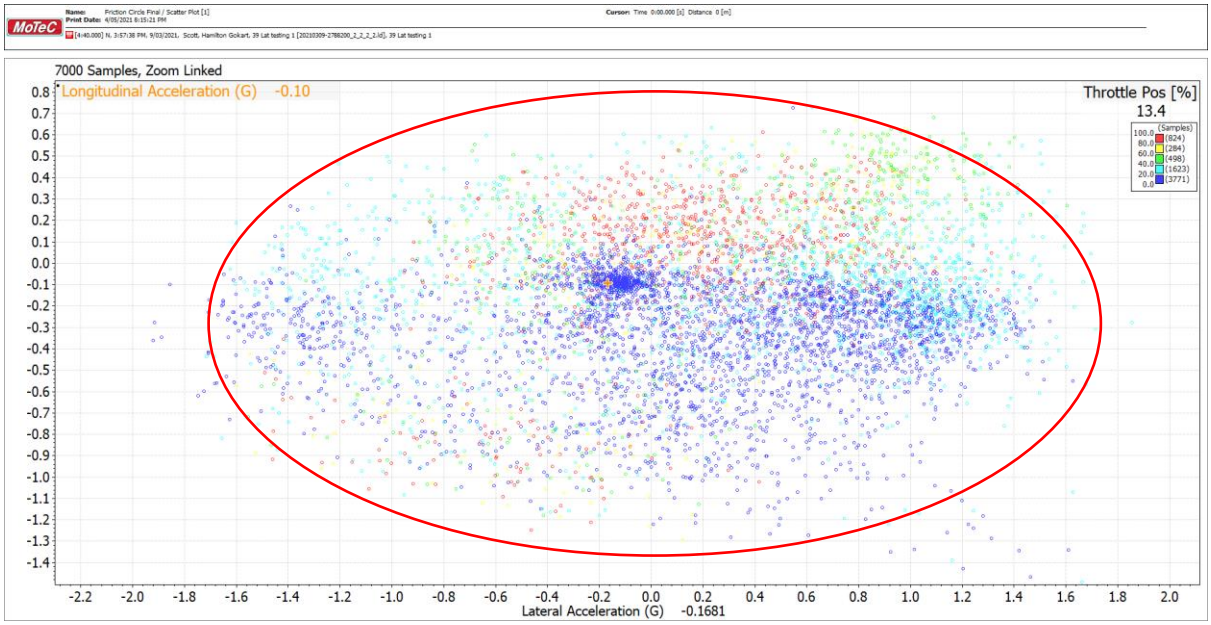

Figure 70: Testing traction circle with 39-tooth rear sprocket

A comparison of the traction circle of the 39 and 44-tooth rear sprockets, to that of the 48-tooth sprocket, demonstrates, the peak acceleration achieved by the car is much smaller . The total number of data points in the 90-100% range for the 39-tooth rear sprocket gear ratio was 675 while the 48-tooth sprocket gear ratio only had 274 data points in the 90-100% throttle position range. While some of these high throttle position data points will not be while accelerating due to things like RPM matching on downshifts, etc. the majority of the high throttle position points will be during periods of hard acceleration.

Having more data points that have a high throttle input as well as having positive longitudinal acceleration means that the car was accelerating hard for longer periods of time, which is vital to achieving good lap times.

This data matches up well with the feedback from previous drivers and is definitive proof that having the 48-tooth rear sprocket paired with a 16-tooth driving sprocket does in fact result in a drivetrain gear ratio that is too low, and will not be the optimum gear ratio to choose for the formula student autocross event.

Theoretical traction circle

The tyre limitation traction circle is the maximum combined traction of the tyres of the W-FS-18 car with the current suspension design (with ARB). Since the anti-roll bars have not been installed for any of the testing during this research project, the car has not been able to reach the lateral traction limit. Since the car is power limited while accelerating the longitudinal traction force is also much below the overall traction of the tyres. The peak longitudinal deceleration reaches reasonably close to the theoretical peak braking acceleration. During the 44-tooth testing there were some data points that were approximately 1.8g which is not far off the 2.06g braking limit of the W-FS-18 (Figure 71). The 1.8g braking value could have been achieved with any gear ratio thus all the braking values for the different gear ratios have been assumed to be the same in Figure 71.

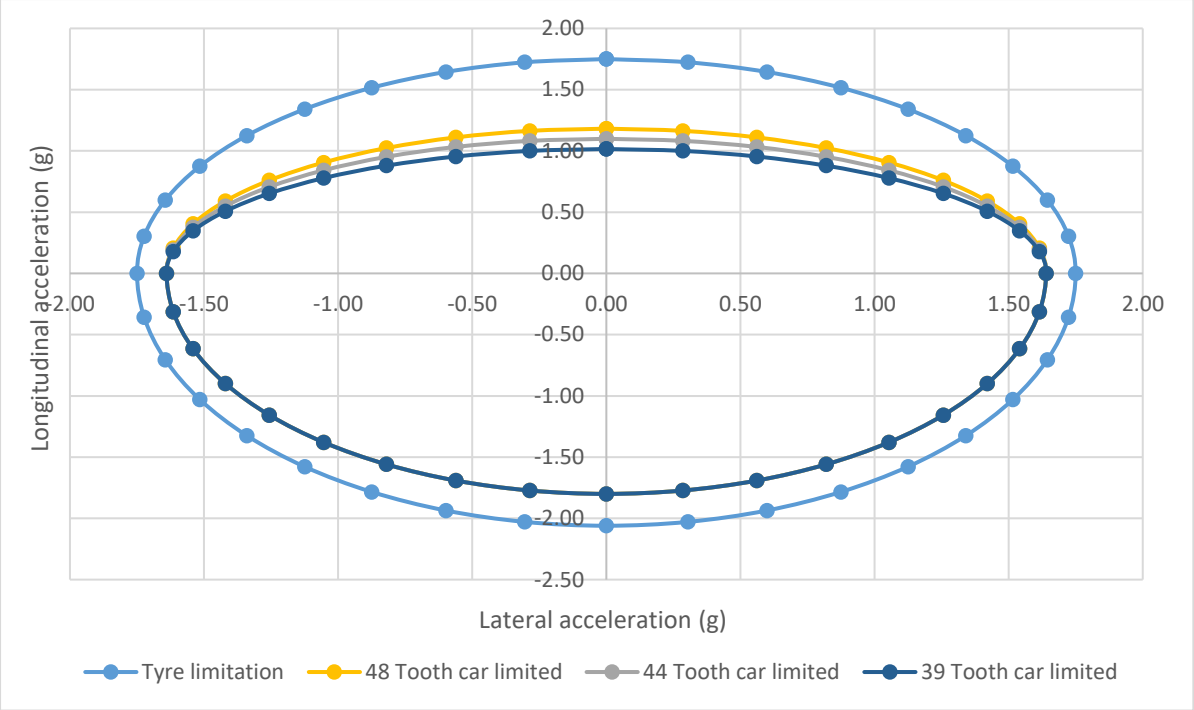

Figure 71: Theoretical traction circles for different W-FS-18 gear ratios

4.4.2. Tyre selection

When comparing the slip ratio to the longitudinal traction force there appear to be multiple different sets of data (Figure 72). Upon further inspection these different trends correlate with different runs. In each of these runs the only variable that was changed was the downforce.

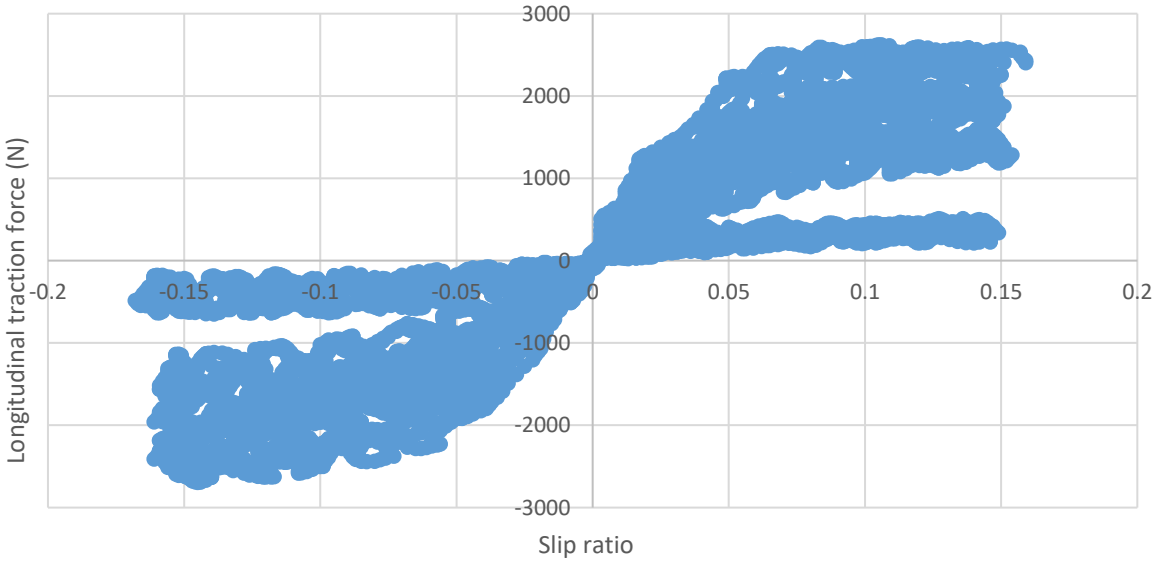

Figure 72: Slip ratio vs longitudinal force for W-FS-18 tyres

Since varying the downforce appears to have a large effect on the longitudinal force regardless of the slip ratio a better way to process this would be to compare the slip ratio against the tyre traction coefficients which are independent of the downforce (Figure 73).

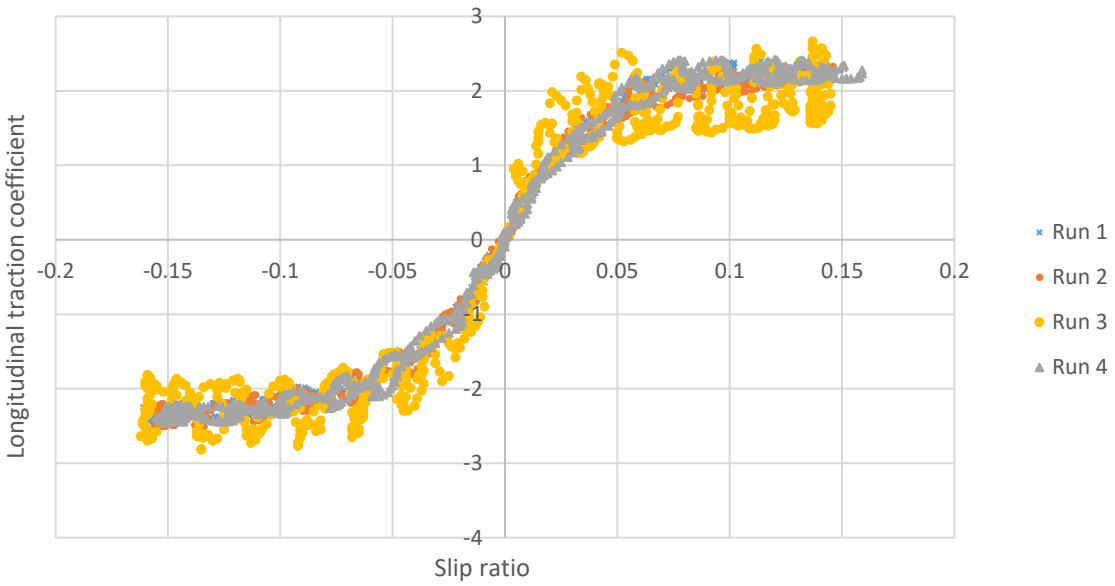

Figure 73: Slip ratio vs longitudinal traction coefficient

After normalising the data to be independent of weight three of the data sets all follow the same trend very closely. The data in run 3 does follow the same trend as the others but has a lot of variation and noise (Figure 74). The reason behind the noisy data is because run 3 was performed with the lowest downforce applied to the wheel (approximately 200N). This low downforce means that any random variation during testing will become considerably larger once the data gets normalised to be independent of downforce. To ensure that the data is accurate I will exclude this dataset and only use the other three accurate datasets.

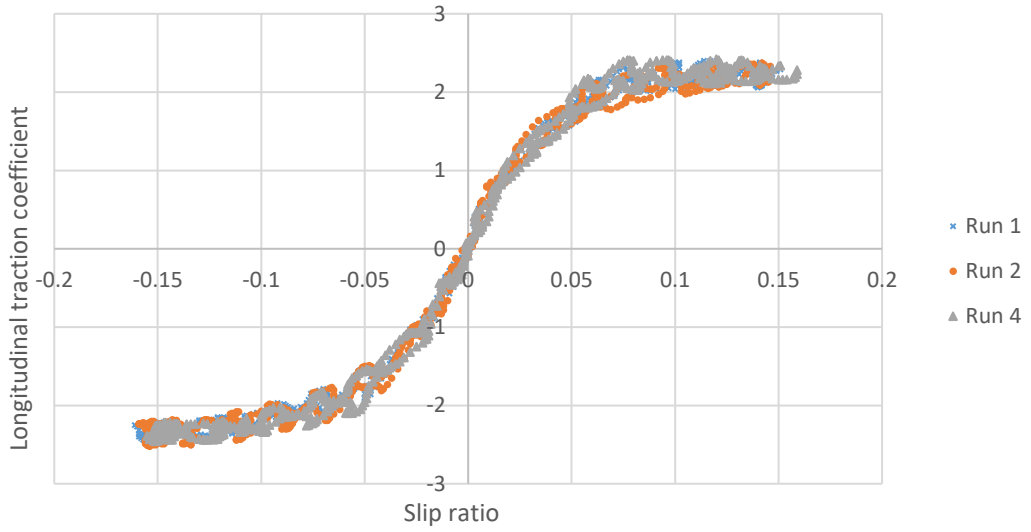

Figure 74: Processed slip ratio vs traction coefficient

To be able to compare the tyres the filtered longitudinal traction force vs slip ratio needs to be generated for each tyre dimension and the equation found from the graph for each. Since the traction is currently being analysed in terms of acceleration, the negative data can be filtered out and a polynomial trend line can be added to find the equation. This equation can then be used to find the longitudinal force at a given slip ratio all that is needed is to find the traction coefficient at the required slip ratio and then multiply the traction coefficient by the downforce on the tyre.

Looking at the longitudinal traction coefficient vs slip ratio, it becomes clear that the tyre construction has a large effect on the traction coefficient with both 20.5 tyres following roughly the same trend. Both 18-inch tyres also followed roughly the same trend until the slip ratio reached approximately 0.06, after that the 18x7.5-inch tyre was far superior. **Error! Reference source not found.** shows that the wider tyres clearly have a higher traction coefficient then their skinnier equivalents. Unfortunately, the loading range where the wider tyres have the largest benefit is when the tyres are under small loads (< 400 N) which will very rarely happen so is not very useful. The loading range that the tyres will most commonly be between 500-1000N. in this range both the wider tyres definitely do have a slightly larger traction coefficient when compared their skinnier counterparts. This is especially apparent for the 18x7.5-inch tyre which is the standout in terms of longitudinal performance (Figure 75).

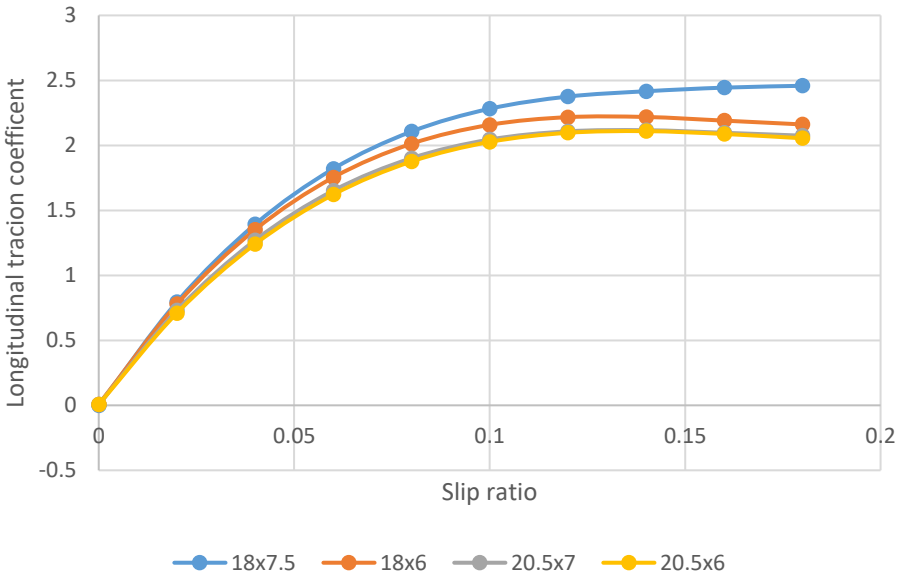

Figure 75: Summary of longitudinal traction coefficient vs positive slip ratio for different tyre selections

The lateral traction coefficient also is very dependent on the geometry of the tyre. The standout tyre in terms of lateral traction coefficient is the 20.5x7 inch for low slip angles and the 18x7.5 for high slip angles (Figure 76)

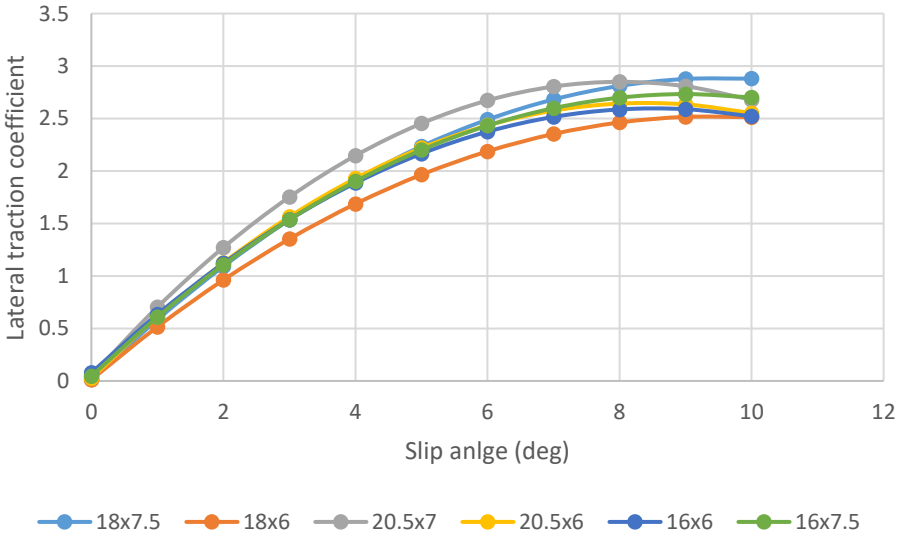

Figure 76: Summary of lateral traction coefficient vs positive slip ratio for different tyre selections

4.4.3. Generating a 16-inch tyre longitudinal traction coefficient

As the tyres are all made using the Hoosier RB25 compound the rubber should have the same friction coefficient and the friction coefficient should have the same rate of change when the rubber is exposed to stress. The sidewall construction is also the same for tyres of the same

diameter, e.g., the 18x6 and the 18x7.5-inch tyres will have almost identical sidewall characteristics despite having differing widths. The geometry of the tyre will result in different tyres having different stresses due both different spring rates as well as different geometric properties to loading.

A tyre is effectively a spring, with the spring rate of a tyre being proportional to the sidewall thickness and height. Due to the round shape of a tyre the contact patch area is proportional to the displacement of the tyre at the contact patch. This means that as the tyre gets more loading on it, the contact patch area increases. Under transient loading with the correct tyre pressure the contact patch can be assumed to be rectangular in shape. This means that if we find out the depth of the contact patch and assuming correct inflation pressure and that the width of the contact patch is equal to the width of the tyre, we can create an approximation of the area of the contact patch and then find the stress that the contact patch rubber is exposed to.

The area of the contact patch is assumed to be rectangular for simplicity purposes as to find the actual shape of the contact patch under longitudinal load is difficult without doing experimental testing on each of the tyres.
This means that the contact patch is simply the contact patch depth multiplied by the width of the tyre. The contact patch depth (L) can be calculated using the radius of the tyre along with the effective radius of the tyre under loading (Equation (4.11).

$$l = \sqrt{r^2 - {r_e}^2} \tag{4.11}$$

Once the area is found the force acting on the tyre at the contact patch needs to be calculated. The longitudinal forces that act on the contact patch are downforce as well as the longitudinal traction force. These two component forces can be used to find the actual force on the contact patch. Using this force, the theoretical stress of the rubber at the contact patch can be calculated using Equation(4.10). To be able to estimate the traction coefficient tyres of the same widths were assumed to be exposed to the same stress (Table 19) and calculating the longitudinal and lateral traction at different downforce intervals a model of the traction coefficient vs downforce can be generated.

Table 19: Contact patch stress for theoretical calculations

Assumed stress at contact patch for calculation					
16x7.5	18x7.5	20.5x7	18x6	16x6	20.5x6

0.03750	0.03750	0.04031	0.04376	0.04376	0.04376
0.05150	0.05150	0.05536	0.06008	0.06008	0.06008
0.06350	0.06350	0.06826	0.07408	0.07408	0.07408
0.07350	0.07350	0.07901	0.08575	0.08575	0.08575
0.08150	0.08150	0.08761	0.09508	0.09508	0.09508

The 200N downforce value was chosen to be excluded as the measured data had a large amount of variation. One potential reason for this variation is that during the testing of tyres there would have been experimental inaccuracies, and with low downforce loading cases those inaccuracies will have a larger percentage error when compared to larger downforce tests. The tractive force at low downforce is not commonly needed as at l have a relatively small contribution to the overall traction of the car. For this reason, the low downforce traction coefficient have been excluded and the range of downforce with which the longitudinal traction coefficients will be calculated from will be from 400N to 1200N.

To judge how accurate the theoretical traction coefficients were, the theoretical models were first calculated for tyres dimension with which there was already measured traction coefficients (Figure 77,). Using the assumption that the tyres of the same construction are all under the same level of stress at when the maximum longitudinal loading, the theoretical traction coefficients were calculated from the stress instead of the other way around.

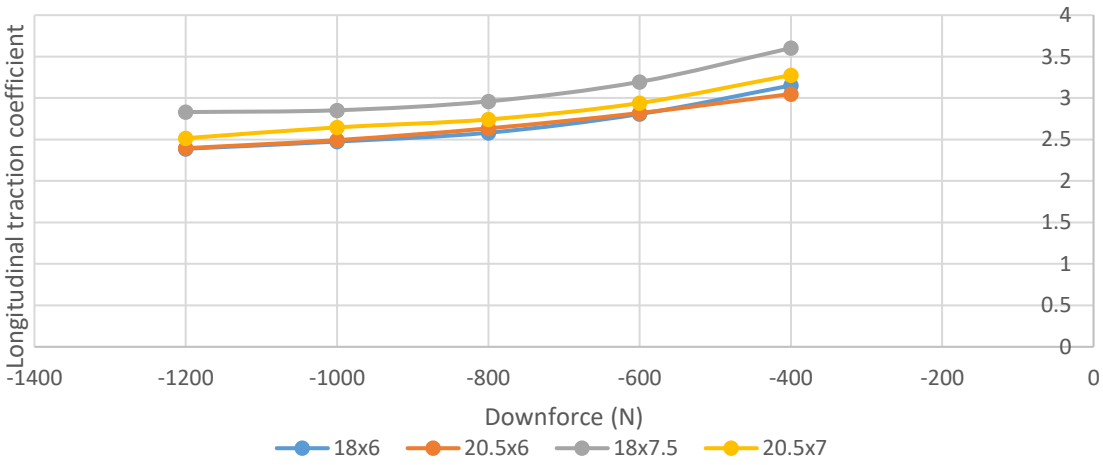

Figure 77: Longitudinal traction coefficient vs downforce for different tyre sizes

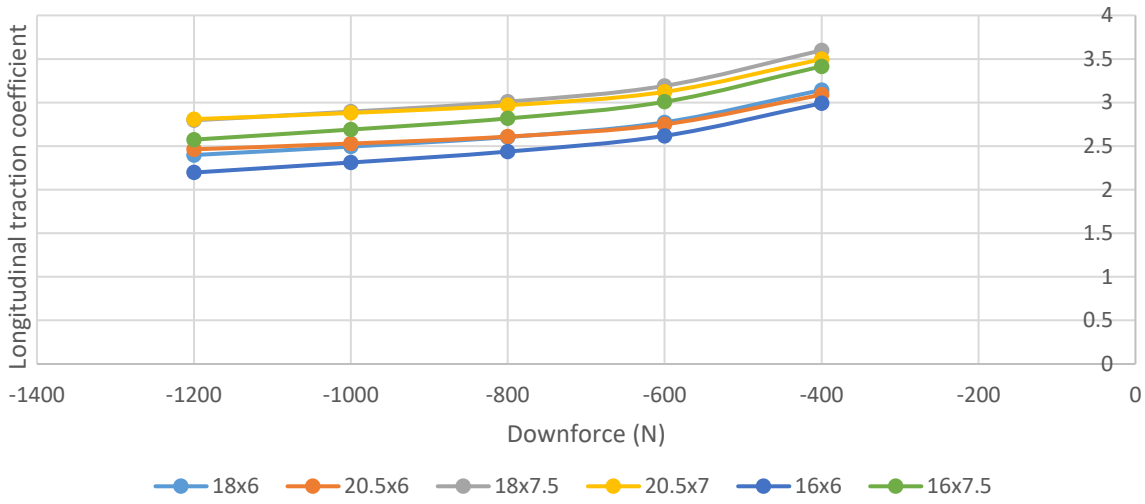

Figure 78: Longitudinal traction coefficient vs downforce for different tyre sizes

Table 20:Margin of error of theoretical longitudinal traction coefficients

Error of theoretical longitudinal traction coefficients				
Downforce (N)	18x6	20.5x6	18x7.5	20.5x7
-400	-0.25%	1.35%	1.81%	4.78%
-600	-1.21%	-2.46%	1.83%	4.21%
-800	0.86%	-0.95%	3.71%	6.17%
-1000	0.77%	1.45%	3.53%	6.75%
-1200	0.38%	2.82%	0.76%	9.50%

The lateral traction coefficients (Figure 79) were also compared to the theoretical lateral traction coefficients (Figure 80), to try find out if the 20.5x7 has the same inaccuracy in terms of lateral data. Based off the results in

Table 21, where the 20.5x7 had approximately the same error as the other tyres the longitudinal traction coefficient for the 20.5x7 is lower than it should be. The lateral traction coefficient had an error range of ±4% for all data values except the 18x7.5- inch tyre at 400N of downforce.

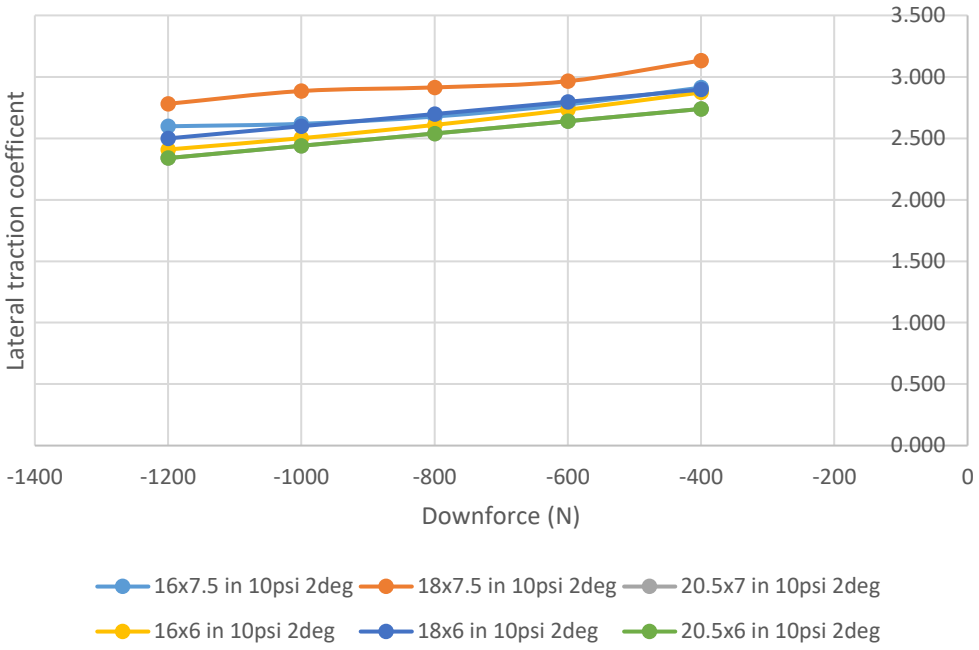

Figure 79: Lateral traction coefficient vs downforce for different tyre sizes

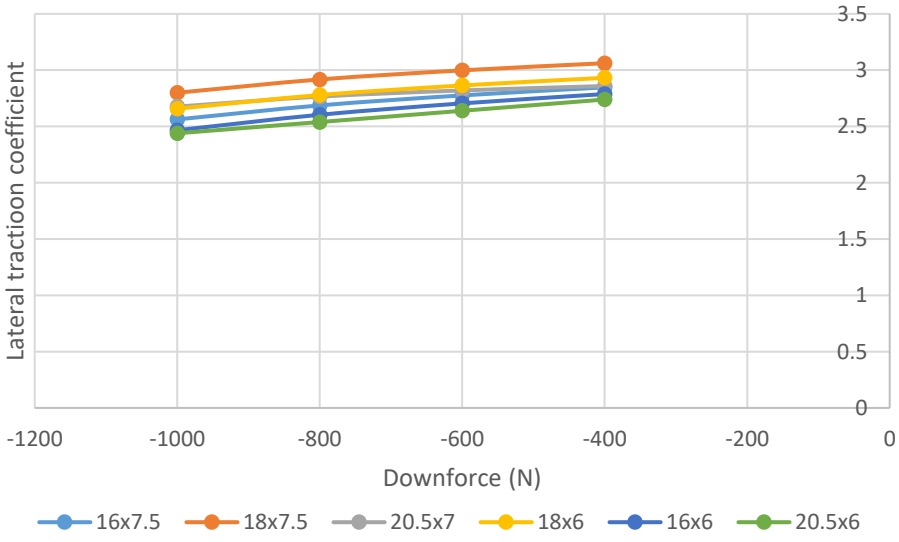

Figure 80: Theoretical lateral traction coefficient vs downforce for different tyre sizes

Table 21:Margin of error of theoretical lateral traction coefficients

Margin of error of theoretical lateral traction coefficients						
Downforce (N)	18x7.5	20.5x7	18x6	16x7.5	16x6	20.5x6
200	-7.59%	-1.68%	4.06%	-1.78%	-1.50%	3.65%
400	-2.28%	-1.23%	1.22%	-2.25%	-2.97%	3.79%
600	1.12%	2.37%	2.40%	0.01%	-1.03%	3.94%
800	0.11%	4.48%	3.02%	0.36%	-0.21%	4.10%

1000	-2.96%	4.11%	2.29%	-2.12%	-1.38%	4.27%

Based off the errors the errors of the predictions for both lateral and longitudinal an assumption of the longitudinal traction coefficient will have an acceptable error and can be used in any further calculations.

4.5. Yaw moment

4.5.1. Theoretical yaw moment calculations

Before the effect that the differential has on the yawing of the car can be calculated, the overall yawing properties of the W-FS-18 car are required. Fortunately, this has already been researched and the yaw moment diagram for the W-FS-18 car have been generated (Figure 81). This previous research did not take into consideration how the differential settings will affect the overall yaw of the car.

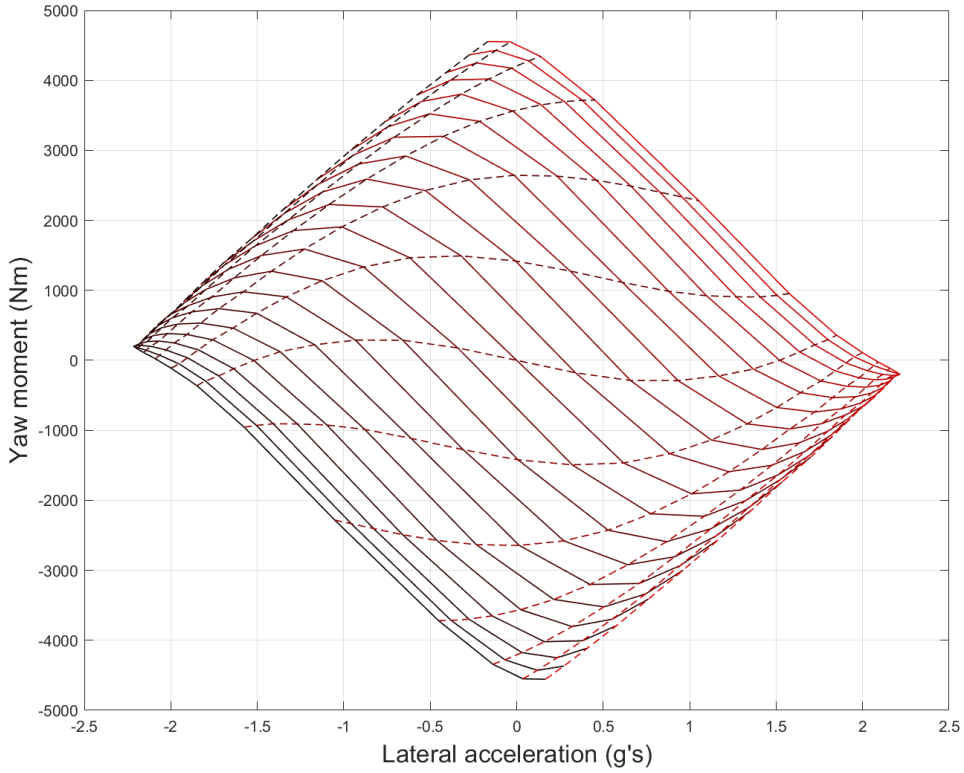

Figure 81: YMD for W-FS-18 with 55% roll stiffness distribution at Vx = 16 m/s (Ashburn, 2020)

This yaw moment diagram only works for transient cornering. This means that it models the handling of the car during cornering when the car is not braking or accelerating. This is a simplified model dealing with transient conditions. Because there will be no acceleration or deceleration the model does not need to consider load transfer or reduction in lateral traction due to longitudinal traction requirements.

Table 22: W-FS-18 differential locking percentages

Differential locking percentages		
	Accelerating	Decelerating
Option 1	27	23
Option 2	25	17
Option 3	40	25

The first part of finding how the differential settings effect the overall yaw velocity of the car is to find a relationship between slip ratio and longitudinal traction force. This has been found previously in the tyre data processing.

The standard convention for yaw moment diagrams is to have them in terms of the yaw moment (Nm) produced by the car's lateral acceleration (g). As the yaw moment due to the differential locking is proportional to the difference in wheel speeds which happens due to difference in corner radii of each of the wheels, the yaw moment caused by the differential locking will need to be converted to be in terms of lateral acceleration rather than the radius of the corner (Equation (4.12).

$$Ac = \frac{V^2}{r} \tag{4.12}$$

"Since yaw motion imparts a differential slip ratio between the inside and outside tires, any locking in the differential will generate a higher yaw-resisting moment" (Vogel, 2020). This yaw moment happens as the two rear wheels are connected but they will have different speeds resulting in the outside wheel having to undergo slip. This slip of the outside wheel creates a force in the longitudinal direction at the contact patch of this tyre, thus creating a moment.

The difference in radii of the rear wheels is found using Equation his is done by adding half the track width of the rear wheels onto the radius of the outer wheel and subtracting half the track width from the inner wheel. The difference in the travel path can be calculated by using the turning radius for each of the wheels (Equation (4.13)**Error! Reference source not found.**.

$$\Delta d = 2 * \pi * \left(r + \frac{tw_r}{2}\right) - 2 * \pi * \left(r - \frac{tw_r}{2}\right) \tag{4.13}$$

Using the difference in distance of the two driven wheels along with the differentials locking percentage, the slip ratio of the outside wheel can be found (Equation (4.14) (Figure

82)**Error! Reference source not found.**. The differential locking percentage has one of 3 options depending on the ramp angle. As the differential in the car is a 1.5-way LSD, this lock percentage will have a different value if the car is accelerating when compared to it coasting or decelerating.

$$slip\ ratio\ (outside\ wheel) = \frac{(\Delta d)}{d_i} * Diff\% \tag{4.14}$$

The minimum radius of the corners for the formula student autocross event is 4.5m. For this reason, the range of the corner radii used for the differential yaw moment calculations were between 4.5m and 100m. 100m was selected as the maximum corner radius because a 100m radius corner is close enough to a straight line, that the slip ratio of the outside wheel is almost zero, while still being fast to compute.

It was found that the slip ratio of the outside wheel increased exponentially as the radius of the corner decreased. The actual slip ratio of the outside wheel was quite small with a maximum slip of 3.5% or 0.035 which occurred with the differential set up with the smallest ramp angle. When compared to each other settings option 3 with the ramp angles of 30/45 had a considerably higher slip ratio for the outside wheel, with the other two settings being fairly close in slip values but having approximately two thirds the slip ratio of setting 3.

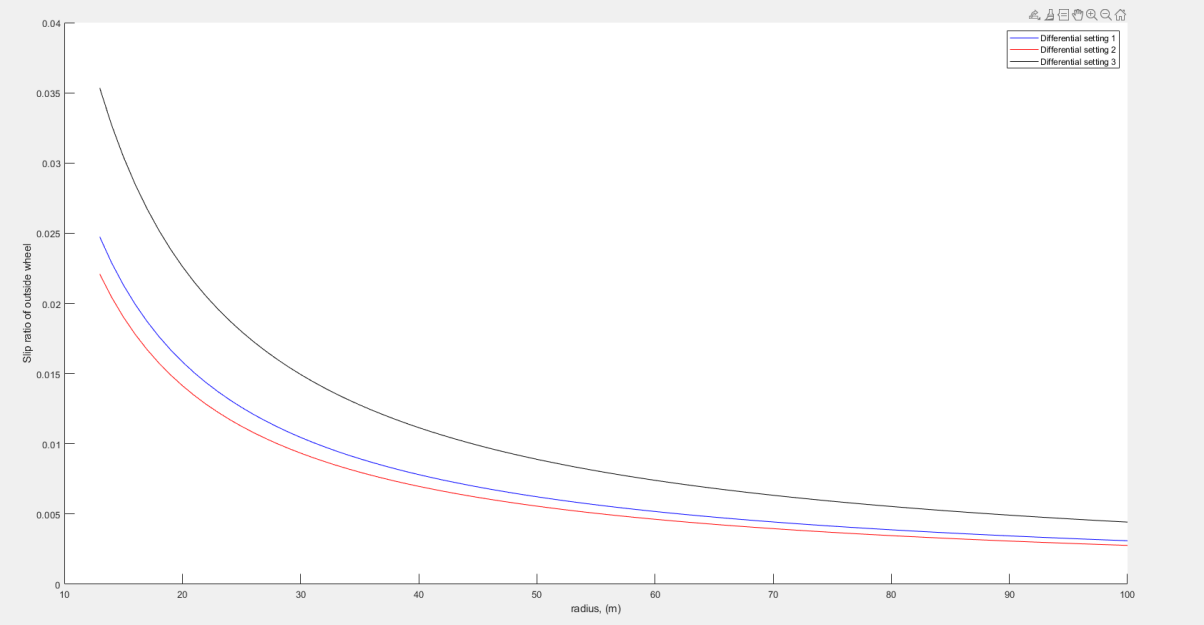

Figure 82: Outside wheel slip ratio at 16m/s for different radii corners

Once the slip ratio of the outer driven wheel is known the longitudinal force can be calculated by using the equation for slip ratio vs longitudinal force found from processing the slip ratio tyre data (Figure 83).

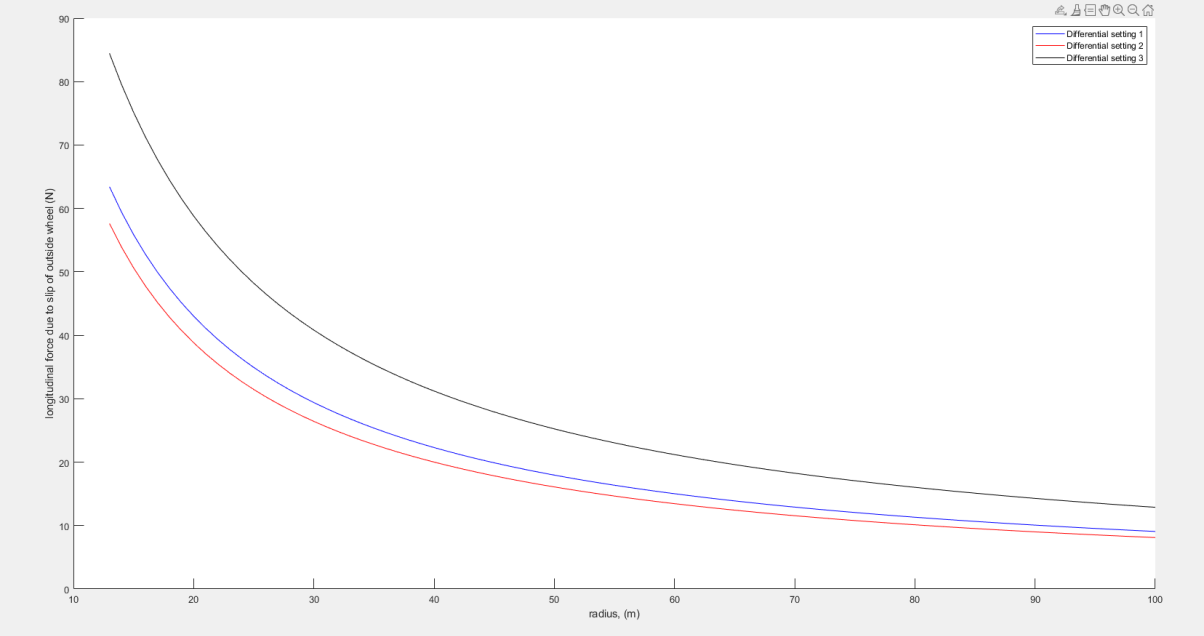

Figure 83: Longitudinal force due to slip ratio of outside wheel

This longitudinal force will result in a moment as the force is acting at a distance from the CoG. The moment that is produced is a yaw moment and will always be in the opposite direction to the yaw moment produced by steering inputs, so will reduce the cars overall yaw moment (Figure 84). Reducing the yaw moment of the car will reduce the yaw velocity, meaning that the car will not be able to turn as quickly or sharply.

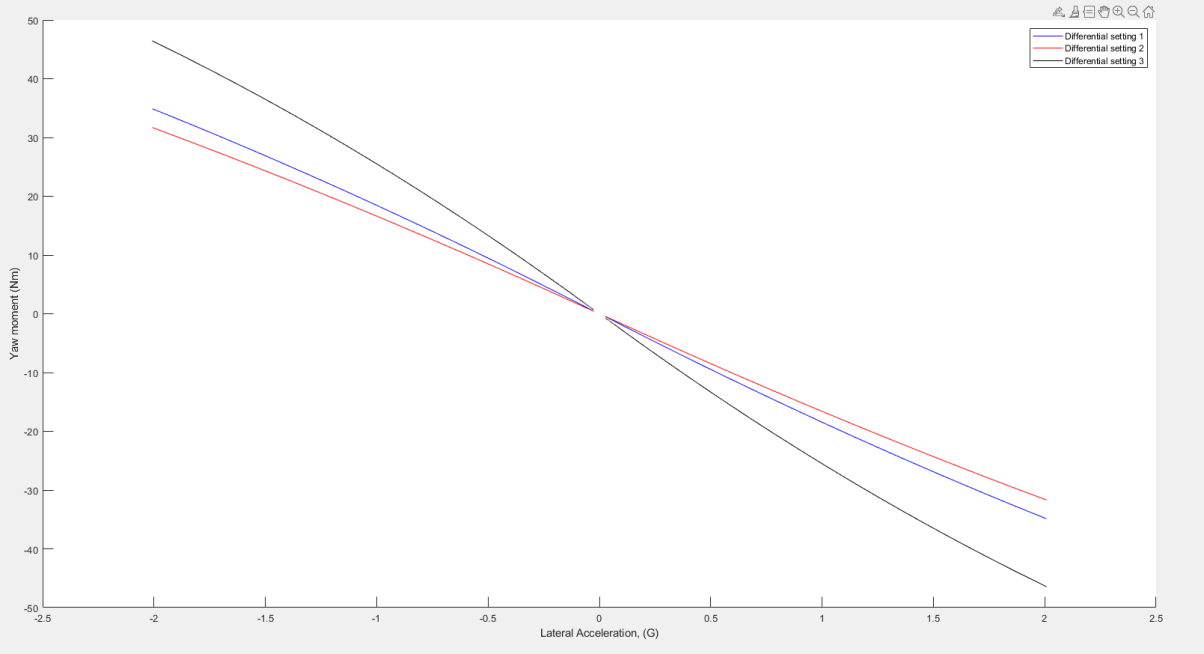

Figure 84: Resistive yaw moment from differential vs lateral acceleration

Though the yaw moment produced by the differential in terms of the radius of the corner is useful, it needs to be converted to be in terms of lateral force and then lateral acceleration to be useful for further analysis. This is because the standard convention for yaw moment diagram uses lateral acceleration in terms of gravitational acceleration force or G's rather than radius. This is easily solved as the lateral force can be calculated from the radius using the centripetal force equation (Equation**Error! Reference source not found.** and then using newtons first law (Equation **Error! Reference source not found.**.

Given the 16m/s constraint with which the yaw moment diagram was generated with, the minimum radius that thew car could be able to manoeuvre given the traction limit of the car is a corner with a radius of approximately 12.5-13m.

The yaw moment values at the peak lateral loads are arbitrary values that do not mean much by themselves. They can however be used for comparison of the handling characteristics of the car with a greater absolute yaw moment value meaning that the car has moved further away from neutral and thus the tendency to understeer or oversteer has increased. As the W-FS-18 car tends to understeer running a higher differential percentage will further increase that understeer tendency which is not ideal (Table 23) (Appendix 6, Appendix 7, Appendix 8).

Table 23: Yaw moment values at peak lateral acceleration for different differential settings

	lateral acceleration	Yaw moment
No differential locking	-2.1978	148.408
	2.1978	-148.408
Differential option 1	-2.1987	181.473
	2.1987	-181.473
Differential option 2	-2.1987	177.384
	2.1987	-177.384
Differential option 3	-2.1987	197.688
	2.1987	-197.688

Though the differential does affect the steady sate characteristics of the car it will have a larger effect on the handling of the car in combined loading cases. Modelling the handling characteristics of combined loading is extremely complicated due to having to consider loads transfer both in the form of roll as well as pitch, as well as having to calculate the reduced lateral traction limit that comes when the tyre needs to produce both longitudinal and lateral forces. “As I have mentioned before, the differential is important far beyond simple steady state cornering. The most significant performance differences lie in mixed conditions such as corner entry and corner exit” (Vogel, 2020).

4.5.2. Yaw Moment testing

The yaw rate is one of the variables recorded by the MoTeC unit however the yaw velocity is not useful by itself (**Error! Reference source not found.**). By differentiating the yaw velocity, the yaw acceleration can be found.

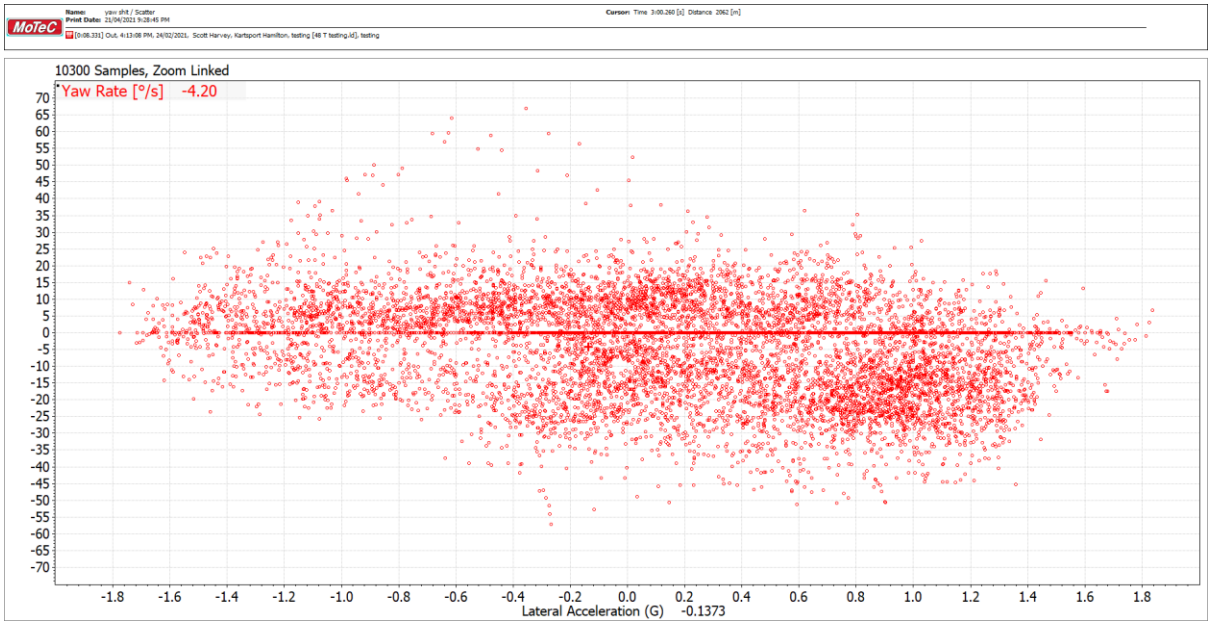

Figure 85: Yaw rate (velocity) MoTeC plot of 48-tooth autocross testing

As the yaw acceleration is just the angular acceleration about the z axis this means that the yaw moment can be found using the rotational inertia of the car about the z-axis (I_{ZZ}) (Equation (2.12).

The yaw moment data that was be gathered during testing was quite different then the corresponding data from the theoretical calculations, with the maximum theoretical maximum yaw moment being approximately 4500 Nm and the experimental being yaw moments both having peak values much higher than 7500 Nm. Generating an experimental yaw moment diagram from the autocross testing is not a good representation of the actual transient yaw moment diagram of the car (**Error! Reference source not found.**, Figure 86). The main problem with using autocross data is that during the autocross testing the car is almost never in transient conditions and the load transfer that comes from longitudinal acceleration/deceleration will have a large effect on the yaw moment as the lateral force the tyres can produce will change To make an accurate experimental YMD the car would have to be tested in a spiral path at a constant speed., the test would involve two clockwise and two anticlockwise runs on the spiral course with one of the runs in each direction maintaining constant slip angle and the other maintaining constant steering angle. The other flaw with trying to generate a yaw moment from the autocross is that the steering and slip angles are constantly changing and the majority of the corners have positive lateral acceleration due to circular nature of the track.

There was a lot of variation between **Error! Reference source not found.** and Figure 86, a considerable amount more than can be justified as purely coming from the alteration of the differential settings (**Error! Reference source not found.**, Figure 86).

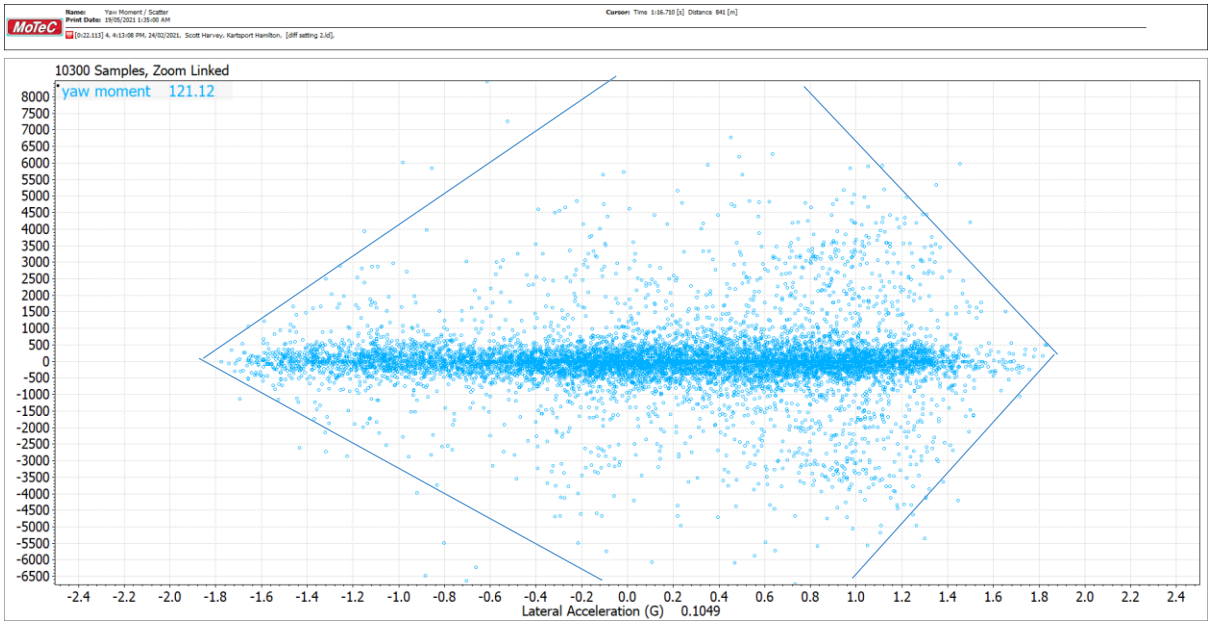

Figure 86: Yaw moments calculated from raw MoTeC data with differential setting 1

Due to the inaccuracy of the experimental data, the experimental data cannot be used as verification of the theoretical yaw moment diagram and cannot be used to access what effect the differential setting will have on the car. Based purely off theoretical calculations the car would benefit from running differential option 2 however, using a 1-way differential with the same accelerating ramp angles would be considerably better as it would reduce the understeer tendency of the car, at the cost of rear wheel braking stability.

4.6. Setbacks encountered during testing

With testing requiring near perfect weather conditions and with the driver away during the summer period when the weather was consistently good, the number of testing sessions achieved was not as much as had been initially planned, due to many being cancelled due to sub-par weather. Of the testing sessions that went ahead, many more sessions had major setbacks than had been planned with over half of the track days having a serious setback resulting in that track sessions data to being too incomplete to be used. The original plan was to run 5 different final drive ratios with the rear sprocket followed up with testing the 3 different differential settings. In the end only three gear ratios could be tested these were the 48-tooth ,the 44-tooth and the 39-tooth rear sprocket gear ratio. Only two of the differential settings could be tested, these were option three and two which have the steepest and shallowest ramp angles. This had been considered and so the order of testing weas changed to enable the three gear ratios that were tested to cover the full range if gear ratios.

During testing there were multiple setbacks that were encountered. Table 24 lists the major

setbacks that resulted in a track testing session having to be cancelled before all the relevant data could be collected.

Table 24: Setbacks during each testing session

Testing setbacks	
48-tooth session 1	Chain tensioner
48-tooth session 2	None
39-tooth session 1	GPS + Wheel bearing
39-tooth session 2	Exhaust tube
39-tooth session 3	Gear shifter
39-tooth session 4	Drivetrain mounts
44-tooth session 1	Chain tensioner
Differential testing 2	None

The first set back was when the GPS sensor stopped working during the second track testing session (Table 24). This was eventually going to happen as the GPS sensor degrades when exposed to vibrations, which is the case during testing and running. The reason the old sensor was expected to fail soon was because it had been used in all WESMO cars since around 2013. To minimise cost the sensor was used until failure and then subsequently upgraded with a higher quality sensor.

On the same track testing day that the GPS sensor failed, it was noticed once the car was up on the dolly that the front right wheel was not spinning freely, and the bearings needed to be replaced. The bearings not spinning as freely as they should, will have a small effect on the data. Though this was one of the reasons for changing the bearings it was not the main reason. The main reason for replacing the bearings is due to the substantial increase in heat produced from a worn bearing and the potential for parts failing due to the increased temperature.

The upright was disconnected from the suspension and removed from the car and the brake disk removed. Once the disk was removed the safety lockwire was removed and the hub assembly bolts undone. The outside half of the hub was pulled out by clamping the centre lock wheel stud in the vice and pulling upwards on the upright. The inside half of the hub was removed using a hydraulic press. Once both halves of the hub were out the bearings needed to be pressed out. There is a spacer in between the two bearings which could be pulled out by hand once one of the bearings was pressed out. The new bearings (SKF 61815-2RS1 – with low friction seals) were the same as the old bearings and were installed using an Arbor press making sure that the spacer was orientated the same as when it came out. Once the new

bearings were installed the inner half of the hub was pressed back in ready for the outer half to be tapped in with a mallet (Figure 87).

Figure 87: Upright with disassembled hub after bearing replacement

Once the outer half was tapped in and the assembly bolts were tightened up and the safety lockwire reinstalled (Figure 88).

Figure 88: Hub assembly with safety locking wire for bolts holding the hub together

The third setback was when a weld failed on the exhaust tube between the first bend after the coupling to the engine and a straight piece of tube (Figure 89). The failure was likely due to heat from the engine softening the material, and vibrations from the engine.

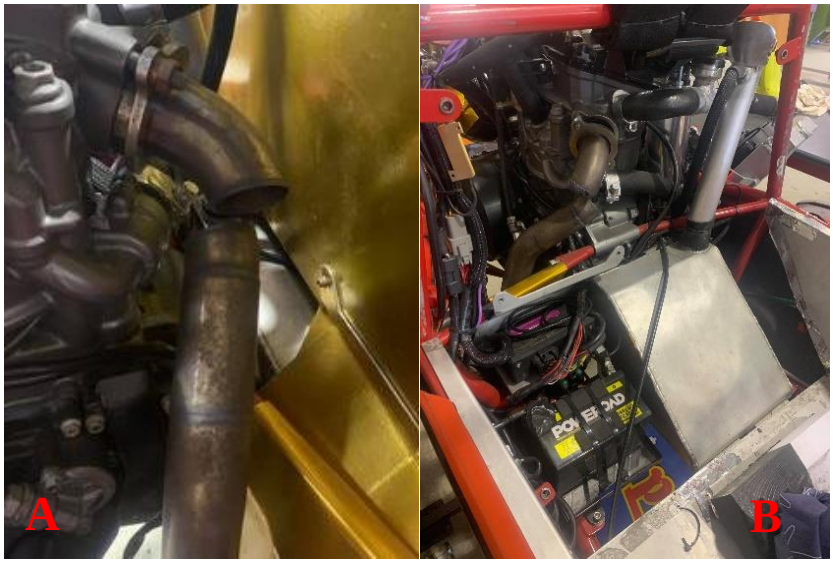

Figure 89: Broken exhaust due to testing

Upon disassembly it was found that the exhaust had been mounted incorrectly as there were two different thickness spacers, and furthermore the spacers had been installed the wrong way around meaning that the exhaust pipe would have been under constant stress further increasing the chance of failure. To access the exhaust, the firewall, seat and hip harnesses were removed. The exhaust was then removed, and the edges of the break and surrounding steel cleaned using a linisher, a file and steel brush. The exhaust was reinstalled, and the break tack welded using a TIG welder before the exhaust was removed again for final welding (Figure 90a) and then reinstalled (Figure 90b).

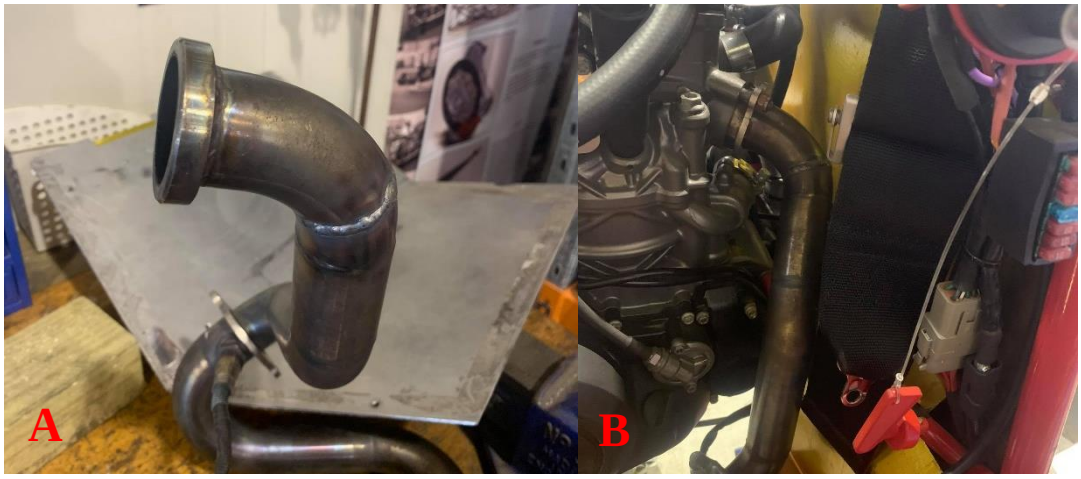

Figure 90: Repaired exhaust

During the next testing session, another setback was encountered when the first gear on the car stopped working. Once the car was back in the workshop, it was discovered that the shift

lever on the engine had come loose and had enough play such that the shifter no longer had the range of motion to be able to engage first gear (Figure 91).

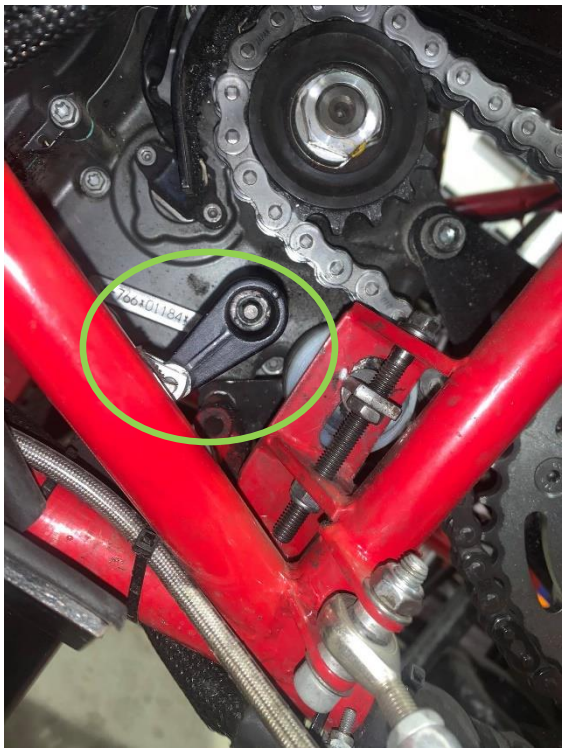

Figure 91: Engine shifting lever that came loose

Once the engine shifting lever was tightened it was also decided that tensioning the cable would be beneficial and could be done by adjusting the positioning nut (Figure 92). The driver also requested that the length of the shifting cable be lengthened which would result in the resting angle of the shifting lever being in a more comfortable position. In the process of extending the shifting cable it was noticed that the shifting lever had been hitting its mount meaning that it did not have the full range of motion which would have made downshifting gears more difficult. Moving the shifter to the requested position gave the interfering section of the lever more clearance which was an added benefit from moving the position.

Figure 92: Gear shifting cable tensioner

The next major setback was when one of the engine bolts loosened fell out (Figure 93). This loosening of the bolt meant that all the weight of the engine as well as the now undampened vibrations were being loaded through the drivetrain mounts along with the force applied from the tension in the chain. This extreme loading then buckled the left drivetrain bracket resulting in a 45-degree step (Figure 94). The buckling of the left bracket then resulted in a large force being pushed through the drivetrain cross bracing which then caused the right drivetrain bracket to bend as well.

Figure 93: Engine bolt that fell out

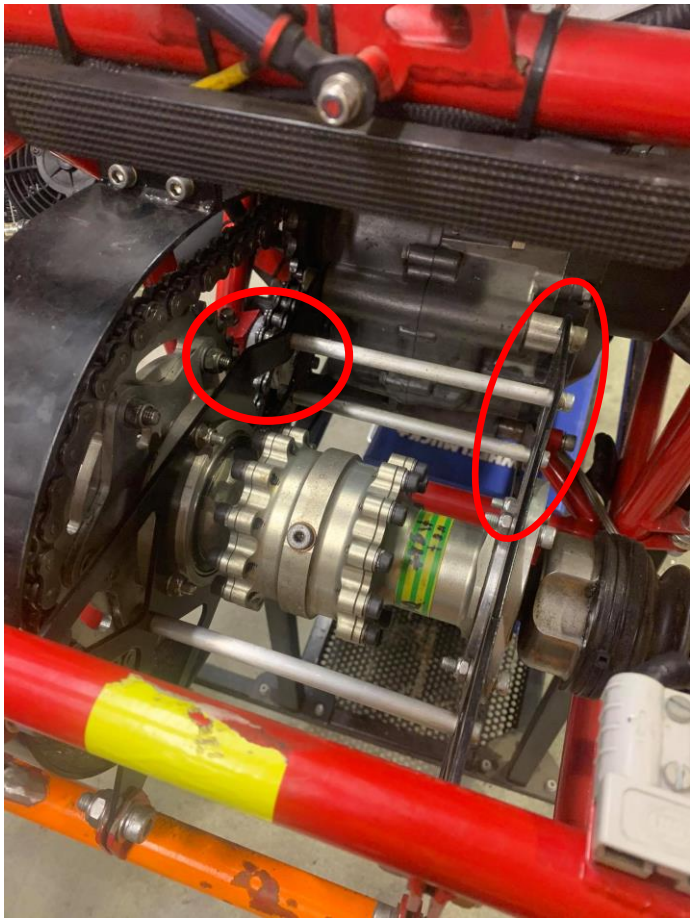

Figure 94: Buckled left and bent right drivetrain brackets

This loosening of the bottom engine bolts is a continual problem. The bolt keeps loosening off because the bolt is constantly exposed to high levels of vibrations as well as being threaded into a tapped collar that has no locking system. One potential fix to this problem would be to drill a hole through both the bolt and the collar and then thread locking wire through the hole.

The tensioner design for this car is not well designed as the nylon roller needs to be replaced after approximately 4 testing. This problem could be fixed by mounting the roller on bearings instead of having a metal sleeve pressed into it and have

Some suggestions for future WESMO teams to increase the reliability of their Formula student car is to ensure that when the hub is being designed and machined that the hole with which both bearings will press into is machined from one side. On the W-FS-18 car the hole which the bearings are pressed into was designed in a way where it had to be flipped mid machining resulting in the two holes being non-concentric, with them estimated to have a slight misalignment. This slight misalignment is causing a constant axial or thrust load, which

was not considered in the design process. Another recommendation is to redesign the engine mounting so that it is both easier to work on as well as including a mounting bolt retention system. During the duration of the testing for this report extra checks were added to the pre track testing check list as some checks were being neglected such as checking the engine mounting and brackets. Checking that the differential had even wear as well as was having the correct amount of oil was also added onto the list as although it was done throughout this research project prior to that it was almost never checked.

4.7. Putting everything together

As a lot of the ideas for improvement are not able to be tested on the W-FS-18 car due to the complicated nature of these improvements, a theoretical run was made where all the potential modifications suggested in this report were implemented and the car was able to complete the 75m run in approximately 3.8 seconds which is approximately half a second faster than the current W-FS-18 car (Figure 95).

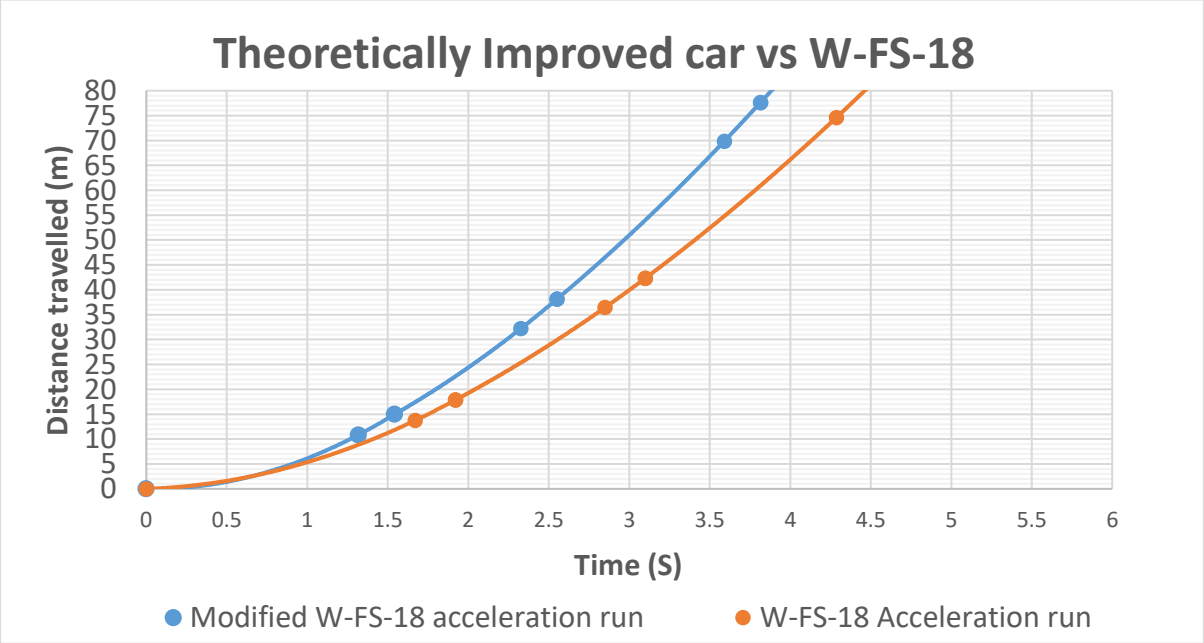

Figure 95: Theoretical car with improvements vs W-FS-18

Of these suggestions the ones that have the most benefit for the least effort would be to use a 44-tooth sprocket or 42-tooth sprocket during competition as this is the gear ratio that was best suited to the autocross track and was ideal as it had the highest torque of the gear ratios that could finish in third gear and would only loose traction from suddenly releasing the

clutch as the peak force generated at the wheels was less than the dynamic traction limit. In terms of changing the tyre to different sized tyre, the 16 by 7.5-inch tyres performed well and also resulted in a net increase in efficiency of the drivetrain. However, to implement this tyre dimension on the car, the suspension on the WESMO car would have to be completely redesigned and none of the previous designs and research would be valid due to the change in wheel diameter. A more practical choice would be to change to the 18x7.5-inch tyres because even though this tyre size result in an increase in weight and inertia, it proved to have the greatest traction both in terms of longitudinal and lateral traction, which will greatly benefit any future cars assuming they can fully utilise the gain in traction. The wider 18-inch tyre will also require a less drastic redesign in terms of the suspension as the tyre has the same diameter as the current tyres and has a fairly similar spring rate.

5. Conclusion and recommendations

In the acceleration run with the 39-tooth driven sprocket the test driver said that “the acceleration run was much easier because it doesn’t wheelspin as easily and the shifting time in first gear is more manageable”. The data gathered from the MoTeC also shows that the car was much less prone to wheelspin because on the 39-tooth gearing chart there is not the cluster of data points that sit in the high RPM range while having low wheel speeds. The MoTeC data also shows that with the 39T rear sprocket the 75m acceleration run could be completed in third gear which means that the gear only needed to be changed twice, meaning that the car had 0.25 seconds more time accelerating when compared to the 48-tooth rear sprocket gear ratio which had to change gear 3 times.
The 44-tooth sprocket on average did the best as it was far better in the autocross and also performed well in the acceleration event.
If there was more time testing with a 42-tooth sprocket during an acceleration run would have been ideal as it would have been able to easily finish in third gear unlike the 44-tooth and 48-tooth sprocket and would have more torque than the 39-tooth sprocket.

Designing and manufacturing the outer shells of the rim as well as the half shafts out of carbon fibre would save approximately 3kg weight reduction, as well as reducing the rotational inertia by approximately $7x10^{-3}kg/m^2$, which would result in approximately 3.25% more torque applied at the wheels.
Incorporating more carbon fibre into future WESMO cars drivetrains would be beneficial, however due to the size and budget of the WESMO team it probably is not very feasible unless WESMO manages to obtain sponsorship from a company that is willing to supply the carbon fibre as well as help out in a technical regard by advising the team about how to effectively design and manufacture parts out of carbon fibre.

Changing the tyres would be largely beneficial to the overall performance for future WESMO teams as moving to a 7.5-inch-wide tyre will increase both the lateral and longitudinal grip of the car. Though the 16x7.5-inch tyre offers both a decrease in rotational inertia as well as an increase in lateral grip and potentially an increase in longitudinal grip, they are not the tyres that would be recommended to future WESMO teams, the recommended tyres would be the 18x7.5-inch tyres. The reason these are the tyres that will be recommended to future WESMO teams is because it had far superior grip when compared to all other tyre

dimensions. Changing to the 7.5-inch wide tyres would still require the suspension to be redesigned however, this redesign would be less drastic than if the WESMO car was to go to 16-inch tyres, due to the tyre still having the same diameter.

Based off the theoretical yaw moment calculations having the car set up with the minimum slip angle would be beneficial as it would reduce the understeer tendency of the car which would improve the handling characteristics of future WESMO cars that are a variation of the W-FS-18. The car could be improved by an even greater margin by installing 1-way Drexler 2010 Formula student limited slip differential. Using a 1-way differential will result in the differential only locking up under acceleration and will be unlocked during coasting/ deceleration. Having no locking under deceleration will decrease the cars overall stability during braking but will also eliminate the destructive yaw moment that is produced by the locking of the differential. Fortunately the W-FS-18 car is very stable under braking, and although the decrease in stability under braking will have a small detrimental effect on the overall performance of the car, the potential performance gains from reducing the tendency for the car to understeer in hard transient cornering outweighs these shortcomings .

6. References

Aleksander. (2010). PROBLEMS OF ROTATIONAL MASS IN PASSENGER VEHICLES . *TRANSPORT PROBLEMS*, 33-35.

Ashburn, S. (2020). *Development and use of Yaw Moment Diagrams for FSAE cars.* Hamilton.

Bakker, E., Nyborg, L., & Pacejka, H. (1987). *Tyre Modelling for Use In Vehicle.* Detroit: SAE.

Balkwill, J. (2018). *Performance Vehicle Dynamics.* Elsevier Inc.

Beckman, B. (1991). *The Physics of Racing.* Burbank, CA 91503.

Bergman, A., & Byrhult, P. (2009). *Automated shifting of a manual sequential.* Lund University, Dept. of Industrial Electrical Engineering and Automation.

Blundell, M., & Harty, D. (2004). *The multipbody approach to vehicle dynamics.* Jordan Hill, Oxford: Elsiver.

Budynas, R., & Nisbett, J. (2005). *Shigley's Mechanical Engineering Design Tength Edition.* New York: McGraw-Hill Education.

Childs, P. (2003). *Mechanical Design.* Elsevier Science & Technology.

Cinar, K., Ersoy, N., & Unal, M. A. (2018). *DESIGN OF A REAL-SIZED COMPOSITE DRIVE SHAFT AND CRITICAL POINTS FROM BEGINNING TO END.* Tekirdag, Corlu, 59860, TURKEY: Mechanical Engineering Department, Namik Kemal University.

Cinar, K., Esroy, N., & Unal, M. A. (2018). DESIGN OF A REAL-SIZED COMPOSITE DRIVE SHAFT AND CRITICAL POINTS FROM BEGINNING TO END. *European Conference on Composite Materials*, (pp. 1-8). Athens.

Cobi, A. (2012). *Design of a Carbon Fiber Suspension System for FSAE Applications.* MASSACHUSETTS: MASSACHUSETTS INSTITUTE OF TECHNOLOGY.

Crolla, D. (2009). *Automotive Engineering: Powertrain, Chassis system and Vehicle body.* Burlington, MA 01803, USA: Elsevier.

Dhasarathy, D. (2010). *Estimation of vertical load on a tire from contact patch length and its use in vehicle.* Virginia Polytechnic Institute and State University.

Flintsch, G., McGhee, K., EIzeppi, & Najafi, S. (2012). *The Little Book of Tire Pavement Friction.*

Gadola, M. (2018). *The Mechanical Limited-Slip Differential Revisited: High-Performance and Racing Car Applications.* Brescia, Italy: Research India Publications.

Gadola, M., Chindamo, D., & Lenzo, B. (2018). *On the passive limited slip differential for high performance vehicle applications.* Bejing, China: Sheffield Hallam University.

Hadula, P., Kaczmarczyk, & Ł., F. (2017). *Powertrain damage analysis for Formula Student car WT-02.*

Hancock, M. (2011). *Vehicle handling control using active differentials.* Matthew Hancock.

Heilsler, H. (2002). *Advanced vehicle technology second edition.* Burlington: Elsevier Butterworth-Hinemann.

Hoseinnezhad, R. &.-H. (2011). *Efficient Antilock Braking by Direct Maximization of Tire–Road Frictions.* Industrial Electronics.

Hunting, B. (2019). WHEEL ALIGNMENT BASICS FOR HIGH PERFORMANCE DRIVING: THREE IMPORTANT ADJUSTMENTS YOU CAN DO YOURSELF. *DRIVINGLINE*.

James, R. A. (2004). *Design of an Aluminum Differential Housing and Driveline.* Massachusetts Institute of Technology.

Jazar, R. N. (2008). *Vehicle dynamics theory and application.* New York: Springer Science+Business Media, LLC.

Kasprazk, E., & Genz, D. (2006). *The Formula SAE Tire Test Consortium—Tire Testing and Data.* Society of Automotive Engineers, Inc.

Kolte, S., Srinivasan, A. K., & Srikrishna, A. (2016). *Development of Decentralized Integrated Chassis Control for Vehicle Stability in Limit Handling.* Michigan: SAE International.

Kopf, L. (2019). *Dynamic Analysis Of The WESMO FSAE Car's Suspension.* Hamilton.

Korntved, K., Hersbøll, J., Lauritsen, M., Bording, K., & Leto, H. (n.d.). *Design and Analysis of a Formula Student Carbon Fibre Rim.* Aalborg East, Denmark: Department of Materials and Production, Aalborg University.

Lechner, G., & Naunheimer, H. (1999). *Automotive transmissions Fundamentals, selection, design and application.* Stuttgart Germany: Springer.

Milliken, W., & Milliken, D. (1995). *Race car vehicle dynamics* . Society of Automotive Engineers, Inc.

MoTeC. (2018). *i2 V1.1.1.4 Feature guide.* MoTeC.

Patton, C. (2013). *Development of Vehicle Dynamics Tools for Motorsports.* Oregon State University.

Popp, K., & Schiehlen, W. (1993). *Ground Vehicle Dynamics.* Stuttgart: Springer.

Pütz, R., & Serné, T. (2017). *Rennwagentechnik - Praxislehrgang Fahrdynamik (Racing car technology - practical course in driving dynamics).* Springer Vieweg.

Rouelle, C. (November 2018). Lateral thinking on tyre load variations. *RACECAR ENGINEERING - TECHNOLOGY*, 51-64.

SAE International. (2019). *2019-2020 Formula SAE Rules.* Warrendale: SAE International.

Segers, J. (2014). *Analysis techniques for racecar data acquisition - second edition.* SAE International.

Seward, D. (2014). *Race Car Design.* Palgrave.

Smith, C. (1978). *Tune to Win: The art and science of race car development and tuning.* Fallbrook, CA : Aero Publishers, Inc.

Société de Technologie Michelin. (2001). *The tyre - Grip.* Société de Technologie Michelin.

Stone, R., & Ball, J. (2004). *Automotive engineering fundamentals.* Warrendale, PA: SAE International.

Szcs, G., & Bári, G. (2018). Generating MMM diagram for defining the safety margin of self driving cars. *IOP Conference Series: Materials Science and Engineering*, 2.

Taylor, C. (2010). *Differntials and chassis setup.* Plano, Tx.

TIRES-EASY. (2012, Feburary). *The Tire Contact Patch – Where the Rubber Meets the Road*. Retrieved from tires-easy.com: https://www.tires-easy.com/blog/the-tire-contact-patch-where-the-rubber-meets-the-road/

US department of commerce. (1971). *Mechanics of Pneumatic tires.* Ann Arbor Michigan: National Bureau of Standards.

Vogel, J. (2020). *Limited Slip Differential Characterization*. Retrieved from jovogel.com: https://www.jovogel.com/limited-slip-diff-characterisation

Walther, H. (2016). *DEVELOPMENT OF A LIGHTWEIGHT LAMINATED COMPOSITE WHEEL FOR FORMULA SAE RACE VEHICLES.* Kansas: University of Kansas.

WESMO. (2018). *2018 Design Report.* Hamilton.

.

7. Appendix

Appendix 1: Torque at wheels for different final drive ratios

Torque at wheels					
1st gear (2.5)	14	15	16	17	18
36	931.071	869.000	814.688	766.765	724.167
38	982.798	917.278	859.948	809.363	764.398
40	1034.524	965.556	905.208	851.961	804.630
42	1086.250	1013.833	950.469	894.559	844.861
44	1137.976	1062.111	995.729	937.157	885.093
46	1189.702	1110.389	1040.990	979.755	925.324
48	1241.429	1158.667	1086.250	1022.353	965.556
2nd gear (1.75)					
36	651.750	608.300	570.281	536.735	506.917
38	687.958	642.094	601.964	566.554	535.079
40	724.167	675.889	633.646	596.373	563.241
42	760.375	709.683	665.328	626.191	591.403
44	796.583	743.478	697.010	656.010	619.565
46	832.792	777.272	728.693	685.828	647.727
48	869.000	811.067	760.375	715.647	675.889
3rd gear (1.33)					
36	496.571	463.467	434.500	408.941	386.222
38	524.159	489.215	458.639	431.660	407.679
40	551.746	514.963	482.778	454.379	429.136
42	579.333	540.711	506.917	477.098	450.593
44	606.921	566.459	531.056	499.817	472.049
46	634.508	592.207	555.194	522.536	493.506
48	662.095	617.956	579.333	545.255	514.963
4th gear (1.1)					
36	407.898	380.705	356.911	335.916	317.254
38	430.559	401.855	376.739	354.578	334.879
40	453.220	423.005	396.567	373.240	352.504
42	475.881	444.156	416.396	391.902	370.130
44	498.542	465.306	436.224	410.564	387.755

46	521.203	486.456	456.053	429.226	405.380
48	543.864	507.606	475.881	447.888	423.005
5th gear (0.96)					
36	356.236	332.487	311.707	293.371	277.072
38	376.027	350.958	329.024	309.669	292.465
40	395.818	369.430	346.341	325.968	307.858
42	415.609	387.901	363.658	342.266	323.251
44	435.400	406.373	380.975	358.564	338.644
46	455.190	424.844	398.292	374.863	354.037
48	474.981	443.316	415.609	391.161	369.430
6th gear (0.87)					
36	323.851	302.261	283.370	266.701	251.884
38	341.843	319.053	299.112	281.517	265.878
40	359.834	335.845	314.855	296.334	279.871
42	377.826	352.638	330.598	311.151	293.865
44	395.818	369.430	346.341	325.968	307.858
46	413.810	386.222	362.083	340.784	321.852
48	431.801	403.014	377.826	355.601	335.845

Appendix 2: traction coefficient vs slip for different tyres

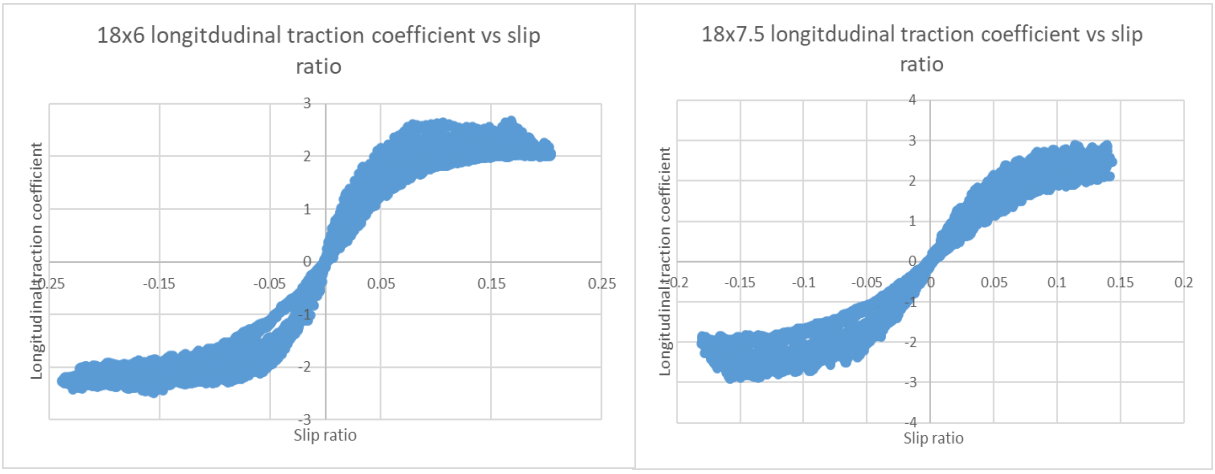

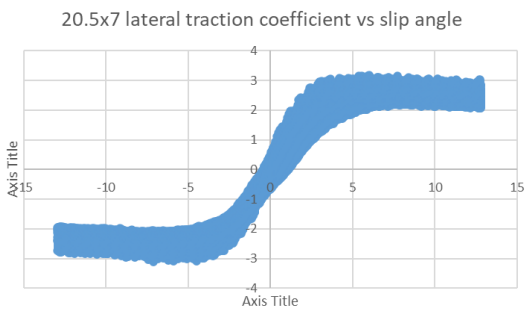

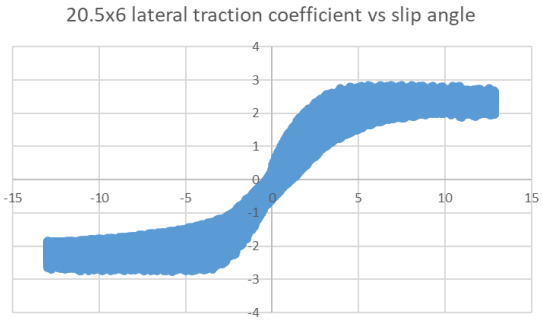

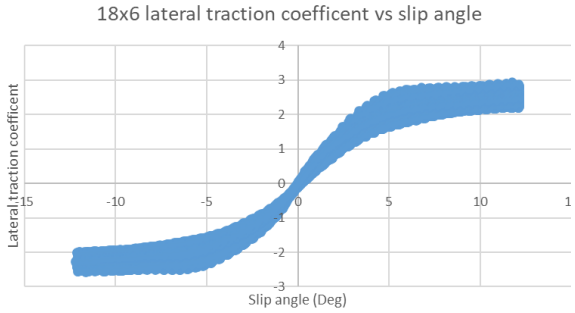

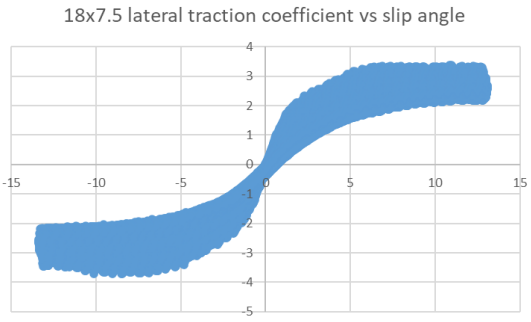

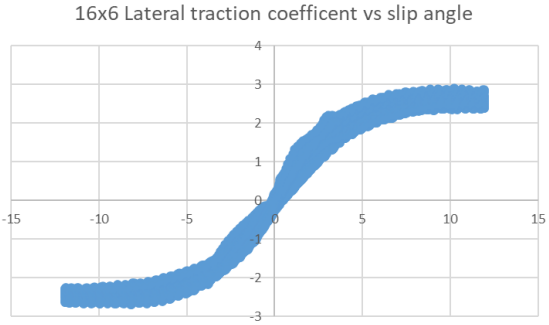

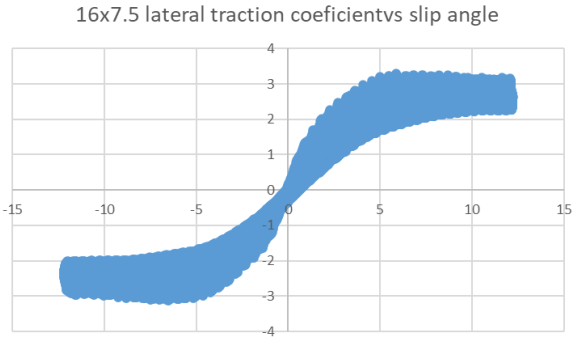

Appendix 3:MoTeC mathematical correction factors

18x6	-400	-600	-800	-1000	-1200
Stress (MPa)	0.064	0.072	0.081	0.09	0.0985
k value measured	9018.266	9018.266	9018.266	9018.266	9018.266
r	0.2286	0.2286	0.2286	0.2286	0.2286
x	0.044354	0.066532	0.088709	0.110886	0.133063
r l	0.184246	0.162068	0.139891	0.117714	0.095537
CP depth	0.13532	0.16122	0.180799	0.195963	0.207679
cp width	0.1524	0.1524	0.1524	0.1524	0.1524
CP area (m2)	0.020623	0.02457	0.027554	0.029865	0.03165

CP area (cm2)	206.2278	245.6989	275.5383	298.6472	316.5033
stress pa	64000	72000	81000	90000	98500
long traction theory	3.144465	2.773623	2.604443	2.494875	2.397794
long traction actual	3.152299	2.807627	2.582155	2.475883	2.388811
difference	-0.00249	-0.01211	0.008632	0.007671	0.003761

Appendix 4:MoTeC mathematical correction factors

$$Actual\ lateral\ acceleration = (\textbf{'G Force Lat'}[G] * sin(14) + \textbf{'G Force Long'}[G] * cos(14) - \textbf{'G Force Vert'}[G] * cos(61.35) - \textbf{'G Force Long'}[G] * sin(61.35)) * cos(14)$$

$$Actual\ longitudinal\ accelration = (\textbf{'G Force Lat'}[G] * sin(14) - \textbf{'G Force Long'}[G] * cos(14)) - \textbf{'G Force Vert'}[G] * sin(61.35) * sin(14)$$

Appendix 5: YMD for W-FS-18 with 55% roll stiffness distribution at Vx = 16 m/s No locking percentage

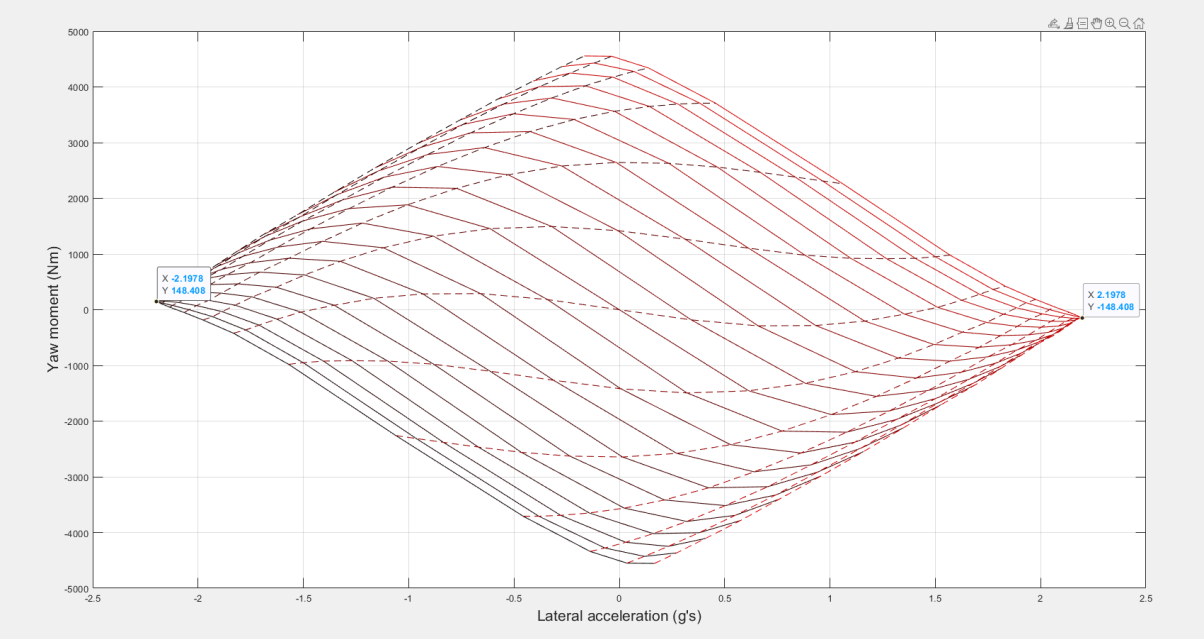

Appendix 6: YMD for W-FS-18 with 55% roll stiffness distribution at Vx = 16 m/s, differential option 1

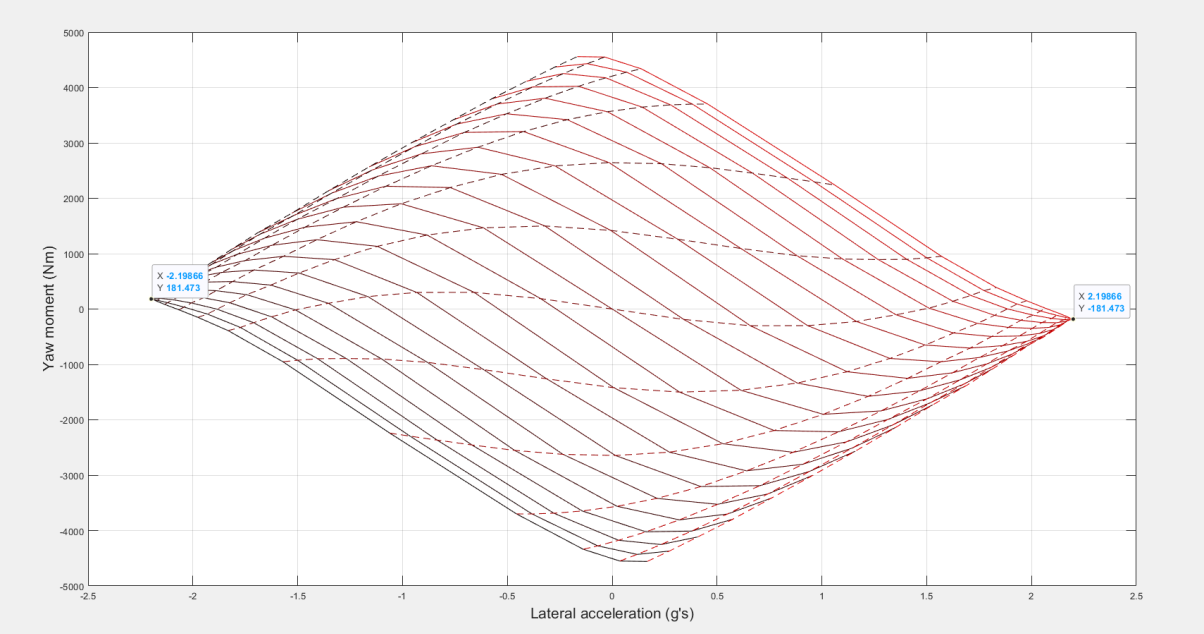

Appendix 7: YMD for W-FS-18 with 55% roll stiffness distribution at Vx = 16 m/s, differential option 2

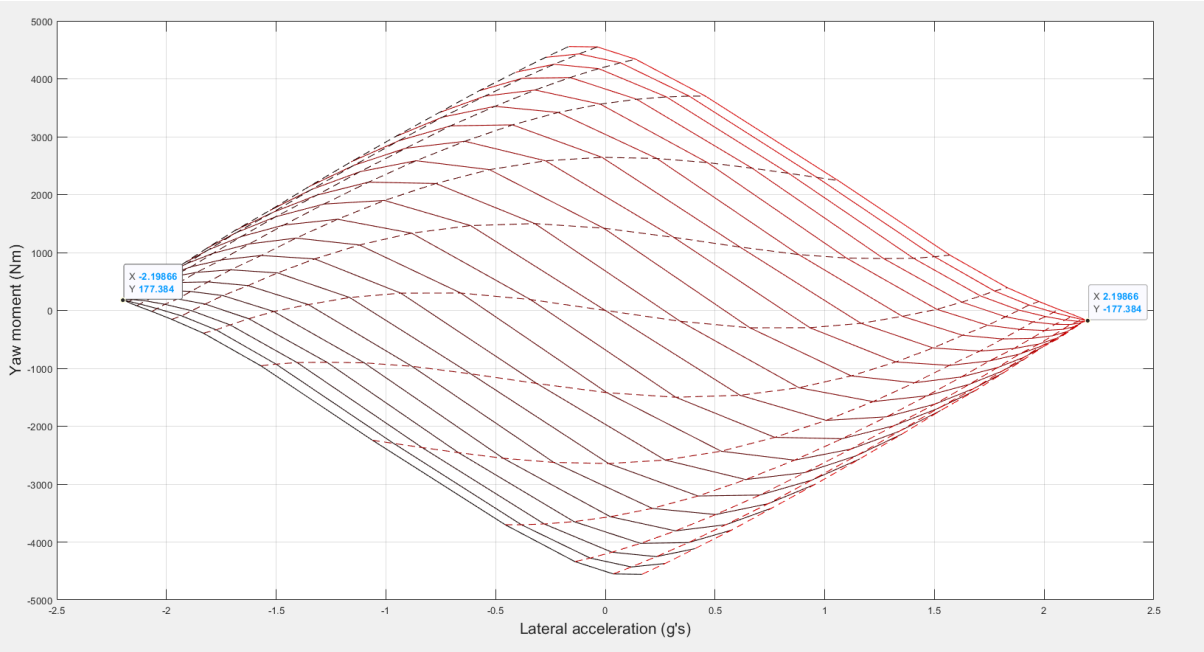

Appendix 8:YMD for W-FS-18 with 55% roll stiffness distribution at Vx = 16 m/s, differential option 3

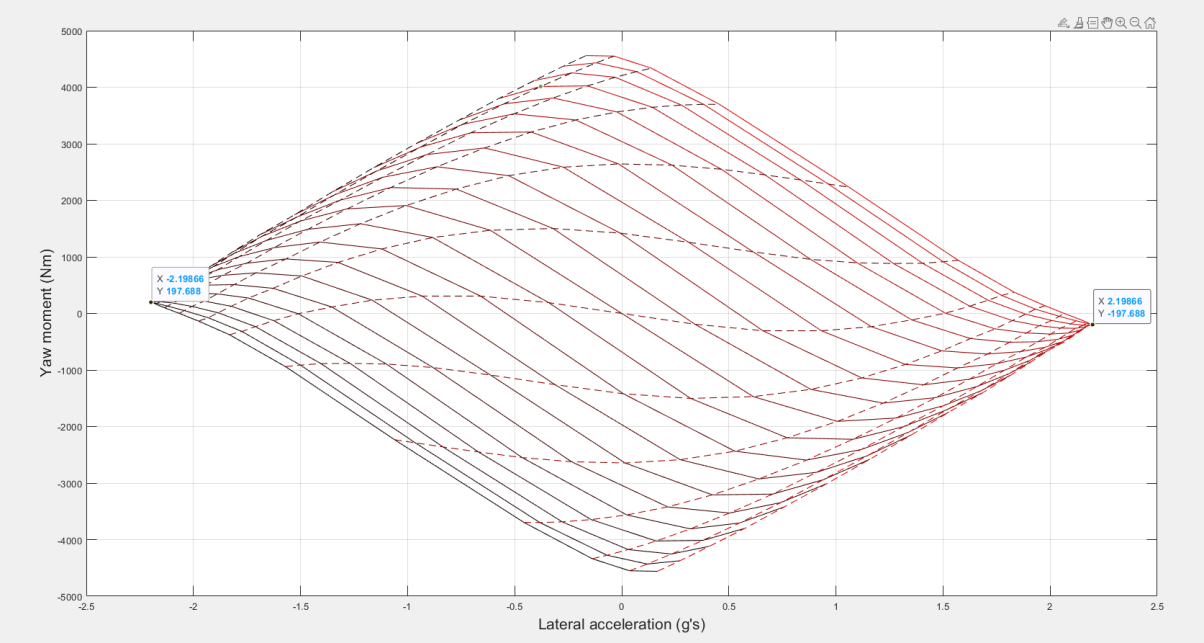

Appendix 9: code for YMD

```
Basic YM calcs

clear;
clc;
close all;

wb = 1.575;
twr = 1.1;
twf = 1.15;
mdriv = 75;
mcar = 191;
mtot = mdriv+mcar;
g = -9.81;
Minrad = 13;

fz = g*mtot/4;

ia = 2;

if ia == 0
  tx = 1*10^-9*(fz)^3 + 4*10^-6*(fz)^2 + 0.0055*(fz) + 4.886;
elseif ia == 2
  tx = 1*10^-9*(fz)^3 + 4*10^-6*(fz)^2 + 0.0053*(fz) + 4.7383;
```

```
else
  tx = 1*10^-9*(fz)^3 + 4*10^-6*(fz)^2 + 0.0056*(fz) + 4.9032;
end




for r = Minrad:100          % finding sr, force and ym for different radii
of corners
  v=16
  Flat = mtot*v^2/r
  ac = Flat/mtot/g
  d1 = pi*(r+twr/2)/(r*pi)
  d2 = pi*(r-twr/2)/(r*pi)


  for diffset = 1
  lp = 28;
  sr1 =((d1-d2)/d2)*lp/100
  %resforce = (-818.61*(sr)^3 -8.4989*(sr)^2 + 32.059*(sr) + 0.0776)*mtot/4
  resforce1 = (611.59*(sr1)^3 -285.81*(sr1)^2 + 45.295*(sr1) -
0.0011)*mtot/4;
  ym1 = 0.5*resforce1*twr;
  end


  for diffset = 2
  lp = 25;
  sr2 =((d1-d2)/d2)*lp/100
  %resforce = (-818.61*(sr)^3 -8.4989*(sr)^2 + 32.059*(sr) + 0.0776)*mtot/4
  resforce2 = (611.59*(sr2)^3 -285.81*(sr2)^2 + 45.295*(sr2) -
0.0011)*mtot/4;
  ym2 = 0.5*resforce2*twr;
  end


  for diffset = 3
  lp = 40;
  sr3 =((d1-d2)/d2)*lp/100
  %resforce = (-818.61*(sr)^3 -8.4989*(sr)^2 + 32.059*(sr)
+ %0.0776)*mtot/4
  resforce3 = (611.59*(sr3)^3 -285.81*(sr3)^2 + 45.295*(sr3) -
0.0011)*mtot/4;
  ym3 = 0.5*resforce3*twr;
  end
```

```
  %Flatbin (r+1-Minrad) = Flat
  %vbin(r+1-Minrad) = v;
  rbin(r+1-Minrad) = r;
  acbin(r+1-Minrad) = ac;
                                                % making a bin of the
different variables being plotted
  srbin1(r+1-Minrad) = sr1;                     % bin of sr for diff 1
  resforcebin1(r+1-Minrad) = resforce1;         % bin of Force for diff 1
  ymbin1(r+1-Minrad) = ym1;                     % bin of YM for diff 1

  srbin2(r+1-Minrad) = sr2;                     % bin of sr for diff 2
  resforcebin2(r+1-Minrad) = resforce2;         % bin of Force for diff 2
  ymbin2(r+1-Minrad) = ym2;                     % bin of YM for diff 1

  srbin3(r+1-Minrad) = sr3;                     % bin of sr for diff 3
  resforcebin3(r+1-Minrad) = resforce3;         % bin of Force for diff 3
  ymbin3(r+1-Minrad) = ym3;                     % bin of YM for diff 1


end
 figure(1);
    hold on;
    plot(rbin,srbin1,'color','blue');           %plotting r vs sr
    plot(rbin,srbin2,'color','red');            %   change variables being
    plot(rbin,srbin3,'color','black');          %   plotted to suit
    hold on;
    %plot(-acbin,-ymbin1,'color','blue');  unsuppress for YM calc
    %plot(-acbin,-ymbin2,'color','red');
    %plot(-acbin,-ymbin3,'color','black');
    %plot(-acbin,resforcebin);
    %plot(rbin,srbin);
    %xlabel('Lateral Acceleration, (G)');      %use label of variable above
    xlabel('radius, (m)');
    %ylabel('longitudinal force due to slip of outside wheel (N)');
    ylabel('Slip ratio of outside wheel');
    %ylabel('Yaw moment (Nm)');
  legend('Differential setting 1', 'Differential setting 2', 'Differential
setting 3')
```

```
Calulate YM for YMD


function[Ay, YM] = calcYM(Ay, aFL, aFR, aRL, aRR) % Ay input initial is
zero, Ay output iterated new value, Ym output


global mtot delta a b Vx Vy r ym tr resforce R acmat


for i = 1:1 %ignore
    convergence = false
        while convergence == false
        [FL, FR, RL, RR] = wt(Ay); %calculate load transfers


        [FyFL, FyFR, FyRL, FyRR] = calcFY(FL, FR, RL, RR, aFL, aFR, aRL,
aRR); %calculate lateral forces
        Pr = 0.6; %relaxation parameter to prevent unstable iterations,
necessary below 12 m/s
                  %0.6 seems to work okay


        newAy = (FyFL + FyFR + FyRL + FyRR)./mtot; %new calculated Ay
        newAy = newAy.*(1-Pr)+Ay.*Pr; %apply relaxation parameter to Ay
        percent_diff = abs((abs(Ay-
newAy)./((Ay+newAy)./2)).*100); %calculate percent difference between old
and new Ay


        if percent_diff < 0.6 %can set this at 0.1 or even lower for magic
number
                              %from 0.2 to 0.8, if you want to simulate
                              %aoutside this range or no ARB front rear
(i.e.
                              %magic number = 0 or 1) set to around
                              %0.8-1.2% otherwise will not convergre
            convergence = true;


        else


            Ay = newAy;
            r = Ay./Vx;
```

```
        [aFL, aFR, aRL, aRR] = calcSA(Vy, delta, Vx, r);


    end

    if Ay ~= 0
        R = Vx^2/(Ay/9.81)
        else
        R =100;
        end


    end




        R1 = abs(R);
        diffset = 3;
        g = 9.81;

        if diffset == 1
        lp = 28;
        elseif diffset == 2
        lp = 25;
        elseif diffset == 3
            lp = 40;
        else lp =0;
        end

        d1 = pi*(R1+tr/2);
        d2 = pi*(R1-tr/2);

        sr =((d1-d2)/d2)*lp/100;
        resforce = (611.59*(sr)^3 -285.81*(sr)^2 + 45.295*(sr) -
0.0011)*g*mtot/4;
        if  R <0
             ym = 0.5*resforce*tr;
        else
```

```
                ym = -0.5*resforce*tr;
            end



    Fyfront = FyFL + FyFR;
    Fyrear = FyRL + FyRR ;
    YM = (((Fyfront.*(cos(delta))).*a)-(Fyrear.*b))+ym;

    convergence = false;
end
end
```

YMD code

```
clear all

load('tyrefit.mat');
%car parameters

global ksf ksr wb a b ms h2 hf hr tf tr huf hur muf mur msf msr hs...
    CoGdistrb h mtot Vx Vy r delta R ym sr resforce Acmat

wb = 1.575; %wheelbase m
magic = 0.5; %note: for magic number outside of range of 0.2 - 0.8
           %must change convergence percentage in calcYM function to
           %around 0.6-1 %

kdes = 832; %desired roll rate Nm/deg
kdesf = kdes.*magic;
```

```
kdesr = kdes.*(1-magic);
ksf = kdesf.*(180./3.141592654); %rear roll stiffness Nm/rad
ksr = kdesr.*(180./3.141592654); %front roll stiffness Nm/rad

mtot = 266; %total mass
ms = 236; %sprung mass kg
CoGdistrb = 0.5; %CoG distribution to rear %
a = CoGdistrb.*wb;
b = wb.*(1-CoGdistrb);
tf = 1.10; %front track width m
tr = 1.05; %rear track width m
hs = 0.305; %height of sprung mass CoG
huf = 0.23; %height of unspruing mass CoG front
hur = 0.23; %height of unspruing mass CoG rear
muf = 12; %unsprung mass front kg
mur = 18; %unsprung mass rear kg
msf = (ms.*b)./wb;
msr = (ms.*a)./wb;
hf = 0.09409; %height of front roll centre, 2018: 0.09409
hr = 0.05001; %height of rear roll centre, 2018: 0.05001
h = (((hr-hf)./wb).*a)+hr; %height of roll axis at longitudinal position of
sprung mass CoG
h2 = hs-h; %lever arm between sprung mass CoG and roll axis

Vx = 16;

%set your range for beta and delta sweeps
betamax = 6; %car sideslip angle
deltamax = 10; % steering angle relative to car

q = 1;
for i = -betamax:betamax
    betadeg(q) = i;
    q = q+1;
end

q = 1;
for i = -deltamax:deltamax
    deltadeg(q) = i;
    q = q+1;
```

```
end

betabin = deg2rad(betadeg); %slip angle at CG
deltabin = deg2rad(deltadeg); %steering angle (at wheel)




for m = 1:numel(deltabin) %sweep for all deltas
    delta = deltabin(m);



    for i = 1:numel(betabin) %sweep for all betas
        if i == round((numel(betabin))./2) & m ==
round((numel(deltabin))./2); %for beta and delta at zero, set Ay and YM to
zero manually
                            %otherwise percent difference equation is
                            %divided by zero (see calcYM)
            Aybeta(i, m) = 0;
            YMbeta(i, m) = 0;
                    else                        %account for zero values
(straightline)
            beta = betabin(i);
            Vy = -beta.*Vx;
            Ay = 0;
            r = Ay./Vx;    % r is yaw rate unit 1/s




            [FL, FR, RL, RR] = wt(Ay); %LT funciton check
            [aFL, aFR, aRL, aRR] = calcSA(Vy, delta, Vx, r); %calculate
slip angles for current vehicle state (Ay=0)


            [FyFL, FyFR, FyRL, FyRR] = calcFY(FL, FR, RL, RR, aFL, aFR,
aRL, aRR); %lateral force function check, a is slip angle




            [Ay, YM] = TRIALcalcYM(Ay, aFL, aFR, aRL, aRR); %start yaw
moment calculation function for given beta & delta
```

```
            Aybeta(i, m) = Ay./9.81; %store converged Ay and yaw moment
result
            YMbeta(i, m) = YM;



        end
    end
    Acmat=Aybeta;


end
figure



%%%%%%%%%%%%%%%%%%plots


for n = 1:numel(deltabin)
    plt(n) = plot(Aybeta(:, n), YMbeta(:, n), '-',
'LineWidth',0.8 ,'MarkerSize',0.5,...
        'MarkerEdgeColor','b','MarkerFaceColor',[0.5, 0.5, 0.5],'Color',
[1.*(n./25), 0, 0]);
    %legend('Delta = 10', 'Delta = 9', 'Delta = 8', 'Delta = 7', 'Delta =
6', 'Delta = 5', ...
        %'Delta = 4', 'Delta = 3', 'Delta = 2', 'Delta = 1', 'Delta = 0',
'Delta = -1', 'Delta = -2', 'Delta = -3', ...
        %'Delta = -4', 'Delta = -5', 'Delta = -6', 'Delta = -7', 'Delta = -
8', 'Delta = -9', 'Delta = -10');
    grid on
    hold on
    xlabel('Lateral acceleration (g''s)', 'fontsize', 16)
    ylabel('Yaw moment (Nm)', 'fontsize', 16)
end


for j = 1:numel(betabin)
    plot(Aybeta(j, :), YMbeta(j, :), '--',
'LineWidth',0.8,'MarkerSize',0.5,...
        'MarkerEdgeColor','b','MarkerFaceColor',[0.5, 0.5, 0.5],'Color',
[1.*(j./15), 0, 0]);
    hold on
    grid on


end
```